Removal of Nitrogen containing Hydrocarbons from Wastewater by Catalytic and Non-Catalytic Hydrothermal oxidation, in Sub- and Supercritical conditions

by

Oluwaponmile Olumayowa Osibo

A thesis submitted to the University of Birmingham
for the degree of
DOCTOR OF PHILOSOPHY

School of Chemical Engineering
College of Engineering and Physical Sciences
The University of Birmingham
September 2010

ABSTRACT

The results of the hydrothermal oxidation of 1,8-diazabicyclo[5.4.0]undec-7-ene (DBU), a toxic nitrogen-containing organic compound by different processes is presented here. Subcritical experiments (wet air oxidation (WAO) and catalytic wet air oxidation(CWAO)), were conducted in a batch reactor and supercritical water oxidation (SCWO) experiments were conducted in a tubular reactor.

The key operating parameters investigated were temperature, pressure, initial organic concentration; for catalytic experiments, the effect of catalyst metal loading and weight were also investigated. Commercially available Ru/Al_2O_3 pellets were selected for catalytic study after various catalysts were screened.

Results indicated that temperature was the key operating parameter in all 3 processes that affected DBU removal, TOC removal and ammonia yield. Ru/Al_2O_3 pellets enhanced the DBU removal, TOC removal and decreased ammonia yield compared to WAO. Complete DBU removal was achieved by catalytic wet air oxidation and supercritical water oxidation. Kinetic data was acquired and a pseudo first order kinetic model was used to quantify the oxidation rate.

WAO and CWAO were investigated for the treatment of hazardous industrial effluent with a high initial ammonia concentration and complete ammonia removal was achieved using Ru/Al_2O_3 pellets. A novel ruthenium coated reticulated foam monolith was investigated as a nalternative for heterogeneous catalyst instead of Ru/Al_2O_3 pellets, the results show that it improved catalyst stability and could be an alternative to pellets for wastewater treatment.

To My Parents and Brother

ACKNOWLEDGEMENTS

I wish to express my gratitude to the following people, who helped me accomplish this work:

Dr Bushra Al-Duri for your supervision, advice and encouragement. I am very grateful for the opportunities you gave me to travel, partake in research overseas and develop.

Dr Regina Santos for your supervision, advice and encouragement.

Professor Yoshito Oshima, Professor Motonobu Goto and Assistant Professor Mitsuru Sasaki for the privilege to work in your laboratories.

Dr Mauricio Angeles, Dr Zoe Brown, Peter Bath, Dr Tiejun Lu, Dr Abdul Alao, Dr Idoko Ochuma, Alireza Bahari, Naeema Al-Darmaki, Ricardo Roque, Dr Muhammad Baig, Dr Raslan Alanezi for your friendship, discussions and the great moments we spent together.

The main office staff for your administrative support and the workshop staff for your technical assistance with experimental equipment.

TABLE OF CONTENTS

LIST OF FIGURES

LIST OF TABLES

NOMENCLATURE

A = pre-exponential factor

E = Activation Energy (KJ mol^{-1})

k = rate constant (min^{-1})

C_{org} = organic compound concentration (mM)

$C_{o2,L}$ = oxygen concentration in the liquid

R = universal gas constant

T = reaction temperature (K)

ΔH - heat of formation of a compound

K_0 - adsorption pre-exponential factor

[Organic] = concentration of organic

[O_2] = concentration of oxidant

[H_2O] = concentration of water

C_{aq} = concentration of molecular oxygen in pure water (mol O_2 / kg H_2O)

P_{O2} = partial pressure of oxygen gas (MPa)

k = equilibrium constant (mol O_2 / kg H_2O) (MPa^{-1})

C_o = initial concentration of DBU and TOC (mM)

C = concentration of DBU and TOC at time t (mM)

C_{NH3} = molar concentration of nitrogen atoms in ammonia after 90 minutes

C_{Nin} = molar concentration of nitrogen atoms in the feed

Superscript

a = reaction order relative to the organic

b = reaction order relative to the oxidant

c = reaction order relative to water

m = reaction order relative to the organic reactant

n = reaction order relative to oxygen

Subscript

j = refers to a compound formed

org = refers to the organic compound

CHAPTER 1 - INTRODUCTION

It is currently forecasted that global water demand will grow by 50% over the next 20 years; it is estimated that such levels of water usage will result in a 40% supply shortage. To put this in context, it is estimated that with current trends, clean water will run out before oil. 87% of the global water demand comes from industry and agriculture. The efficient treatment of industrial and agricultural wastewaters was highlighted as one of the important steps in water management (McKinsey&Company, 2009).

The World Health Organisation (WHO) 2006 estimates, suggest that 1.2 billion people lack hygienic drinking water, and this figure will grow with population increase. To tackle this, governmental organisations have brought in more stringent regulations and guidelines to govern the effective disposal of industrial wastewater and control the accepted levels of pollutants in the wastewater (European Economic Community, 2008). One of these regulations is "The Environment Agency Integrated Pollution Control Guidance", which gives guidance for production processes prescribed for Integrated Pollution Control (IPC) in Regulations made under Section 2 of the Environmental Protection Act. It is a guide on techniques and standards relevant to batch and fine organic chemicals manufacture including pesticides and pharmaceuticals. Benchmark release guidelines to surface water are provided in the Table 1.1 below.

Substance	**Concentration (mg/L)**
Total hydrocarbon oil content	1-3
Biological Oxygen Demand (BOD)	20-30
Chemical Oxygen Demand (COD)	150-1100
Ammoniacal Nitrogen (as N)	10-20
Suspended Solids (SS)	30-40

Table 1.1 Benchmark releases to surface water

The levels shown above are ranges achievable after effluent treatment and are not release limits. No information on pharmaceutical active ingredients is provided. For pollutants resistant to biodegradation, achievement of the levels quoted above will require isolation at source and separate specialised treatment.

Industrial wastewaters regularly contain compounds which are not amenable by municipal wastewater treatment methods, this is mainly due to the toxicity of the compounds or the secondary compounds they form when treated. Therefore the ideal or preferred treatment method must be able to completely mineralise the primary pollutant or a mixture of pollutants, and any secondary products formed; whilst being cost effective.

Incineration is a commonly used technology to treat wastewater because it indiscriminately destroys a wide range and varying concentrations of organic compounds and is appropriate for treating wastewater with high Chemical Oxygen Demand (COD) of 400 g/ dm^3 or above (Luck, 1996, Imamura, 1999). The process is handicapped by large energy cost which demands a minimum solution concentration of 40% to be energy efficient, corrosion problems and products of incomplete combustion (Bhargava *et al.*, 2006). This coupled with the fact that some industrial processes produce wastewaters with low concentrations (10 - 2000 mgL^{-1} TOC) of highly toxic compounds, has led to a push for alternative and novel wastewater treatment technologies (Oliviero *et al.*, 2003).

Apart from biological and physical methods of wastewater treatment, a variety of novel treatment technologies called Advanced Oxidation Processes (AOPs) have been developed and applied for the treatment of wastewaters; these can be broadly classified into hydrothermal (Sub and Supercritical Water Oxidation); catalytic (Photo Catalytic and Catalytic Wet Air Oxidation) and chemical (Ozone, Hydrogen peroxide, Ultraviolet, Ultrasound) processes. Selection of the appropriate treatment process is dependent on the

feasibility of treatment and process economics, as each process has its range of application depending on the composition and volume of wastewater and the concentration of pollutants.

Hydrothermal oxidation (Wet Air Oxidation (WAO) and Supercritical Water Oxidation (SCWO)), have been shown to be an effective treatment method of wastewaters contaminated with toxic and non-biodegradable compounds, and have garnered strong research interest over the past 30 years.(Luck, 1999, Cansell *et al.*, 1998, Aki and Abraham, 1998, Bhargava *et al.*, 2006, Gogate and Aniruddha, 2003). The use of hydrothermal oxidation for wastewater treatment has been motivated by the desire to create a cleaner and more environmentally benign process.

Wet Air Oxidation (WAO) is an attractive treatment for aqueous waste streams, that are too dilute to incinerate or too concentrated or toxic for biological treatment. WAO becomes energetically self-sustaining when the Chemical Oxygen Demand (COD) of the wastewater exceeds 20 g/dm^3 compared to 400 g/dm^3 for incineration (Deiber G. et al., 1997).

Wet Air Oxidation process enhances contact between molecular oxygen and organic matter in solution, at high temperature. The liquid phase is maintained at high pressure which also increases the concentration of dissolved oxygen (Debellefontaine and Foussard, 2000; Zimmermann and Diddams, 1960). Several researchers have investigated and proven the effectiveness of WAO as a wastewater treatment technology. The variety of wastes treated by WAO include contaminated soil, organic solvents, chemical and pharmaceutical wastes containing dyes and polymers (Deiber G. *et al*., 1997; Imamura,1999; Oliviero L. *et al*., 2002; Thomsen and Laturnus, 2001)

Supercritical Water Oxidation is a very effective treatment method as it is able to completely mineralise many compounds rapidly, due to the unique properties of supercritical water. (Crain *et al.*, 1993, Savage *et al.*, 1984). A variety of wastes have been effectively treated with SCWO include rocket propellants, warfare agents, cutting oils, and petrochemical

wastes(Harradine *et al.*, 1993, Downey *et al.*, 1995, Portela *et al.*, 2001a, Onwudili and Williams, 2007b).

The motivation for this research is to asses the performance of WAO and SCWO for the treatment of organic pollutants containing heteroatoms only, and demonstrate that the use of catalysts in CWAO improves degradation and could possibly reduce operating temperature and pressure. Furthermore it would demonstrate the potential of these technologies to be applied to industrial waste water treatment.

Chapter 2 is a literature survey on WAO, SCWO and CWAO of pollutants and this chapter includes sections on generalised theory and mechanism, kinetic models, oxidation treatment technologies, catalysts, advances and future challenges.

Chapter 3 covers experimental materials, equipment, procedures and analytical methods.

Chapter 4 discusses the Wet Air Oxidation of DBU as a model pollutant, chapter 5 discusses the Catalytic Wet Air Oxidation of DBU and while chapter 6 discusses the Supercritical Water Oxidation of DBU.

Chapter 7 compares and discusses the results of DBU treatment using the various Hydrothermal Oxidation processes. Chapter 8 includes conclusions drawn from the studies presented in this thesis and recommendations for future work. The appendices include properties of materials used, sample calculations, and supporting graphs.

Research Objectives

The overall aim of this thesis is to increase the collective knowledge and understanding of oxidation chemical reactions under hydrothermal conditions. Ultimately, the information gained from the study of the various systems may play an important part in the

effective design of future hydrothermal systems for wastewater treatment, and may provide further documentation of their strengths and weaknesses.

The research objectives are to:

i) **Study the oxidation of the model pollutant 1,8-diazabicyclo [5.4.0] undec-7-ene (DBU) and evaluate its kinetic parameters.** This involves identifying the range of operating conditions for Wet Air Oxidation (WAO) and Supercritical Water Oxidation (SCWO), at which the pollutant oxidises with reasonable efficiency but is incomplete; thereby making the use of a catalyst viable. This will be done by measuring the oxidation rates of DBU under defined conditions of temperature, pressure and organic concentration. These data will be used to determine the fundamental kinetics of DBU destruction. In addition, where possible intermediates formed will be identified and quantified to determine how they change with experimental conditions.

ii) **Screen various catalysts and select one suitable for optimising the oxidation of DBU.** This involves selecting one suitable catalyst type for study under similar conditions to Wet Air Oxidation.

iii) **Evaluate the ability of the hydrothermal processes to effectively treat industrial waste containing nitrogenous compounds**. Ultimately the aim of all wastewater treatment processes is to effectively treat industrial wastewater; therefore a sample of industrial wastewater will be treated using the hydrothermal processes.

CHAPTER 2 - LITERATURE SURVEY

2.1 Understanding Sub and Supercritical water

The principle idea behind hydrothermal oxidation processes is the use of high temperature and high pressure water as a reaction medium. As the temperature and pressure of water is increased its physical and chemical properties change from those of ambient water and become favourable for its use as a reaction medium. High temperature water can be broadly defined as subcritical and supercritical water. Subcritical water is classified as water between 150 - 300ºC with a maximum pressure of 10 MPa, while supercritical water is above the critical point of water, which is 374ºC and 22 MPa (Portela *et al.*, 1997, Lee and Park, 1996). Above the critical point of water, it can no longer be classified as a liquid or gas, because the boundary between the two layers disappears and they become one phase. This is demonstrated in Figure 2.1, which shows a Temperature-Pressure graph of a pure substance.

Subcritical and supercritical water have lower dielectric constants, fewer and weaker hydrogen bonds than ambient water. Hydrogen bonding is the source of many of the unique properties of liquid water. The hydrogen bonding in water becomes weaker with increasing temperature and pressure. For example, water at 773 K and ~0.1 g/cm^3 retains 10–14% of the hydrogen bonds that exist at ambient conditions, whereas water at 673 K and ~0.5 g/cm^3 retains 30–45% (Hoffmann and Conradi, 1997). This is due to the breakdown of infinite percolating network of hydrogen bonds in ambient water; at high temperatures and pressures this network now exists as small clusters of hydrogen bonded molecules (Akiya and Savage, 2002).

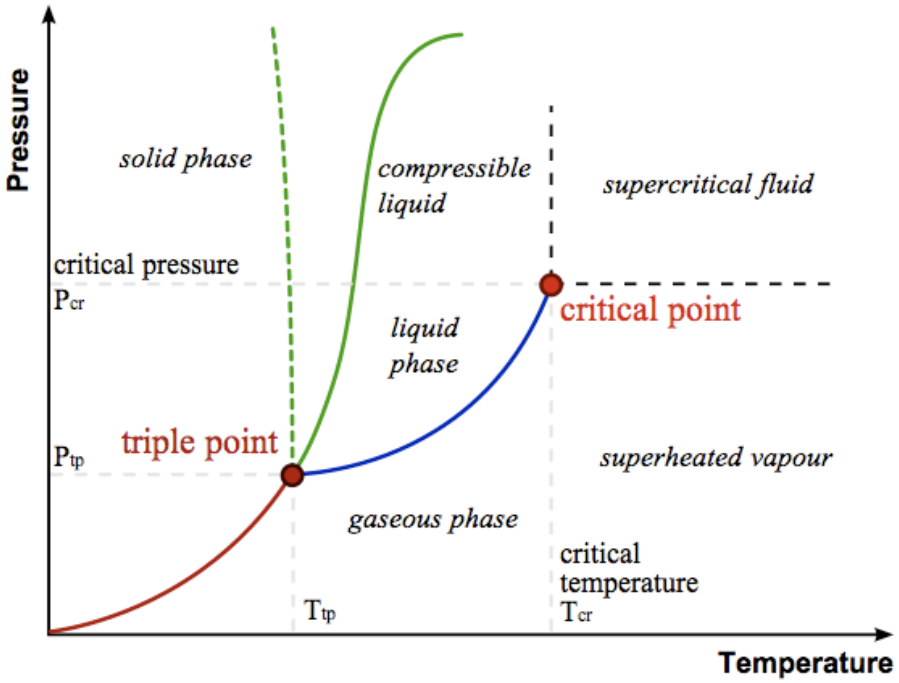

Figure 2.1 Generic Temperature-Pressure diagram of a pure substance

The static dielectric constant (ε) is a measure of the polarity of a solvent and with increasing temperature, pressure and decreasing density, the static dielectric constant of water decreases. For example, the dielectric constant is 21 at 300 ºC and density of 0.75 g/cm^3 and 4.1 at 500 ºC and density of 0.30 g/cm^3, compared to 78 for ambient water (Heger *et al.*, 1980). With such a low dielectric constant, high temperature and pressure water behaves more like polar organic solvents rather than ambient water (Rebert and Kay, 1959), as a result, the solubility of small organic compounds increases in subcritical water, and they are completely miscible in supercritical water, while the solubility of most gases in liquid water initially decreases as the temperature increases above ambient, but a minimum is soon reached and then the gas solubility increases. For oxygen, for example, this minimum occurs at around 100ºC (Akiya and Savage, 2002).

The ion product (*Kw*) of water is another property that changes with temperature and pressure. The ion product (*Kw*) of water at subcritical conditions is about 3 orders of

magnitude higher than that of water at ambient conditions(Akiya and Savage, 2002), water at these elevated conditions also has higher concentrations of H^+ and OH^- ions making it an effective medium for acid and base catalysed reactions(Marshall and Franck, 1981). On the other hand, (*Kw*) for supercritical water at gaslike densities (<0.1g/cm^3) can be tens of orders of magnitude lower than for water at ambient conditions, and accordingly free radical chemistry dominates at these high temperature and low density conditions. Antal *et al.*(1987) found that Ionic mechanisms are favoured when $Kw > 10^{-14}$ and free radical mechanisms are favoured when $Kw << 10^{-14}$. In summary, high temperature and pressure water can support ionic, polar non-ionic, and free-radical reactions(Akiya and Savage, 2002).

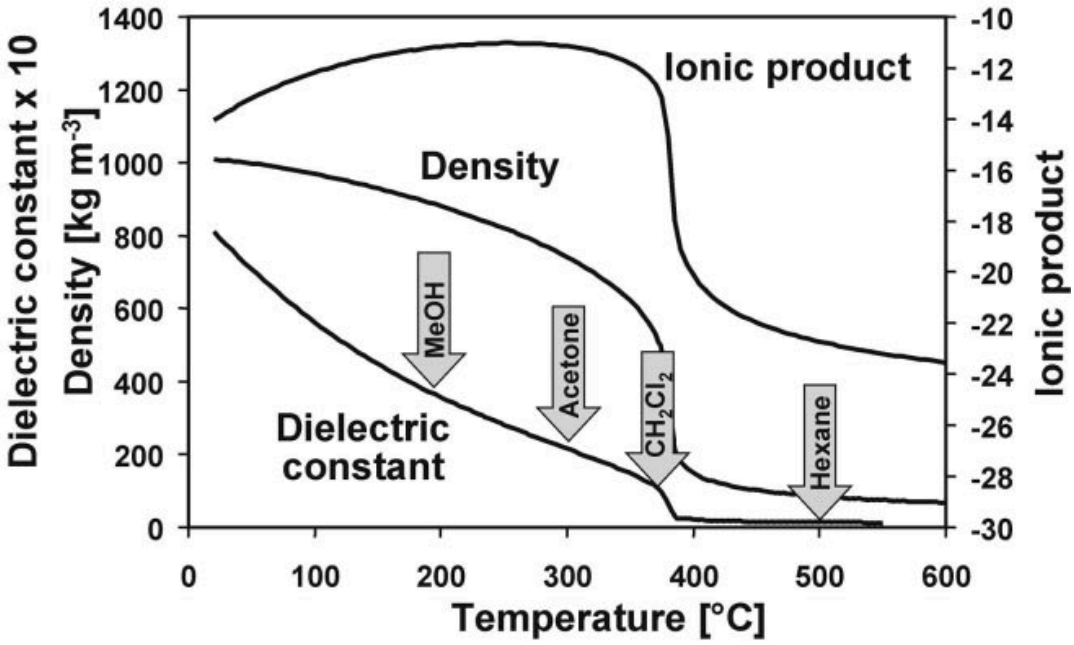

Figure 2.2. Physical properties of water at a pressure of 24MPa versus temperature. Dielectric constants of typical organic solvents at room temperature are indicated. (Kritzer and Dinjus, 2001)

2.2 Other oxidation processes

There are many chemical treatment processes for wastewater treatment and these employ oxidation, and they mineralise the organic compounds to final products (water, carbon dioxide, nitrogen) with varying efficiency. These processes work on the principle of the

generation of free radicals and their subsequent attack or the direct attack of the oxidants on the contaminant molecules. They are mainly applicable to bio-refractory molecules with an aim to either completely mineralise the contaminants or convert them into less harmful compounds which can then be treated biologically. The efficiency of the process depends strongly on the rate of free radical generation and, the extent of contact between the free radicals formed and contaminated molecules. Some major oxidative processes will be summarised in this section.

2.2.1 Ozone/H_2O_2

Ozone is an unstable, reactive compound that is produced from air, high purity oxygen or oxygen enriched air. The capacity of ozone in oxidising various pollutants by direct attack on the different bonds and aromatic rings(Andreozzi *et al.*, 1991), is further enhanced in the presence of hydrogen peroxide due to generation of highly reactive $OH^{\cdot}$ radicals. The dissociation of hydrogen peroxide results in the formation of hydroperoxide ion, which attacks the ozone molecule resulting in the formation of hydroxyl radicals(Staehelin and Hoigne, 1985, Forni *et al.*, 1982). Ozone loading is usually in the range of 0-20 mg/l with recommended ratio of 0.33 hydrogen peroxide(Perkowski *et al.*, 2000).

This technique has been applied in the treatment of short chain acids(Paillard *et al.*, 1988), organochloride compounds(Ormad *et al.*, 1997), ammonia solutions(Kuo *et al.*, 1997), synthetic dyes(Arslan and Balcioglu, 2001), paper mill and pharmaceutical wastes(Gulyas *et al.*, 1995). Radical scavengers such as humic acid, bicarbonate and chloride ions present in the effluent were found to inhibit mineralisation. (to overcome this, pretreatment of waste streams was required to remove the inhibitors or lower their concentrations) Experimentally, reactor design is a critical factor with various reactor configurations (bubble columns, spray

columns, static mixers) and multistage injection systems have been tested (Martin and Galey, 1994).

2.2.2 Fenton's Reagent and Photo-Fenton

The reaction of ferrous iron with hydrogen peroxide is known as Fenton's reaction (Fenton 1894).

$$Fe^{++} + H_2O_2 = Fe^{+++} + OH^- + {}^{\bullet}OH \qquad (2.1)$$

The •OH formed during the reaction can either react with more ferrous iron or oxidise organic contaminants in the wastewater. The decomposition of peroxide is also catalysed by ferric iron regenerating ferrous iron. These processes are effective only at pH of 3 or lower (Dominguez et al. 2005). Fenton's Reagent has obvious advantages: it is a cheap and simple way of producing hydroxyl radicals. Balanced against this, low pHs are required and significant sludge production occurs, adding to overall process costs.

Addition of near-UV and visible light gives the Photo-Fenton reaction (Ruppert et al. 1993). This process provides enhanced reaction rates, most probably due to photo-reduction of ferric to ferrous iron, and photolysis of hydrogen peroxide. Fenton and photo-Fenton reaction processes have been evaluated for a range of organic molecules. An interesting application is the removal of toxic or inhibitory pollutants, such as 2,4,6-trichlorophenol or dichlorodiethylether prior to biological treatment (Basu and Wei, 2001; Gurol et al. 2001). A potential limitation of Fenton or photo-Fenton process however, is illustrated by certain azo dyes that are not easily oxidised, because they form insoluble iron precipitates (Mackay and Pignatello, 2001)

2.2.3 Photocatalysis

A photocatalytic oxidation reaction is a photochemical process that must be preceded by the absorption of radiation of the appropriate energy by the reacting molecules. Upon radiation absorption, the photo-excited molecule can be transformed, in one or more steps, into a product. The excited molecule may also be converted into an intermediate product or component that can take part in subsequent reactions of thermal nature as occurs, for instance, in chain reactions.

One of the concepts that has received an increasing degree of attention is photocatalytic oxidation in which catalysts such as titanium dioxide (TiO_2) are used for the light-induced degradation of organic pollutants (Li Puma and Yue, 2001, Toepfer *et al.*, 2006). Photocatalytic oxidation employs the energy in ultra violet light range. Catalysis by illuminated titanium dioxide is the outcome of the chemical interaction of the electrons and holes generated in the photo-activated TiO_2 with the surrounding medium; thus upon light absorption, electron-hole pairs are formed in the solid particles which can recombine or participate in reduction and oxidation reactions (Cassano et al. 1995).

2.3 Wet Air Oxidation

The Wet Air Oxidation process, which has attracted significant research attention for the treatment of wastewater contaminated with toxic and non-biodegradable compounds was extensively developed and patented by Zimmerman over 50 years ago(Luck, 1999), mineralises organic compounds in liquid phase by oxidising them completely to carbon dioxide and water using an oxidant, usually oxygen or air. The process can treat a variety of wastes produced by industry including sludge(Harada and Yamasaki, 1994)

It is a clean process, because it does not involve the use of any harmful chemical reagents and the final products (If complete mineralisation is achieved) are carbon dioxide and water; If not

complete mineralisation is not achieved various carboxylic acids can be formed as by-products(Foussard *et al.*, 1989).

Wet Air Oxidation operating conditions are typical in the range of 130 - 315 ºC and 2-15 MPa. The oxidant (oxygen or air) is fed into the reactor with the wastewater stream, the reactor conditions promote the oxidation due to the increased solubility of the oxidant and accelerated reaction rates at these conditions. It should be noted that there are process advantages including reduced capital costs in using oxygen instead of air as an oxidant (Kolaczkowski *et al.*, 1999). Prasad and Materi(1990) compared air and oxygen based WAO systems for two levels of organic waste concentration and found that oxygen based systems showed lower capital costs and profitability than air based systems, because using air, a larger pump size was required to achieve the necessary concentration of oxygen.

Figure 2.3 shows the a simple flow diagram of the wet air oxidation process.

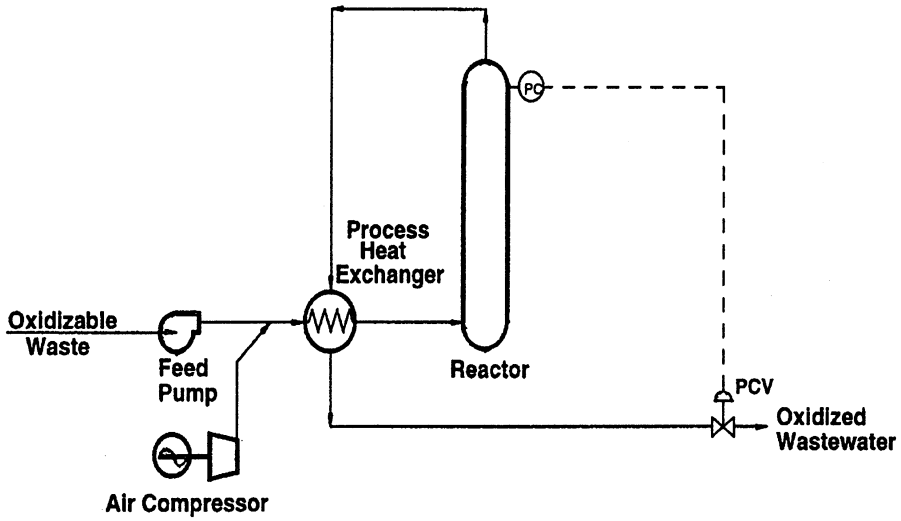

Figure 2.3 Basic flow diagram of a wet air oxidation process (Luck, 1999)

In the simplest terms, the wet air oxidation of an organic compound occurs in two stages; (i) a physical stage, involving the transfer of oxygen from the gas phase to the liquid phase and (ii) a chemical stage, involving the reaction between the transfer oxygen (or an active species formed from the oxygen) and the organic compound. There are some other

phenomena that occur but these two stages ultimately govern the oxidation rate of the organic compound.

2.3.1 Physical stage

Debellefontaine *et al.,* (1996) found that the only significant resistance to oxygen transfer is located at the gas/liquid interface (film model) with three limiting cases: (i) oxygen reacts within the film because of the rapid chemical reaction, enhancing the oxygen transfer rate; (ii) oxygen reacts rapidly within the bulk, where its concentration is close to zero, the overall rate of reaction is equal to the rate at which oxygen is transferred; (iii) the oxygen concentration within the bulk liquid is equal to the interface concentration, in this situation the overall rate is the chemical step rate and it is usually low.

The effect of the oxygen transfer rate on the overall reaction rate can be eliminated through high mixing efficiency, which would allow the chemical kinetic rates to be determined (Winterbottom and King, 1999).

2.3.1 Chemical reaction stage

Many factors can influence the chemical reaction rate of wet air oxidation, the most important factors include temperature, dissolved oxygen concentration (oxygen partial pressure), solution pH, nature of organic compounds, reactor geometry and composition of reactor walls (Kolaczkowski *et al.*, 1997).

2.4 Reaction Mechanisms and Rate Equations in WAO

In the WAO process, the knowledge of the reaction kinetics is fundamental. The effort of research should focus on the establishment of both the reaction pathways followed during the oxidation reactions and the kinetic laws that can describe them. This knowledge, apart from giving a fundamental insight into WAO can lead to significant improvements in the operation and design of WAO units.

2.4.1 Chemistry of WAO

The chemistry of Wet Air Oxidation can be complex, and this complexity is partially due to the different types of chemical reactions that can occur for various organic compounds under typical WAO conditions and the high number of reactions that can occur even in the oxidation of a simple organic compound.

Under typical WAO conditions there are various reactions that result in the oxidation of organic compounds. These include but are not limited to: auto oxidation (free radical reactions involving oxygen), heterolytic/homolytic cleavage (oxidative or non-oxidative thermal degradation), hydrolysis, decarboxylation, alkoxide formation followed by subsequent oxidation (alkaline solution)(Bhargava *et al.*, 2006). The total number of reactions that occur can be high even for a simple low molecular weight compound, for example Day *et al.*(1973) proposed a 16 step free radical reaction mechanism for the wet air oxidation of propionic acid.

Various researchers have investigated the types of reactions that occur during WAO and the general concensus is that the chemical reaction occurs mainly via free radical reactions(Rivas *et al.*, 1998, Lixiong *et al.*, 1991, Robert *et al.*, 2002, Ingale *et al.*, 1996) Numerous free-radical reactions, from each of the three main types of free-radical chemical

reactions (initiation, propagation and termination) have been suggested to occur during WAO of organic compounds. These are shown below:

Initiation

$$RH + O_2 \rightarrow R^{\bullet} + HO_2^{\bullet} \quad (2.2)$$

$$H_2O + O_2 \rightarrow H_2O_2 + O^{\bullet} \quad (2.3)$$

$$H_2O + O_2 \rightarrow HO_2^{\bullet} + OH^{\bullet} \quad (2.4)$$

Free radicals are formed by the reaction of oxygen with the weakest C-H bonds of the organic compound (reaction 2.2), and the reaction of oxygen with water (reaction 2.4). The hydrogen peroxide formed, reaction 2.3, then decomposes into water and oxygen.

Propagation

$$R^{\bullet} + O_2 \rightarrow ROO^{\bullet} \quad (2.5)$$

$$ROO^{\bullet} + RH \rightarrow ROOH + R^{\bullet} \quad (2.6)$$

$$ROOH \rightarrow RO^{\bullet} + OH^{\bullet} \quad (2.7)$$

$$RH + OH^{\bullet} \rightarrow R^{\bullet} + H_2O \quad (2.8)$$

$$O^{\bullet} + H_2O \rightarrow OH^{\bullet} + OH^{\bullet} \quad (2.9)$$

$$H^{\bullet} + H_2O \rightarrow OH^{\bullet} + H_2 \quad (2.10)$$

The formation of the hydroxyl radical $\left(OH^{\bullet}\right)$ plays an important role because it is highly reactive with organic compounds. The oxidation of the organic compounds by hydroxyl radicals as shown in (reaction 2.8), follows a hydrogen abstraction mechanism. The organic radical $\left(R^{\bullet}\right)$ reacts with oxygen (reaction 2.5) to form an organic peroxy radical $\left(ROO^{\bullet}\right)$. The organic peroxy radical further abstracts a hydrogen atom from the organic

compound, producing an organic hydroperoxide $(ROOH)$ and another organic radical (reaction 2.6).

Termination

$$2ROO^{\bullet} \rightarrow ROOR + O_2 \quad (2.11)$$

$$2HO_2^{\bullet} \rightarrow H_2O_2 + O_2 \quad (2.12)$$

$$HO_2^{\bullet} + OH^{\bullet} \rightarrow H_2O + O_2 \quad (2.13)$$

The organic hydroperoxides formed are relatively unstable, the decomposition of such intermediates often leads to molecular breakdown and the formation of intermediates with lower carbon numbers (Bhargava *et al.*, 2006). These scission reactions continue rapidly until the formation of acetic or formic acid. These acids will eventually be converted into carbon dioxide and water.

2.4.2 Ionic Reactions

Although the majority of reactions that lead to oxidation via WAO are free radical in nature, there are other reactions that can also result in oxidation. These are classified as ionic reactions, where ions present at typical WAO conditions react with compounds/intermediates up(Bhargava *et al.*, 2006). Examples of these are shown below:

$$XCH_3 + {}^{-}OH \rightarrow XCH_2^{-} + H_2O \quad (2.14)$$

Equation 2.14, shows the removal of an α -hydrogen from a carboxylic acid and a hydroxide ion, where X represents the carboxylate group (Wakabayashi *et al.*, 1988).

$$C_6H_5OH + {}^{-}OH \rightarrow C_6H_5O^{-} + H_2O \quad (2.15)$$

The removal of an alcoholic hydrogen from phenol by hydroxide ion is shown in Equation 2.15 (Rivas *et al.*, 1998).

2.4.3 Wet Air Oxidation Kinetics

Power law kinetics

WAO reaction rates are generally described by the global rate law

$$-\frac{dC_{org}}{dt} = k\left(C_{\text{org}}\right)^{m}\left(C_{O_2'\text{L}}\right)^{n} = A\,\mathrm{e}^{-E/(RT)}\left(C_{\text{org}}\right)^{m}\left(C_{O_2'\text{L}}\right)^{n}$$

(2.16)

where

k = rate constant

C_{org} = organic compound concentration in liquid

$C_{o2,L}$ = oxygen concentration in the liquid

A = pre-exponential factor

E = activation energy

R = universal gas constant

T = reaction temperature

m = reaction order relative to the organic reactant

n = reaction order relative to oxygen

Numerous kinetic studies have been performed on various compounds and wastes for WAO, these include phenol (Portela *et al.*, 1997, Kolaczkowski *et al.*, 1997, Joglekar *et al.*, 1991, Willms *et al.*, 1987a), glucose (Skaates *et al.*, 1981), acetic acid (Foussard *et al.*, 1989). The partial order with respect to the organic compound is in the range of 0.5 - 1, whereas the order with respect to oxygen is in the range of 0 - 0.5. In situations where oxygen is present in the bulk liquid in stoichiometric excess, many researchers have approximated equation 2.16 to

a pseudo first order model (it is assumed that since oxygen concentration is in excess, its partial order becomes 0), as shown in 2.17

$$-\frac{dC_{org}}{dt} = k\left(C_{\text{org}}\right) = A\, e^{-E/(RT)}\left(C_{\text{org}}\right) \qquad (2.17)$$

For complex wastestreams that contain a mixture of organic compounds, more detailed kinetic models have been used to explain the effects of the main reaction parameters on the rate of WAO. These models are usually based on the existence of two types of intermediate compounds present in complex solutions: (i) compounds and intermediates that are quickly oxidised to carbon dioxide, water and other final products and (ii) compounds and intermediates that are difficult to oxidise (refractory). Many reserachers have developed generalised kinetic models for complex wastewater streams using this concept (Debellefontaine *et al.*, 1996, Lixiong *et al.*, 1991). Lixiong *et al*., (1991) proposed the model shown in Figure 2.4, they determined that acetic acid was their refractory intermediate.

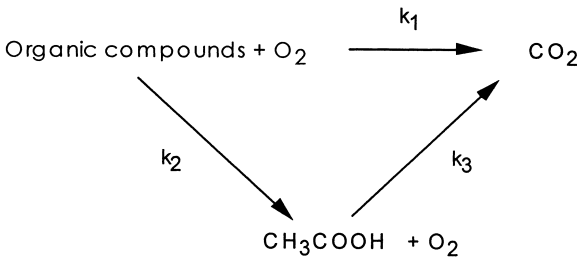

$$\frac{[O.C. + CH_3COOH]}{[O.C. + CH_3COOH]_0} = \frac{k_2}{k_1 + k_2 - k_3} e^{-k_3 t} + \frac{k_1 - k_3}{k_1 + k_2 - k_3} e^{-(k_1 + k_2)t}$$

Figure 2.4 Simplified kinetic model for wet air oxidation(Lixiong et al., 1991)

where k_1 is determined from the initial reaction rate, k_3 is determined from Foussard's rate equation for acetic acid oxidation (Foussard *et al.*, 1989), and k_2 is determined from the rate of acetic acid formation.

2.5 Previous WAO Research

WAO has been investigated for the oxidation of various types of organic compounds, not limited to carboxylic acids, alcohols, aldehydes, ketones, amides and sulfonates. In this section previous research conducted on the WAO of organic compounds is discussed.

2.5.1 Carboxylic Acids

Carboxylic acids, particularly low molecular weight carboxylic acids such as acetic acid, have been studied extensively (Day *et al.*, 1973, Debellefontaine *et al.*, 1996, Shende and Mahajani, 1997, Ichinose and Okuwaki, 1990, Bjerre and Sorensen, 1992), as they are usually the most refractory and as such provide a barrier to complete mineralisation(Foussard *et al.*, 1989).

Imamura *et al*., (1982) found that pH significantly affected the WAO of these compounds, with higher mineralisation (in terms of TOC conversion) at a lower pH. Furuya et al., (1985) found that structurally similar acids such as 1,3-benznedicarboxylic acid and 1,4-benznedicarboxylic acid are not mineralised to the same degree, WAO of 1,3-benznedicarboxylic acid resulted in 21% TOC conversion, while WAO of 1,4-benznedicarboxylic acid resulted in 3.2% TOC conversion under the same WAO conditions.

2.5.2 Phenol and other aromatic compounds

Phenol is found in the wastewater streams from petrochemical, coke, paper and plastics industries and therefore the global oxidation kinetics and effect of process operating conditions such as reaction temperature, pressure, oxygen partial pressure and reactant concentration been investigated by several researchers(Lin and Chuang, 1994, Joglekar *et al.*, 1991, Chang *et al.*, 1995, Portela *et al.*, 1997, Kolaczkowski *et al.*, 1997). The oxidation of phenol was found to be strongly influenced by reaction temperature and oxygen partial

pressure. The TOC and COD conversions of phenol and other aromatic compounds are higher than those for carboxylic acids, and complete mineralisation would be achieved if refractory carboxylic acids (such as acetic acid) were not formed as intermediates. Imamura(1999) achieved 88% TOC conversion of phenol after 2 hours reaction time, at 220 ºC and oxygen partial pressure of 3 MPa but achieved 8% and 15% TOC conversion for succinic and propionic acid at the same reaction conditions.

Kolaczkowski *et al*.,(1997) investigated the factors that may influence the global kinetics of phenol oxidation. According to their findings, the solution pH had an influence on the oxidation of phenol, at pH less than 2 and 7-10, no oxidation of phenol occurred at 200ºC and total pressure of 3 MPa, whereas at pH 2-7 and greater than 10, phenol oxidation occurred. This was attributed to changing oxygen solubility with pH and the effect of pH on the reactions necessary for the formation of key free-radical species.

Portela *et al*.,(1997) studied the effect of temperature and pressure on the oxidation of phenol with a stoichiometric oxygen excess to obtain kinetic data. They found the influence of temperature was more pronounced than pressure on phenol and COD conversion. Induction times were seen for phenol and COD conversion, which represent the time needed for free-radical species to reach a critical concentration. The induction times shortened significantly as temperature increased.

Other compounds investigated include 1,2-benzenediol and cyclohexanol (Furuya *et al.*, 1985), 2,4-dimethylphenol (Dietrich *et al.*, 1985), p-chlorophenol(Qin *et al.*, 2001), 2-chlorophenol(Chang *et al.*, 1995, Wilhelmi and Knopp, 1979), o-cresol(Imamura, 1999), cellulose(Robert *et al.*, 2002) and glucose(Sonnen *et al.*, 1997)

2.5.3 Nitrogen containing compounds

Some nitrogen containing compounds are produced naturally like amine acids, proteins or humic substances; ammonia and urea are also produced by human metabolism. However majority of nitrogen containing compounds originate from industrial activity and in particular from chemical, petrochemical and pharmaceutical industries. Sewage treatment units and agriculture are also responsible for the presence of a large range of nitrogenous compounds in the environment (Kiwi *et al.*, 1994). One such compound is aniline and its derivatives, which are used extensively in the manufacturing and application of dyes in the textile industry. It is estimated that up to 15% of the worlds production of dyes are lost during their fabrication and use, this corresponds to a worldwide loss of 128 tonnes per day (Sarasa *et al.*, 1998). Table 2.1 summarises the toxicity of some nitrogenous compounds.

Products	Toxicity
Ammonia	350 mg/kg
Aniline	250 mg/kg
4-Nitrophenol	20 mg/kg
Phenylacetamide	800 mg/kg
Nitrobenzene	200 mg/kg
1,8-diazabicyclo[5.4.0]undec-7-ene	300 mg/kg

Table 2.1 Toxicity of nitrogenous compounds (LD50 oral), some data adapted from Oliviero *et al*., (2003) and Sigma Aldrich MSDS database

Ammonia is considered to be a particularly refractory nitrogen compound to oxidise and has been found to be a refractory intermediate of the WAO of nitrogen containing compounds (Oliviero *et al.*, 2003, Martin *et al.*, 2005, Cao *et al.*, 2003), a negative effect of ammonia is seen in the eutrophication of rivers (Fang *et al.*, 1993). In terms of reactivity ammonia is equivalent analogous for nitrogen containing compounds to acetic acid for organic compounds (i.e. phenol)(Pifer *et al.*, 1999). Biological processes can be used to treat industrial wastewater containing low amounts of ammonia (<80 mgL^{-1}). By the action of

Nitrosomona, 90% of initial ammonia can be converted into nitrites, these nitrites are then oxidised by *Nitrobacter* after 1 week and can then be biologically treated to give molecular nitrogen (Fang *et al.*, 1993). However, many industrial effluents polluted by ammonia are generally too concentrated to be treated by biological processes, therefore physical and chemical techniques are required, sometimes as a pretreatment step before biological oxidation.

Hao *et al*., (1993) studied the effect of temperature, oxygen partial pressure on the treatment of TNT manufacturing wastewater. They found that TOC conversion was primarily a function of temperature, and that at lower temperatures (240 ºC) there was an increase in the concentration of 1,3-dinitobenzene and acetic acid. In another study on the WAO of Nitrotoulenesulfonic acid, Hao and Phull (1993), achieved a TOC conversion of 95%, but indicated that some of the byproducts formed during WAO maybe more toxic than the original compound.

Thomsen (1998) examined the reaction products and mechanism of quinoline oxidation and found that a free radical reaction is responsible for transforming 99% of quinoline to other substances, with 30-50% of the quinoline being oxidised to CO_2 and H_2O depending on the initial concentration of quinoline. Fifteen intermediates were identified and quantified with nicotinic acid accounting for 35% of initial quinoline.

Mishra *et al*.; (1995) treated the wastewater from an acrylonitirile manufacturing plant with an initial acrylonitirile concentration of 1330 mgL^{-1} and COD concentration of 120,000 mgL^{-1}. They achieved 96% conversion of acrylonitirile after 4 hours reaction time and found that the oxygen partial pressure did not affect the rate of oxidation (between 0.69 and 1.38 MPa), they also modeled the oxidation rate using a pseudo first order rate equation.

Owing to the success of WAO research, various large scale industrial WAO were built and are currently in use. These are the Wetox process, that combines a series of agitated tank

reactors, the Vertech process that uses gravity to develop high pressures in a deep shaft reactor, the Kenox process which incorporates novel elements like static mixing and ultrasound energy and the Oxyjet process in which the liquid is fed in the reactor in form of droplets to eliminate oxygen transfer limitations (Luck, 1996, Kolaczkowski *et al.*, 1999).

2.6 Catalytic Wet Air Oxidation

The incorporation of a catalyst has also been considered in combination with all types of advanced oxidation processes, with the aim to reduce the operating temperature and pressure, and treat pollutants that cannot be destroyed during various non-catalytic liquid phase oxidation processes and WAO is no exception.

Homogeneous catalysts, such as copper ions in solution were very effective in oxidising several organics when air was used as oxidant (Imamura, 1999). Homogeneous catalysis simplifies reactor operation as it is in the liquid phase, resulting in mass transfer and reaction kinetics similar to the non-catalytic system. The use of a homogeneous catalyst has the disadvantage of requiring an additional catalyst removal step from the treated effluent, because these metal ions become pollutants (Luck, 1999). In the Ciba-Geigy process, where cupric salt is used as a homogeneous catalyst, it is recovered as cupric sulphide and then recycled back to the reactor (Luck, 1996).

Heterogeneous catalysts, do not need any extra separation step and are thus more attractive. Solid catalysts, mostly noble metals and base metal oxides, have been tested in combination with all types of oxidants. The use of heterogeneous catalysts has shown promising results on a lab scale, but industrial applications have been hindered for the following reasons: the required engineering effort to model and design three phase reactors (Matatov-Meytal and Sheintuch, 1998), catalyst longevity and performance (Stuber *et al.*, 2005), the time and cost required for catalyst development (Imamura, 1999). It has been demonstrated that catalyst deactivation can take place because of the active phase leaching (Fortuny *et al*., 1998), the formation of carbonaceous deposits (Hamoudi *et al.*, 1998) and, to a less extent, the catalyst sintering (Ding *et al.*, 1996).

Dudukovic (1999), in a review of the current trends in catalytic reactor engineering, outlines that simultaneous development of both chemistry and engineering aspects is necessary for any emerging process. A better understanding of the reactor behaviour, would enable to improve the reactor operation and modeling tools, thus eventually minimising the operation costs and, more important, the scale up risks.

In a recent review of CWAO, Larachi (2005) described the characteristics of most common reactor configurations for CWAO namely, Trickle bed, Packed bubble column, Three phase fluidised bed and slurry bubble column. WAO would be further more appealing if a heterogeneous catalyst was successfully incorporated into the process.

Despite its success on a laboratory scale, catalytic WAO has yet not found the industrial recognition met by WAO. The main reason, as pointed out earlier, is that an additional step is required for the removal of homogeneous catalysts, while the heterogeneous catalysts have to be active for long periods.

Process	Waste type	Plant Number	Reactor Type	Temperature (°C)	Pressure (MPa)	Catalyst
Zimpro	sewage sludge and industrial	250	Bubble column	280-325	20	none
Vertech	sewage sludge	1	deep shaft	<280	10	none
Wetox	nk	nk	stirred tanks	200-250	4	none
Oxyjet	ns	nk	tubular jet	<300	nk	none
Ciba-Geigy	industrial	3	-	300	nk	Cu^{2+}
LOPROX	industrial	1	bubble column	<200	5-20	Fe^{2+}
Osaka gas	sewage sludge coke oven	nk	slurry bubble column	250	7	ZrO_2 or TiO_2 with noble or base metals
Nippon Shokubai	nk	>10	monolith	160-270	1-8	TiO_2, lanthanide oxide and noble or base metal

nk: not known

Table 2.2 Industrial processes of WAO and CWAO, compiled from Luck, 1999 and Kolaczkowski *et al*.; 1999

Table 2.2 shows a summary of industrial processes of WAO and CWAO, it indicates that the industrial applications of CWAO operate at temperatures and pressures not significantly lower than those for WAO. This contradicts laboratory scale research that have shown the superior efficiency of CWAO at lower temperatures and pressures (Mishra *et al.*, 1995), yielding greater mineralisation and more biodegradable oxidation products (Donlagic and Levec, 1998). Given the potential of CWAO, extensive research has been made to develop active and stable catalysts for the process, improve reactor design and better understand and describe reaction kinetics.

2.7 Catalysts and Catalyst Support

As described earlier, heterogeneous catalysts are favoured over homogenous catalysts, therefore heterogeneous catalyst will be the focus of this section. Heterogeneous catalysts that have been employed in CWAO can be divided into two main groups, i.e. metal oxides (including mixtures of them) and supported noble metals(Matatov-Meytal and Sheintuch, 1998, Imamura, 1999). Active carbon, without any deposited active phase, has also exhibited catalytic activity (Tukac and Hanika, 1998, Eftaxias *et al.*, 2006).

2.7.1 Noble Metals

Noble metals have been very effective in the treatment of different pollutants such as phenols (Qin *et al.*, 2001, Hamoudi *et al.*, 1998, Oliviero *et al.*, 2000), carboxylic acids, including refractory acetic acid (Gallezot *et al.*, 1996, Barbier *et al.*, 1998, Gomes *et al.*, 2005), ammonia (Oliviero *et al.*, 2003, Ukropec *et al.*, 1999) and kraft effluents [57, 58, 59, 60, 61]. Pd, Pt and Ru have received most attention although Ir or Rh have also been tested (Duprez *et al.*, 1996, Barbier *et al.*, 1998) . Table 2.3 summarises the applications of noble metal catalysts in the CWAO.

They are numerous noble metal catalyst available but for different pollutants different metals may present optimum results. For example, in the case of acetic acid oxidation, Barbier *et al*.;(1998) state that the catalytic activity decreases in the order Ru > Ir > Pd, while for the oxidation of p-chlorophenol, Qin *et al*.;(2001) found out that catalytic activity decreases in a reverse order Pt > Pd > Ru. Noble metals were ranked according to their TOC conversion of polyethylene glycol at 200 ºC by Imamura *et al*., (1988). They found the activity of noble metals to be Ru = Rh = Pt > Ir.

Occasionally, synergistic effects in bimetallic catalysts improve catalyst activity and/or selectivity (Luck, 1999). Better N_2 selectivity was achieved during ammonia oxidation when a mixed Ru−P d/CeO_2 catalyst was used (Barbier *et al.*, 2002).

Noble metal	Support	Organic compound	Temperature (°C)	Pressure (MPa)	Reference
Ru, Ir, Pd, Ag	CeO_2, TiO_2, ZrO_2	acetic acid	200	2	Barbier *et al.*, 1998
Pt	Y-Al_2O_3	maleic acid	>120	>0.4	Rivas *et al.*, 1999
Pt	C	carboxylic acids	200	0.69	Gomes *et al.*; 2000
Ru	C, CeO_2/C	phenol	160	2	Oliviero *et al.*; 2000
Pt	Y-Al_2O_3	phenol	>155	2	Kim *et al.*; 2002
Pd	C	ammonia	280	2	Takayama *et al.*; 1999
Ru, Ir, Pd, Pt	TiO_2, CeO_2, C	ammonia	>150	1.5	Ukropec *et al.*, 1999
Pd-Pt-Ce	Y-Al_2O_3	kraft effluent	>130	>1.5	Zhang and Chuang, 1998
Ru, Ir, Pd, Pt	CeO_2	polyethylene glycol	200	3	Imamura *et al.*, 1988

Table 2.3 Application of noble metal catalysts in CWAO

Promoters are occasionally used with noble metal catalysts. An Ag promoted Pt over MnO_2/ CeO_2 catalyst enhanced the CWAO of phenol when compared to the non promoted catalyst (Hamoudi *et al.*, 2000).

The noble metal support also influences catalyst performance. Metal oxides, like alumina, ceria, titania and zirconia, as well as active carbon or high specific area graphite have been mainly studied. In the treatment of Kraft bleach effluents increasing the support surface area increased catalyst activity (Pintar *et al.*, 2001). The dispersion of the active phase was also shown to be important for the CWAO of phenol, as demonstrated by a comparative study of two Pt/Al_2O_3 catalysts prepared by different methods(Kim and Ihm, 2002). The deposition of noble metals on hydrophobic supports, i.e. certain active carbons, or styrene

divinyl benzene co-polymer, was very effective for the destruction of volatile pollutants such as ammonia (Takayama *et al.*, 1999).

2.7.2 Metal Oxides

The other class of catalysts used in CWAO is metal oxides. Copper oxide, alone or combined with other oxides, has received special attention in the CWAO of aqueous effluents (Sadana and Katzer, 1974, Baldi *et al.*, 1974). Phenol was successfully oxidised by a commercial catalyst "Harshaw Cu0803 T1/8", comprising of 10% copper oxide supported over alumina (Sadana and Katzer, 1974, Ohta *et al.*, 1980). Baldi *et al.*;(1974) and Goto and Smith(1975) tested a commercial CuO/ZnO catalyst to oxidise Formic acid while Levec *et al.*; (1976) used a catalyst combining Cu, Mn and La oxides supported on Al_2O_3 and ZnO to oxidise acetic acid. In the early nineties, other commercial catalysts comprising CuO, ZnO and $\gamma - Al_2O_3$ (Pintar and Levec, 1992) or CoO were successfully employed by Pintar and Levec to oxidise phenol and substituted phenols. Table 2.4 summarises some of the applications of metal oxide in CWAO

Metal oxide	Support	Organic compound	Temperature (°C)	Pressure (MPa)	Reference
Cu/Cr oxides	-	phenol	>127	0.32	Santos *et al.*; 2001
CuO	Y-Al_2O_3	phenol	140	0.9	Miro *et al.*; 1999
CuO/ZnO/CoO	cement	phenol	>130	7	Pintar *et a*l.; 1997
MnO_2, Co_2O_3	-	p-chlorophenol	>170	>1.3	Chang et al.; 1995
Fe_2O_3	-	acetic acid	>252	>6.7	Levec and Smith, 1976
MnO/CeO	-	ammonia	263	1	Imamura, 1999
MnO_2, CeO_2	-	alcohol distillery waste	>180	>0.5	Belkacemi et al.; 2000

Table 2.4 Application of metal oxide catalysts in CWAO

Ceria oxide, manganese-ceria mixed oxides and promoted ceria catalysts have also exhibited high activities. In the eighties, Imamura *et al*., (1982) developed Mn/Ce oxide catalysts for the CWAO of ammonia, which proved to be very effective for other organic compounds. Hamoudi et al.; (1999) found that that CeO/MnO catalysts can effectively oxidise phenol and 4-chloroguaiacol (Hamoudi *et al.*, 2001). Later, Chen *et al*.; 2001 showed that a Mn/Ce ratio of 6/4 was the most active for phenol oxidation. The performance of the catalyst was further improved by the incorporation of potassium(Hussain *et al.*, 2001a), although this modification mainly affected catalyst stability.

Metal oxide catalysts not based on copper or cerium have been tested in fewer cases. The use of ferric oxide gave good results for the oxidation of acetic acid under severe conditions (T > 250 ºC, P > 6.7 MPa), while the copper based catalysts suffered severe deactivation (Levec and smith, 1994). Nickel oxide catalysts have also been used to remove effectively phenol at atmospheric pressure conditions (Christoskova and Stoyanova, 2001).

2.7.3 Catalyst support

In heterogenous catalysis, the support material plays a crucial role in the performance of the catalyst. It increases the surface area of the metal catlayst (oxide or noble) by providing a matrix which disperses them as small particles, it also improves hydrolytic and chemical stability, while inhibiting sintering (Matatov-Meytal and Sheintuch, 1998).

The activity of metal catalyst can also be improved dependent on the support used, as shown by Imamura *et al*., (1988). They found in their study of polyethylene glycol oxidation by CWAO using a Ru catalyst with various supports that the TOC conversion decreased in the following order CeO_2 > ϒ-alumina > NaY zeolite > ZrO_2 > TiO_2.

2.7.4 Catalyst stability

Currently, the main drawback of CWAO, preventing it from a broad industrial application, is due to catalyst deactivation, which occurs mainly due to active phase leaching, support sintering or formation of carbonaceous deposits, during the oxidation process. The catalysts most prone to leaching of their active phase are mixed oxides catalysts. Pintar and Levec(1994) investigated the CWAO of nitrophenol and chlorophenol over a catalyst comprising CuO, ZnO and CoO in a liquid full fixed bed reactor and detected metal ions from all the above oxides in the solution. Similar trends were also observed for other copper catalysts like $CuO/\gamma{-}Al_2O_3$ (Fortuny *et al*., 1995, Alejandre *et al*., 1998), bimetallic copper containing catalysts, copper on activated carbon (Alvarez *et al*., 2002) and zeolites Wu *et al*., (2001). Under continuous operation, this decline leads to a continuous activity loss. Therefore, the development of more stable supported metal catalysts can be pointed out as a critical issue in CWAO.

Metal oxide catalysts with promising behaviour have been prepared. Alejandre *et al*.; (1999) developed mixed copper, nickel and aluminium oxide catalysts, which performed without any activity loss for 15 days on stream in a Trickle Bed Reactor. Hocevar et al.; (2000), prepared different $CuO - CeO_2$ catalysts in which copper leaching was significantly reduced. For mixed Ce/Mn oxide catalysts, it was found that measurable amounts of Mn could dissolve (Duprez *et al.*, 1996). Active phase leaching was also reported for noble metal catalysts from during the CWAO of pulp mill effluents over Pd and Pt catalysts (Zhang and Chuang, 1998). Ceramic and cement supports have been investigated as possible alternatives to typical metal oxide based supports. Improved chemical stability, hydrolytic stability and catalyst lifes time were reported (Matatov-Meytal and Sheintuch, 1998). The use of ceramics is touted as feasible solution due to it's extensive use in other high temperature applications which utilise temperatures above 500ºC.

Catalyst deactivation caused by the formation of carbonaceous deposit on the catalyst surface has been observed for several types of catalysts. Ceria oxide based catalysts have been found to suffer from this type of catalyst deactivation during tests carried out in agitated tank reactors(Hamoudi *et al.*, 1998). Further work demonstrated that carbonaceous deposits could be minimised by promoting the catalyst with Pt and Ag (Hamoudi *et al.*, 2000). More recently, it was found that less expensive potassium can also retard such formation (Hussain *et al.*, 2001b). The carbonaceous deposit has to be related both to the nature of the organic pollutant and the reactor type used. The enhanced formation of such deposits has been confirmed by several authors in slurry reactors (Pintar and Levec, 1992), with a characteristic high liquid to catalyst ratio, that promotes the homogeneous polymerisation reactions. Consequently, comparative studies have shown that the extent of these parallel side reactions in the liquid phase are significantly reduced in Trickle Bed Reactors (Alejandre *et al*.; 2001).

2.8 Reaction Mechanisms and Rate Equations in CWAO

In understanding the CWAO process, the knowledge of the reaction kinetics is fundamental. This knowledge, apart from giving a fundamental insight to CWAO can lead to significant improvements in the operation and design of CWAO units.

Catalysts are free radical initiators and two possible methods of radical formation are suggested namely: the catalyst reacts with the molecules directly decomposing them into radicals or the the catalyst accelerates the decomposition into radicals, with the hydroperoxides either being present in the system or being slowly formed by the earlier step (Matatov-Meytal and Sheintuch, 1998).

2.8.1 Mechanism of phenol oxidation

The pathways and mechanism of CWAO reactions have been studied in detail only for pure compounds. Phenol and substituted phenols are commonly present in industrial effluents that are refractory to conventional biotreatment. Also phenol has been shown to be more refractory than most of the substituted phenols, as discussed in the WAO section, CWAO of phenol has been conducted either in slurry, rotating basket or fixed bed reactor.(Hamoudi *et al.*, 2000, Pintar and Levec, 1994, Sadana and Katzer, 1974, Ohta *et al.*, 1980, Fortuny *et al.*, 1999, Santos *et al.*, 2001)

These studies demonstrated that phenol could be readily oxidised although its oxidation is followed by the formation of numerous organic intermediates. It is also well known that phenol oxidation occurs through a free radical chain mechanism (Sadana and Katzer, 1974, Rivas *et al.*, 1998, Pintar and Levec, 1994), that can take place in the homogeneous phase or on the catalyst surface. A simple but accepted mechanism for the CWAO of phenol has been proposed by Pintar and Levec, (1992) and shown below:

$$RH\text{-}OH + cat \rightarrow R^{\bullet}H{=}O + {}^{\bullet}H\text{-}cat \qquad (2.18)$$

$$R^{\bullet}H{=}O + O_2 \rightarrow RHO\text{-}OO^{\bullet} \qquad (2.19)$$

$$RHO\text{-}OO^{\bullet} + RH\text{-}OH \rightarrow ROH\text{-}OOH + R^{\bullet}H{=}O \qquad (2.20)$$

In this mechanism RH-OH corresponds to phenol, $R^{\bullet}H{=}O$ corresponds to the phenoxy radical and $RHO\text{-}OO^{\bullet}$ corresponds to the peroxy radical.

Studies into catalytic aqueous phenol oxidation have shown similar intermediate distribution in the presence of a solid catalyst as that described in detail by Devlin and Harris (1984) for the WAO of phenol. Ohta *et al.*; (1980) reported the formation of catechol,

hydroquinone, maleic acid and oxalic acid, on a copper oxide catalyst. Fortuny et al.; (1999) using the same catalyst, identified in addition benzoquinone, malonic acid, acetic acid and formic acid. These authors calculated that the detected compounds account for more than 95% of the experimentally measured COD.

Pintar and Levec (1992) detected dihydric phenols and small quantities of benzoquinone, using a ZnO, CuO and $\gamma - Al_2O_3$ catalyst in a slurry reactor. Neither maleic, nor oxalic acid were detected, but acetic acid was present in considerable quantities. For this reactor it was found that phenol undergoes not only oxidation reaction but also polymerisation reactions in the homogenous liquid phase. In a related study using a liquid differential packed bed reactor they identified additionally 1,4-dioxo-2-butene and maleic acid (Pintar and Levec, 1994), although no polymers were detected on the catalyst surface. Sadana and Katzer (1974) found the presence of an induction period, indicating the poor generation of radicals during the CWAO of phenol, this was followed by a fast reaction period.

Oliviero *et al*.; (2000) using Ru supported on either CeO_2 or C also detected several of the compounds encountered by Devlin and Harris (1984). They divided the detected compounds into C6: (benzoquinone and small amounts of dihydric phenols), C4: (maleic, succinic and small amounts of fumaric acid), C3: (acrylic acid, 3-hydroxy as well as 3-oxo propionic acid) and refractory acetic acid.

Santos *et al*.; (2000), studied separately the oxidation of the main aromatic and carboxylic acid compounds mentioned above and proposed a scheme that distinguishes between the oxidation pathway of catechol, with that of hydroquinone. These authors concluded that during catechol oxidation alone only oxalic acid is formed, while hydroquinone undergoes a complex scheme that agrees with the Devlin and Harris mechanism.

2.8.2 Pathways of carboxylic acids oxidation

In the case of carboxylic acids both the oxidative degradation and the thermal decomposition, via decarbxylation roots, should take place, explaining the different intermediates observed. For example, during the maleic acid thermal decomposition no acetic acid is detected, the main product being formic acid. In an oxidative environment acetic acid is formed in quantities half of those of formic acid (Shende and Mahajani, 1997). The use of Pt/C and Pt/$\gamma - Al_2O_3$ catalysts clearly affects reaction pathways of maleic acid oxidation, because no acetic acid formation is reported for the when using these catalysts (Lee and Kim, 2000).

2.9 Reaction kinetics

In evaluating rate constants and ultimately rate expressions for CWAO, two expressions are generally used. These are a power law expression (as discussed in the WAO section) and a Langmuir-Hinshelwood expression.

2.9.1 Power law kinetics

Power law expressions have also been considered for CWAO kinetics, and are similar to that shown in equation 2.16. The CWAO of phenol usually yields a first order dependence on phenol (Sadana and Kratzer, 1974, Fortuny *et al*.; 1995), although Ohta *et al*.; (1980) report a value of 0.44. For formic acid, Baldi *et al*.; (1974) also obtained a first order dependence, as well as Klinghoffer *et al*.; (1998) in the case of acetic acid oxidation over Pt/$\gamma - Al_2O_3$. On the other hand, Gallezot *et al*.; (1996) and Beziat et al.; (1999) claimed a zero order for acetic acid and succinic acid using Ru/C and Ru/TiO_2 catalysts respectively. They justified these results by stating that these compounds are strongly adsorbed on the ruthenium surface. Furthermore, a −0.5 acetic acid order was obtained on a Ru/CeO_2 and it was argued

that on this catalyst acetic acid adsorbs even stronger (Barbier *et al.*, 1998). These later findings suggest that the substrate adsorption on the catalyst surface can significantly affect the resulting reaction rate, making evident that in some CWAO cases L-H expressions should be implemented.

For most of the above studies the oxygen order lies within 0.4 and 0.65, i.e. close to 0.5 (Gallezot *et al*., 1997, Barbier *et al*., 1998, Fortuny *et al*., 1995). Nevertheless, Baldi *et al*., (1974) obtained first order oxygen dependence for the CWAO of formic acid in a liquid full fixed bed reactor operating in the kinetic controlled regime. The reported activation energies may even vary for the same compound and catalyst. For phenol, most authors agree in values between 85 and 105 kJ/mol (Chang *et al*., 1996, Ohta *et al*., 1980, Fortuny *et al*., 1995). Conversely, Sadana *et al*., (1974) reported a much higher value of 176 kJ/mol, for the steady state period. The values reported for carboxylic acids are between 81 and 155 kJ/mol (Gallezot *et al.*, 1996, Barbier *et al.*, 1998, Baldi *et al.*, 1974) most values being higher than those for phenol oxidation, a similar trend was also found in WAO of these compounds.

2.9.2 Langmuir-Hinshelwood kinetics

In describing heterogeneous catalytic reactions, Langmuir-Hinshelwood expressions have been proven useful. Surprisingly, they have found less application to CWAO kinetics. A wide scenario of L-H expressions can be developed, although the most popular used in CWAO accounts for the competitive adsorption of the organics on the same active site, omitting the existing adsorption of oxygen. The resulting expression is then given by Eq 2.22 (Eftaxias *et al.*, 2001):

$$r_i = A\exp\left(-E_a / RT\right)\frac{K_0\left[C_{org}\right]^m\left[C_{O_2}\right]^n \exp(-\Delta H_{org} / RT)}{1+\sum K_{0_j}C_j \exp(-\Delta H_j / RT)} \qquad (2.22)$$

where

ΔH - heat of formation of a compound

K_0 - adsorption pre-exponential factor

j - refers to a compound formed

Several studies have considered that only the initial reactant, but not the products, adsorb on the catalysts surface. Nevertheless, it has been demonstrated that phenol adsorption on AC can be affected by the presence of dihydric phenols or benzoquinone, in the solution (Polaert *et al*., 2000)

With this type of equation, first order dependence on the organic compound has been obtained for all the organic compounds tested, i.e. acetic acid (Levec and Smith, 1976), succinic acid, phenol (Hamoudi *et al*., 1999, Alvarez *et al*., 2002) and substituted phenols (Pintar and Levec, 1994). The activation energy values of the range 78 to 90 kJ/mol, although high values between 140 and 170 kJ/mol have also been reported, without any specific trend depending on the compound (Eftaxias *et al.*, 2001). The corresponding heats of adsorption are in the range of, -18 to -109 kJ/mol, although a value close to zero has also been reported for acetic acid oxidation over ferric oxide (Levec and Smith, 1976). Among these studies Beziat *et al*., (1999) took into account competitive adsorption of the succinic acid oxidation products, while Hamoudi *et al*., (1999) took into account adsorption of oxidation products (included as a lump), as well as carbonaceous deposits.

2.10 Supercritical Water Oxidation

The unique physical properties of High Temperature Water (described in section 2.1) above its critical point is driving force behind the past and continuing research into Supercritical Water Oxidation (SCWO). Above this critical point (374 ºC and 22.1 MPa), the boundary layers disappear and it becomes a mono-phasic, homogeneous fluid, it also becomes an excellent solvent for liquids and gases (Gopalan and Savage, 1994, Savage *et al.*, 1984, Thomason and Modell, 1984). The physical properties are tunable by manipulation of the system temperature and pressure (Bermejo and Cocero, 2006).

In a typical SCWO process, the organic waste is dissolved in an aqueous solution and then contacted with an oxidant at system temperature of 400 - 650 ºC and pressures above 22.1 MPa (Modell *et al.*, 1992).

SCWO has been applied for the treatment of various toxic and non-biodegradable wastewaters, i.e. pharmaceutical, chemical and petrochemical. In most circumstances, the complete mineralisation of such wastes occurs via rapid oxidation (≤ 5 minutes residence time) to low molecular weight organic compounds and then benign compounds such as carbon dioxide, nitrogen and water (Lee *et al.*, 1997, Boock *et al.*, 1993). If the original waste contains nitrogen atoms, then virtually no NO_x is detected in the effluent stream, which is ideal from an environmental view point.

Hydrolysis is a side reaction that occurs during SCWO. This occurs when water molecules interact with organic molecules resulting in bond rupturing (Akiya and Savage, 2002). Hydrolysis has been investigated by various authors as a potential route for the oxidation and partial oxidation of organic compounds (Boock *et al.*, 1993, Lee and Gloyna, 1992, Holgate *et al.*, 1995, Meyer *et al.*, 1995, Kramer *et al.*, 1999) and they have shown that hydrolysis can be a medium for the recovery of valuable chemical compounds from complex polymers. For example, waste plastics and resins have been hydrolysed to phenol, cresol

(Suzuki *et al.*, 1999) and oils (Su *et al.*, 2004, Sugano *et al.*, 2009). This shows that supercritical water oxidation is a flexible process controlled by its operating conditions to attain the required level of mineralisation or degradation.

A basic SCWO process consists of 3 main steps: namely (i) feed preparation and pressurisation (ii) reaction (iii) cooling and depressurisation.

The advantages of SCWO are (i) a mono-phase reaction medium eliminates the phase boundary mass transfer limitations present in other advanced oxidation processes, such as WAO. (ii) shortened reactor residence times due to high temperatures enables a high throughput of waste compounds. (iii) benign and low molecular weight compounds are produced as products, and are less toxic than the original waste. The production of NO_x is not prevalent, due to the low temperatures used (Cocero, 2001). (iv) more recently, there has been a drive to recover energy used to preheat reactants and maintain reactor conditions, this has resulted in process integration on scale-up (Cocero, 2002) and making it economically favourable (Griffith and Raymond, 2002). Table 2.5 shows some of the commercial SCWO plants that have been built.

Operating equipment in the supercritical range is not without its challenges; corrosion and salt deposition are seen as the main challenges that need to be solved for SCWO to be widely accepted as a preferential waste treatment solution to incineration. This can be overcome using specialist and innovative materials of construction to overcome the harsh conditions responsible for corrosion, and the development of novel reactor designs (Kritzer and Dinjus, 2001).

2.10.1 The SCWO process

The 3 main steps of SCWO are described here, Figure 2.5 shows a basic SCWO process diagram.

Feed preparation and pressurisation

The feed into a SCWO reactor typically consists of the oxidant and wastewater stream but in some special cases, especially on an industrial scale a secondary fuel is added (The secondary fuel reduces the energy required to attain the reaction temperature, they are usually low molecular weight alcohols such isopropanol) (Cocero *et al.*, 2000a). According to Phenix *et al*., (2002) the process efficiency is independent of oxidant choice (air, oxygen or hydrogen peroxide) on a lab scale. However on an industrial scale, the choice of oxidant is determined by the process economics, as oxygen compression costs are considerably lower than air, and the commercial application of hydrogen peroxide is restricted because of its high cost and related safety concerns (Bermejo and Cocero, 2006).

Reaction

Once the oxidant and organic waste are mixed, they react exothermally producing extra heat. The operating variables are (i) ***reaction temperature*** – the conversion of organics increases with reaction temperature, this also reduces the residence time required for oxidation (Segond *et al.*, 2002). (ii) ***oxidant concentration*** – various studies have conducted into the optimal oxidant concentration and it is suggested that 1-1.2 of the required stoichiometric is necessary for optimal oxidation (Cocero *et al.*, 2000b) (iii) ***residence time*** – the residence time varies dependent on the reaction temperature and the reactant flow rate (iv) ***reaction pressure*** – the conversion improvement is negligible above the critical point of water.

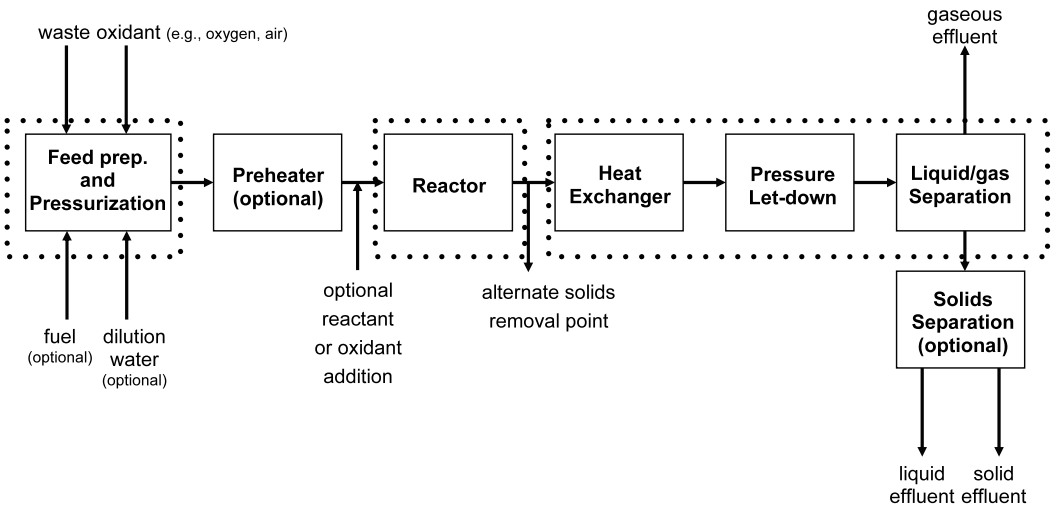

Figure 2.5 A Basic SCWO process adapted from Marrone *et al*., 2004 (*the dotted sections represent the 3 steps discussed in this section*)

Cooling and depressurisation

The exit stream condition from a SCWO reactor is typically > 400 ºC and > 23 MPa. This stream is cooled, depressurised to ambient conditions and then separated into a liquid and gas phase. On a pilot plant or industrial scale, where energy recovery is integrated into the design, excess heat from the exit stream is used to partly heat the feed using heat exchangers (Kritzer and Dinjus, 2001, Bermejo *et al.*, 2004). Cocero *et al*., (2002) performed an energy analysis of the SCWO of different wastes and found that the exit streams from certain feeds can generate an energy content sufficient to preheat the feed from ambient to 400 ºC, and generate the electric power equivalent to that utilised by a high pressure pump and air compressor. A SCWO plant for sludge treatment in the USA is able to harness this excess energy to heat water, which they sell on to a nearby clothing factory(Griffith and Raymond, 2002).

Company	Commercial plant	Country	Application	Related Dates
MODAR	Nittestsu Semicondutor	Japan	Semiconductor manufacture wastes	Built **1998**. No longer in operation.
MODEC	Several companies	Germany	Pharmaceutical wastes, pulp and paper mill waste, sewage sludge	Operation stopped **1996**
General Atomics	US Army Newport Chemical Depot, Newport, IN	USA	Bulk VX nerve agent hydrolysate; Other feeds processed in smaller-scale systems: chemical agent, explosives, and dunnage (US Army), shipboard wastes (US Navy), rocket propellant (US Air Force)	Commisioned **1999**. 1/10 scale plant tested in **2000 - 2001**
Foster-Wheeler	US Army, Blue Grass Army Depot, KY	USA	Chemical agents and aging munitions	Operated from **2009**
Chematur (Aqua Cat®)	Johnson Matthey, Brimsdown	UK	Spent catalyst (recover platinum group metals and destroy organic contaminants)	Operated from **2004**
SRI International	Mitsubishi Heavy Industries	Japan	PCBs, chlorinated wastes	Operated from **2005**
Chematur (Aqua Citrox®)	Krlskoga	Sweden	Nitrogen containing wastes	Operated from **1998**
Hydro Processing	Harlingen Wastewater Treatment Plant No. 2, Harlingen, TX	USA	Mixed municipal and industrial wastewater sludge	Operated from **2000**

Table 2.5 Commercial SCWO plants adapted from Marrone *et al*., 2004

2.10.2 Overcoming SCWO challenges

As stated earlier there are two main challenges facing SCWO, these have resulted in the plant closure of some SCWO plants. Various approaches have been taken to overcome them and will be discussed here.

Construction materials

To address the challenge of corrosion, different materials have been investigated for the construction of SCWO equipment.

Stainless steel is the widely used for the construction of reactors, and is adequate for temperatures between 300 and 500ºC. The presence of heteroatoms in the waste stream enhances the corrosion rate of stainless steels(Kritzer, 2004). Nickel and chromium based alloys have been found to reduce the corrosion at alkaline and acidic conditions respectively. Titanium alloys have a high resistance to strong oxidative environments and have been used to coat other materials, thereby preventing corrosion (Bermejo and Cocero, 2005).

Reactor Design

The reactor design has a strong influence on the performance of the reactor, corrosion and salt formation. Reactor designs broadly fall into 4 groups (Schmieder and Abeln, 1999), namely tubular, transpiring wall, film-cooled and tank reactor. Tubular reactors are used mainly due to their simplicity, especially at lab scale, where kinetic parameters are determined (Benjamin and Savage, 2004). Transpiring wall reactors consist of a reaction chamber surrounded by a wall through which clean water circulates preventing salt deposition on the walls(Bermejo *et al.*, 2005). Tank reactors are preferred when salt formation is present, as it has two reaction zones, the upper reaction zone and lower cool zone, where the salts are formed and can be removed(Marrone *et al*., 2004).

2.10.3 Kinetics and Reaction Mechanism

Similar to WAO and CWAO, a free radical mechanism is accepted for the SCWO of organic compounds. Gopalan and Savage (1994), suggested the following free radical reaction scheme shown below for the oxidation of phenol in SCWO, using oxygen as the oxidant.

Initiation

$$C_6H_5OH + O_2 \rightarrow C_6H_5O^{\bullet} + HO_2^{\bullet} \quad (2.23)$$

$$H_2O + O_2 \rightarrow HO_2^{\bullet} + OH^{\bullet} \quad (2.24)$$

The initial radicals formed are identical to those for WAO, in addition they found that reaction 2.24 was the most likely initiation step. The radicals produced then react with phenol to produce the phenoxy radical (reaction 2.25 and 2.28), reaction 2.26 and 2.27 show the buildup of OH radicals, which are highly reactive.

Propagation

$$C_6H_5OH + HO_2^{\bullet} \rightarrow C_6H_5O^{\bullet} + H_2O_2 \quad (2.25)$$

$$HO_2^{\bullet} + HO_2^{\bullet} \rightarrow \ H_2O_2 + OH^{\bullet} \quad (2.26)$$

$$H_2O_2 \rightarrow 2OH^{\bullet} \quad (2.27)$$

$$C_6H_5OH + OH^{\bullet} \rightarrow C_6H_5O^{\bullet} + H_2O \quad (2.28)$$

As hydrogen peroxide is a powerful source of these highly reactive hydroxyl radicals, it is suggested by Emanuel *et al*., (1984) that it promotes oxidation because reaction 2.27 becomes an initiation reaction.

SCWO Kinetics

Power law

Similar to WAO, Most SCWO reaction rates are derived from the global rate law

$$-\frac{dC_{org}}{dt} = k[\text{Organic}]^a[\text{O}_2]^b[\text{H}_2\text{O}]^c = A\,\text{e}^{-E/(RT)}[\text{Organic}]^a[\text{O}_2]^b[\text{H}_2\text{O}]^c \qquad (2.29)$$

where

[Organic] = concentration of organic

[O_2] = concentration of oxidant

[H_2O] = concentration of water

a = reaction order relative to the organic

b = reaction order relative to the oxidant

c = reaction order relative to water

Numerous kinetic studies have been performed on various compounds, namely specific commercial wastes, such as, Ship wastes (Lopez Bernal *et al.*, 1999), Olive oil mill waste water (Rivas *et al.*, 2001), Cutting oil wastes (Portela *et al.*, 2001a). and then single model compounds, such as Phenol(Portela *et al.*, 2001b, Gopalan and Savage, 1995), Ammonia(Webley *et al.*, 1991, Segond *et al.*, 2002), Methanol(Cansell *et al.*, 1998), Pyridine (Crain *et al.*, 1993), under a narrow range of conditions.

For the commercial wastes typically a reaction order of 1 is found for the organic and a 0 order for the oxidant, the effect of water is not calculated because the pressure (density) is kept constant. For the model compounds studied, a reaction order of 0.5 - 1 is found for the organic, the reaction order for the oxidant is typically in the range of 0.1 - 0.6, and in the cases where the reaction order of water is calculated, this ranges from -0.1 - 1.3. The negative reaction order of water suggests the concentration of water affects the rate of oxidation detrimentally.

It is worth nothing that, while the effect of temperature on the oxidation kinetics in SCWO is understood, the influence of pressure is not yet fully understood. For example, while investigating the kinetics of phenol oxidation in SCWO, Goplan and Savage(1995) and Koo *et al*.,(1997) found that the oxidation rate increased with pressure, while Krajnc and Levec (1996) found that pressure change had no effect on the rate of oxidation, and Oshima *et al*., (1998) found that increased pressure affected the oxidation rate negatively. These experiments were conducted under similar reactor and operating conditions. Li *et al*.,(1991) suggested that the effect of pressure was negligible and should therefore be ignored. Luft (2001) suggested that using the concept of volume activation, the reaction rate constant can be expressed as a function of pressure.

2.10.4 Previous SCWO research results

SCWO occurs rapidly and oxidises but most products to benign compounds, but it is vital to understand to what extent this oxidation occurs and identify the intermediates formed. Results relating to the fate of various compounds will be discussed in this section

2.10.4.1 Nitrogen containing compounds

Some nitrogen containing compounds are readily oxidised by SCW while others are more refractory to this process. Ammonia is also considered a refractory compound under SCWO conditions and has been investigated by various researchers (Webley *et al.*, 1991, Killilea *et al.*, 1992, Cocero *et al.*, 2000a, Bermejo *et al.*, 2008, Helling and Tester, 1988).

Killilea *et al*., (1992) and Bermejo *et al*., (2008), found that ammonia destruction increased with increasing temperature and the presence of other compounds such as ethanol and isopropyl alcohol enhanced the oxidation by acting as auxiliary fuels. Cocero *et al*.,

(2000a) found that N_2 formation is favoured over N_2O at high temperatures. At temperatures above 600 ºC no N_2O is detected in the gas effluent.

Aymonier *et al*., (2000) found that the selection of H_2O_2 rather than O_2 as the oxidant enhanced the oxidation of ammonia, and the use of nitrates as a co-oxidant also enhanced ammonia oxidation.

Crain *et al*., (1993) investigated the SCWO of pyridine and found that pyridine oxidation increased with temperature and pyridine had a reaction order of 1. They also identified reaction intermediates and proposed a simplified reaction pathway.

Vera Perez *et al*., (2004) found a large oxygen stoichiometric excess was required for complete mineralisation of dinitrophenol in 40 s. No CO or NO_x was detected in the effluent gas, unless the oxygen concentration was below the stoichiometric amount.

Fenuron was successfully oxidised by SCWO at 540 ºC, 25 MPa after 39 s by Aymonier *et al*.,(2000). The nitrogen content of the compound was initially converted into ammoniacal nitrogen, nitrate ions, and nitro groups of nitrobenzene. They were then converted into molecular nitrogen by a redox process between ammoniacal nitrogen and the oxidised forms of nitrogen.

Lee *et al*., (1997) investigated the oxidation of p-nitroaniline and found that ammonia was only formed in trace quantities. The low ammonia level was attributed to ammonia oxidation by the nitro group of the decomposed p-nitroaniline. They further suggested that the co-oxidation of nitro group-containing compounds with other nitrogen containing groups could reduce the production of ammonia during SCWO.

Zhang and Hua studied the achieved greater than 95% conversion of nitrobenzene at 600 ºC, 34 MPa after 160 s residence time. Over 90% of organic nitrogen was converted to inorganic species, mainly elemental nitrogen, and over 60% of organic carbon was converted to CO and CO_2, with a higher selectivity towards CO_2.

Similar results were found by Chen *et al*., (2001) who investigated the efficiency of phenol, aniline and nitrobenzene by SCWO. Nitrobenzene was the most difficult to oxidise and needed a temperature of 650 ºC to achieve complete oxidation.

Ogunsola (2000) studied the decomposition of quinoline and isoquinoline (heterocyclic compounds). The compounds reacted differently in SCW due to the varied positions of the N atom in the compound and reaction pathways for both compounds were suggested. Toluene, methyl quinoline and aniline were identified as intermediates.

2.10.4.2 Phenol and other compounds

Most research in SCWO has been focussed on the oxidation of Phenol and substitued phenols, especially for the estimation of global rate kinetic parameters (Koo *et al.*, 1997, Chen *et al.*, 2001, Portela *et al.*, 2001b, Gopalan and Savage, 1995, Martino and Savage, 1997).

Similarities exist between the SCWO reactions of various aromatic compounds. For example, CO_2 is the product with the highest yield, even at low conversion of the original waste and short residence times. This suggests that once ring opening occurs, the oxidation pathway proceeds rapidly towards the formation of CO_2 (Holgate *et al*., 1992).

The oxidation of aromatic compounds appears to proceed by parallel simultaneous reactions, with the formation of dimers and ring opening compounds. Martino and Savage (1997) investigated the SCWO of phenol and mono substituted phenols and found that the substituted phenols were more reactive than phenol, they found that phenol reacts via two parallel paths, leading to the formation of phenol dimers and ring-opening products. The dimers are then converted to ring opening products and then to carbon dioxide.

Other compounds investigated for SCWO are acetic acid (Meyer et al., 1995, Kranjc and Levec, 1997, Lee *et al*., 1990, Aymonier *et al*., 2001). Simple organic compounds namely methane (Savage *et al*., 1998, Sato *et al*., 2003, Aki and Abraham, 1994), methanol (Cansell

et al., 1998, Anitescu *et al*., 1999), formaldehyde (Osada et al., 2003) have also been studied at SCWO conditions.

Halogenated and suphided compounds are another group of compounds that have attracted interest for SCWO. The chlorine ion formed can lead to a corrosive environment or result in salt formation, which complicates treatment. Lee *et al*., (2005) were able to operate a floating type reactor for the treatment of 2, 4-dichlorophenol for 5 months without corrosion or fouling, and achieved 99.9% oxidation.

2.11 Why 1,8-diazabicyclo[5.4.0]undec-7-ene (DBU)?

1,8-diazabicyclo[5.4.0]undec-7-ene is a tertiary amine compound and the a commonly used amidine, as a catalyst for polyurethane and a chemical intermediate. With chemical formula of $C_9H_{16}N_2$, it is a light yellow liquid which has a strong catalyst effect for the reactions of alicyclic and aliphatic isocyanates.

Among the analytes and reagents of environmental concern, aromatic amines constitute a very important class since they have been identified as high priority pollutants. The presence of these compounds, though at very low concentrations, has become a great concern. Therefore, DBU has been selected as a model pollutant representing the group of nitrogen containing pollutants. DBU is specifically a compound of interest to the pharmaceutical industry, hence this investigation to propose an efficient treatment method.

The stoichiometric equation for the complete oxidation of DBU is given by:

$$C_9H_{16}N_2 + 13\,O_2 \rightarrow 8H_2O + 9CO_2 + N_2$$

CAS Registration Number	6674-22-2
Structure	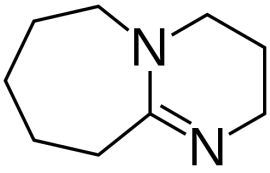
Formula	$C_9H_{16}N_2$
Molecular weight	152.24
Boiling Point	115 ºC
Density	1.019 g/mL

Table 2.6 DBU data sheet

CHAPTER 3 - EQUIPMENT, PROCEDURE AND ANALYTICAL METHODS

This chapter describes the experimental materials and equipment used in this study. Section 3.1 describes the experimental set up and procedure for WAO and CWAO system and section 3.4 describes the SCWO experimental set up and procedure. The catalyst materials used are described in section 3.2. Analytical techniques and methods employed for compound identification are described in sections 3.3 and 3.5.

3.1 WAO and CWAO system

3.1.1 Description of the WAO and CWAO Rig

A schematic diagram of the WAO system is shown in Figure 3.1. The WAO was designed by Baskerville UK, according to Glaxo Smith Kline UK design specifications. The author made modifications and improvements to the rig to enable further analysis to be carried out. All WAO and CWAO experiments were carried out using this batch reactor.

The rig comprises of an 800 ml Hastelloy C-276 steel alloy autoclave and operates as a fed batch process where 99.5% oxygen from a BOC gas cylinder is fed continuously to the bottom of the autoclave. The autoclave has 8 bolts welded to the top face of the vessel and is secured to the rig using eight 24 mm nuts and tightened stepwise, in a diametrically opposite and opposed manner to 100 lb/ft using a torque wrench. The central unit of the rig comprises of the autoclave lid and seal, a variable high speed motor (maximum speed 1000 rpm) attached to a six blade Hastelloy Ruston turbine, a pressure gauge, a cooling coil for temperature control, a gas sparger tube, and a temperature and pressure sensor. All piping utilised in the rig are made of stainless steel and are ¼ in outer diameter (O.D). Water from the laboratory mains serves as the cooling fluid for temperature control.

The Wet Air Oxidation process is controlled entirely from the control panel located on the left of the rig. The control panel houses two Eurotherm temperature controllers, a 2216 PID controller, circuit switches and indicator; a 2116 PID controller acts as a temperature over-rider linked to the start - stop buttons that control the removable heating mantle that surrounds the autoclave. The panel also incorporates a NEWPORT pressure indicator via a transducer set for a maximum pressure of 16 MPa; pressure regulation is via a pneumatically actuated vent valve, with the discharge rate controlled via a needle valve in the outlet line. Two Bronkhorst mass flow monitoring valves for mass flow indication and a rotary potentiometer for speed adjustment with digital display of RPM are housed on the panel. An emergency stop button is housed on the panel as a safety measure.

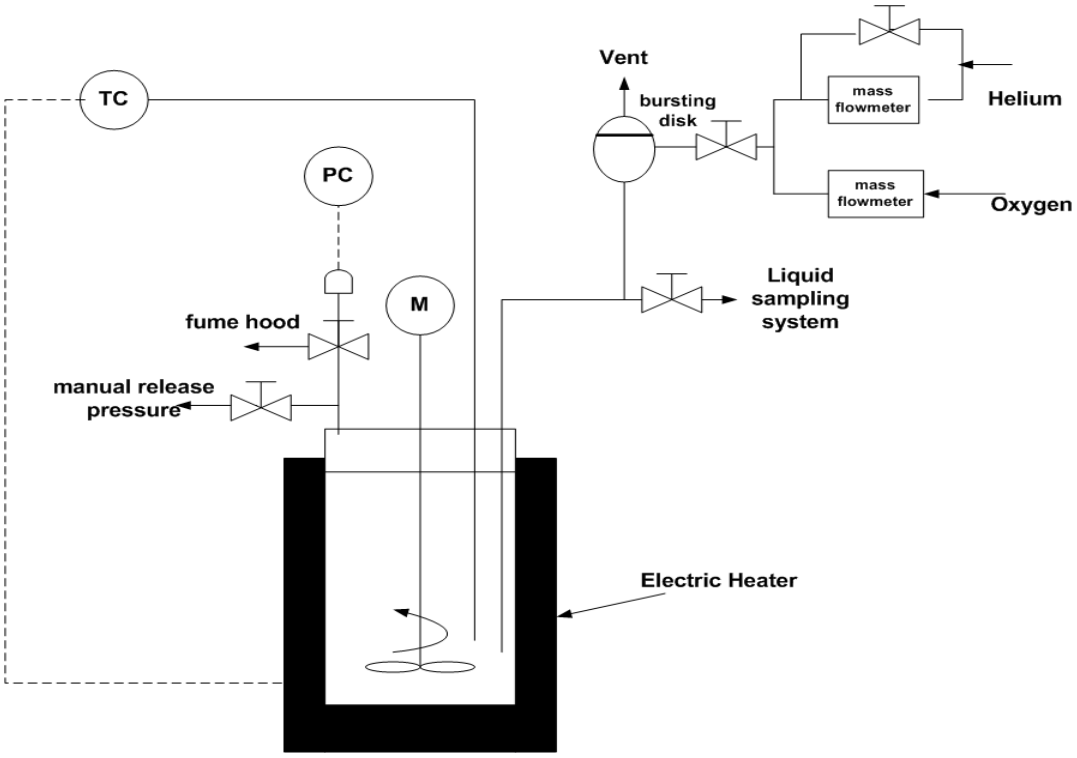

Figure 3.1 WAO and CWAO system

The liquid sampling system comprises of a metering valve, connected to a shell and tube heat exchanger, enabling the liquid to be rapidly cooled from the reaction temperature to ambient temperature, without a significant loss in pressure (less than 0.1 MPa).

The gas sampling system comprises of a metering valve after the manual release pressure valve, which is then connected by teflon tubing to a gas syringe. This syringe is injected into a gas sampling bottle filled with water, which has a second syringe attached to it, enabling the water to be displaced by the gas from the reactor.

3.1.2 Experimental Procedure

3.1.2.1 Reagent Preparation

1,8-diazabicyclo[5.4.0]undec-7-ene (DBU) solutions used as the model pollutants were prepared by diluting DBU (99% Sigma Aldrich, UK) in distilled water to the required concentration. The prepared solution was then sparged with helium for twenty minutes prior to experimentation to remove any dissolved oxygen. A liquid sample of this feed solution was collected for analysis.

For Catalytic Wet Air Oxidation (CWAO) experiments, besides following the procedures outlined above, the weight of catalyst required was measured and then placed in the catalyst basket.

3.1.2.2 Reactor Operation

For experimental runs, the autoclave was charged with 500 ml of DBU aqueous solution. The autoclave was then pressurised to the required operating pressure using 99.8% helium from a BOC gas cylinder, the electric heating jacket and stirrer were switched on. When the desired reaction conditions had been attained, then oxygen is fed through a KHRONE gas flow meter at a constant rate. This is time t = 0. A stirrer speed of 500 rpm was

used to overcome mass transfer limitations. For CWAO runs the catalyst basket was attached to the stirrer before the autoclave was charged with aqueous solution.

A liquid sample (5 mL) was withdrawn every 10 minutes, by opening a metering valve connected to a gas sparge tube at the base of the autoclave; gas samples (60 mL) were withdrawn at the end of the each experiment (t = 90 min) using a gas collection bottle connected to a metering valve from to the vent line.

At the end of the experiment, the heating jacket was removed and the reactor rapidly cooled by increasing the flow rate of water to the cooling coil inside the reactor. The remaining liquid contents of the reactor were collected for further analysis.

When a CWAO run was completed, the catalyst used was allowed to dry and then re-weighed, to indicate if there was any change in catalyst weight.

3.2 CWAO Materials

3.2.1 Catalyst Basket

The catalyst basket used to house the pellets, is made of stainless steel and consists of 3 parts: the top and bottom cylindrical lid (both, 40 mm O.D. and 10 mm I.D.), and a cylindrical mesh grid that forms the body of the basket. (37 mm O.D. x 46 mm). The holes on the mesh grid are 1 mm in diameter. The design of the catalyst basket is shown in Figure 3.2.

3.2.2 Catalysts Used

For the CWAO runs, it was decided to use commercially of the shelf catalysts, as these would be readily available for use in sufficient quantities. The choice of catalyst size was governed primarily by the size of the mesh grid to prevent catalyst escape into the main body of the reactor. The specifications of the catalysts are as follows

- Ruthenium 3.0 wt % on 3.2 mm Alumina trilobe pellets (Johnson Matthey)

- Ruthenium 0.5 wt % on 3.2 mm Alumina pellets (Aldrich)

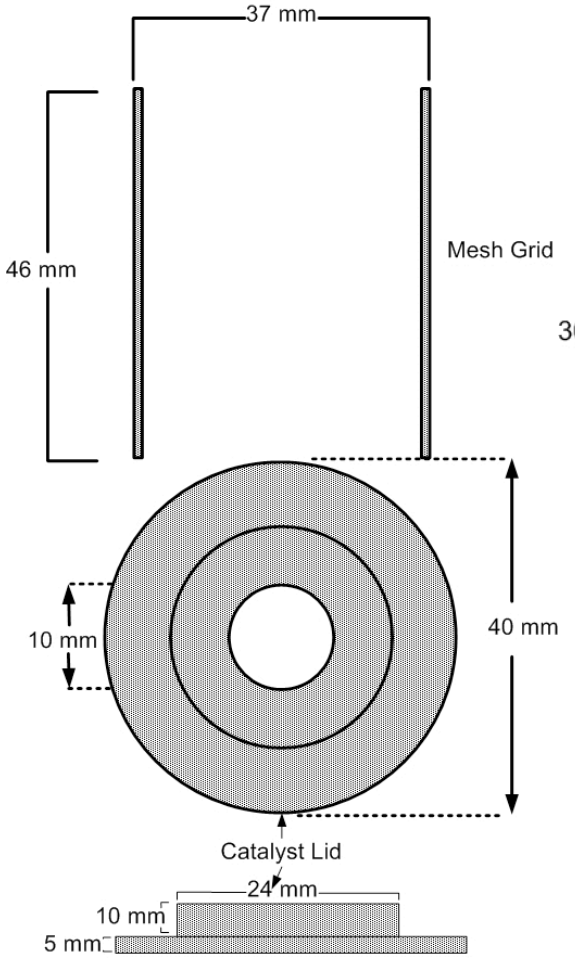

Figure 3.2 Catalyst Basket

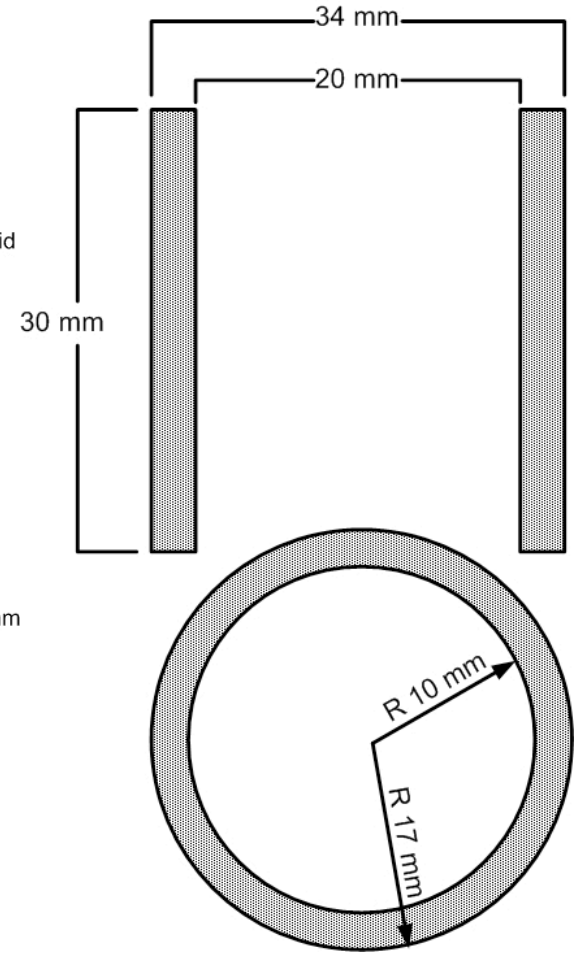

Figure 3.3 Reticulated Foam Design

3.2.3 Reticulated Foam Design

Alumina reticulated foam ceramic were custom fabricated by Vesuvius, UK. The reticulated foam was designed to replace the catalyst basket in the CWAO reactor set up, by fitting exactly between the two lids. It is constructed of 99.5 % Al_2O_3 and has a pore size of 15 PPI (15 pores per inch correspond to a mean pore size of 1100 - 1300 um)

The cylindrical shaped foam dimensions are 34 mm OD, 20 mm ID and 30 mm height. The design and dimensions of the reticulated foam monolith is shown in Figure 3.3. The unique honey comb structure is discussed further in section 5.12.

3.2.4 Coating of the Reticulated Foam

The reticulated foams were custom coated by Johnson Matthey Technology Centre, Reading using a customised and proprietary spray coating technique. This method was chosen for its easy preparation and to ensure the uniform anchoring of the catalyst onto the surface and internal of the reticulated foam. Ruthenium metal (Johnson Matthey) on a milled ceramic support was made into a slurry with ultra pure water (Millipore). Prior to coating, the foams were dried at 105 ºC for 2 hours and weighed. The slurry was then sprayed onto the foams to achieve a uniform coating and specific Ruthenium weight on the foam. The foams were then dried at 120 ºC for 2 hours then calcined at 500 ºC overnight. The weight of ruthenium metal on each foam was determined by calculating the weight difference before and after coating. The weight of ruthenium metal on the reticulated foams were 0.015g, 0.03g and 0.09g.

3.3 Analytical Methods for WAO and CWAO

The different techniques used to evaluate the oxidation efficiency of the WAO and CWAO processes are discussed here and the SCWO analytical techniques are discussed in section 3.5.

	Detected Species	Hydrothermal System	Analytical Technique
Liquid Phase	Model Pollutant (DBU)	WAO/CWAO/SCWO	HPLC
	Total Carbon (TC)	WAO/CWAO/SCWO	TOC Analyser
	Inorganic Carbon (IC)	WAO/CWAO/SCWO	TOC Analyser
	Total Organic Carbon (TOC)	WAO/CWAO/SCWO	TOC Analyser
	Organic By-Products	SCWO	GC-MS
	Ammonia	WAO/CWAO	Ammonia Cell Test
	Ammonia	SCWO	Ion Chromatography
	pH	WAO/CWAO	pH Meter
Gaseous Phase	Nitrogen (N2)	WAO/CWAO	GC-TCD
	Nitrous Oxide (NO2)	SCWO	GC-TCD
	Carbon dioxide (CO2)	WAO/CWAO/SCWO	GC-TCD
	Carbon monoxide (CO)	WAO/CWAO/SCWO	GC-TCD
	Methane (CH4)	WAO/CWAO/SCWO	GC-TCD
Solid Phase	Physical Characteristics	CWAO	Nitrogen Adsorption
	Surface Morphology	CWAO	SEM

Table 3.1 Summary of the detected species and their corresponding analytical techniques

3.3.1 Liquid Phase Analysis

3.3.1.1 High Performance Liquid Chromatography (HPLC)

The main components of the HPLC system are a mobile liquid phase (eluent), a separating column housed within a heating block and a detector. Separations on the column are achieved by the partitioning of solutes between the mobile liquid phase and a stationary phase held on a solid support. The analysis was carried out an Agilent 1100 series system with an auto sampler and variable wavelength detector. The method developed for monitoring DBU utilises HPLC grade water and acetonitrile (Both Fisher Scientific), with 0.05 % w/w Tri Flouroacetic Acid added to both (TFA) (Fisher) as eluents in a gradient mode, at a flow

rate of 1 ml/min. A Phenomenex Luna C18 column (15 cm x 0.46 cm) was used. The column temperature was 50 ºC and the wavelength was set at 230 nm. An calibration curve was developed for the organic compound and used to evaluate the experimental data.

3.3.1.2 Total Organic Carbon Analyser (TOC)

A Shimadzu TOC 5050A with an ASI-5000A auto sampler was used for TOC monitoring. Results are expressed in form of Total Carbon (TC), Inorganic Carbon (IC) and Total Organic Carbon (TOC).

TOC analysis is based on a combustive and non dispersive infrared (NDIR) gas analysis method. High purity air is supplied to the Total Carbon combustion tube, which is filled with oxidation catalyst and heated to 680 ºC. When the liquid sample reaches the TC combustion tube, the TC component is decomposed in CO_2. The carrier gas containing the combustion gas from the TC tube flows through the Inorganic Carbon reaction vessel, where it is cooled and dried. It is then sent through a halogen scrubber into a sample cell set in a non dispersive gas analyser, where CO_2 is detected. The amount of CO_2 generated is used to determine the TC concentration, based on the TC calibration curve.

For IC measurement, the sample is injected into the Inorganic Carbon reactor vessel, where the carrier gas is flows through a solution acidified by IC reagent (Phosphoric Acid). Only the IC component is decomposed to CO_2, which is then detected by the non-dispersive infrared (NDIR) gas analyser. The amount of CO_2 generated is used to determine the IC concentration, based on the IC calibration curve. IC measures carbon, represented in the form of carbonates and hydrogen carbonates.

3.3.1.3 Ammonia Cell Test

In a strongly alkaline solution, ammonium nitrogen is present almost entirely as ammonia, which reacts with hypochlorite ions to form monochloramine. This in turn reacts with a substituted phenol to form a blue indophenol derivative that is measured photometrically. (This method is analogous to EPA 350.1, US Standard Methods 4500-NH3 D, and ISO 7150/1)

The method used consits of 0.10 mL of effluent which was transferred into a reaction cell (Merck) and mixed, then a specified dose of NH_4 - 1K reagent was added and mixed. The cell is left to stand for 15 minutes then measured on a Spectroquant Nova 60 photometer (Merck) .

3.3.1.4 pH meter

The pH of the reaction is monitored using a Mettler - Toledo pH meter (Model - Seven Multi). This was done by direct measurement of the effluent solution after sampling.

3.3.2 Gas Phase Analysis

3.3.2.1 Gas Chromatography with Thermal Conductivity Detector (GC-TCD)

The main components of the GC system are a carrier gas supply, a separating column housed within the oven and a detector. Separations on the column are achieved by the partitioning of solutes between the mobile gas phase and a stationary phase held on a solid support. The analysis was carried out on an Agilent gas chromatograph (model 6890N) equipped with a thermal conductivity detector. An Alltech CTR 1 column (6 in x ¼ in OD and ⅛ in ID) was used. The carrier gas was helium, with a flowrate of 65 ml/min, injector, oven and detector temperatures were 50 ºC, 33 ºC and 250 ºC respectively. The reference gas was also helium with a flow rate of 65 ml/min. Calibration gases (Scientific and Technical and

Matheson Tri-Gas) were used to calibrate the GC, enabling the calculation of gas phase concentrations.

3.3.3 Solid Phase Analysis

3.3.3.1 N_2 Adsorption

A Micromeritics ASAP 2010 was used to obtain the physical characteristics of the catalysts used.

N_2 Adsorption utilizes the principle of physical adsorption to obtain adsorption and desorption isotherms and information about the surface area and porosity of a solid material. It performs surface area analyses plus pore size and pore volume distributions, typically using nitrogen as the standard gas. It calculates the Brunauer-Emmett- Teller (BET) and Langmuir surface areas, average and total pore volume, BJH pore size distribution and performs micro-pore analysis. It employs a range of standard theories for the calculation such as Horvath-Kawazoe, Dubinin-Radushkevich, Dubinin-Astakov, t-plot, MP-method, BET, Langmuir and Density Functional Theory.

3.3.3.2 Scanning Electron Microscope (SEM)

The SEM produces a largely magnified image by using electrons instead of light to form an image. A beam of electrons is produced at the top of the microscope by an electron gun. The electron beam follows a vertical path through the microscope, which is held within a vacuum. The beam travels through electromagnetic fields and lenses, which focus the beam down towards the sample. Once the beam hits the sample, electrons and X-rays are reflected from the sample. Detectors collect the X-rays, backscattered and secondary electrons and convert them into a signal that is sent to a display screen as a final image.

A Joel 6060 SEM was operated in low vacuum mode, using 20 kV voltage and 65 spot size, to view the surface of the catalysts. The catalysts were analysed with no preparation (no coating).

3.3.3.2 X-ray microtomography

X-ray microtomography measures the 3-dimensional (3-D) internal structure of a material's X-ray absorption. Hundreds of radiographs of a sample are taken at small angular increments over 180 degrees of sample rotation. A computer algorithm inverts this data to produce the 3-D absorption map. X-ray microtomography can resolve volume elements within a sample down to approximately eight cubic microns (2 x 2 x 2 μm).

3.4 SCWO system

3.4.1 Description of the Supercritical Water Oxidation Rig

A schematic diagram of the SCWO system is shown in Figure 3.4. The SCWO experiments were undertaken at Oshima Lab at the University of Tokyo, Japan. All tubing used for the preheaters, reactor and connections 1/16 in. , 316 stainless steel, unless stated otherwise.

The rig comprises of oxidant and organic feed tanks connected to their respective high pressure liquid chromatography (HPLC) pump and check valves. The oxidant feed tank is a Taiatsu pressure vessel, where the oxidant is stored under 0.2 MPa of helium pressure. The HPLC pumps are JASCO 9600 HPLC pumps, with a maximum flow rate of 10 ml/min. The pumps were individually calibrated before use to determine the actual flow rate of the pump, in order to design the experiments. The check valves prevent back flow to the HPLC pumps.

The feed streams are heated through their respective preheaters before contacting in the cross piece fitting at the reactor inlet. The preheaters are initially 1 m and then shaped into an 0.08 m diameter coil. The length of the preheaters were based on the surface area needed to ensure that over the operating range, both streams reach reaction temperature and, the oxidant (H_2O_2) will be decomposed into O_2 and H_2O before contacting the organic feed. The decomposition of H_2O_2 into O_2 and H_2O is confirmed by measuring the flow rate of evolved gas, when a known flow rate of oxidant solution is pumped through the reactor. The preheaters and reactor are placed in a fluidised sand bath (Techne) connected to a temperature control unit.

The reactor has a length of 3.3 m and then coiled into a 0.16 m diameter coil. At the reactor inlet (cross piece) and the reactor exit, two K type thermocouples are situated, and the temperatures are displayed on a digital read out. The temperature deviation between the inlet

and the outlet was ± 3 ºC. The pressure within the reactor is achieved and maintained by an automatic back-pressure regulator (JASCO), with a deviation of ± 0.1 MPa.

After leaving the reactor, the effluent stream is first cooled using a shell and tube heat exchanger, then the stream is depressurised as it passes through the automatic back-pressure regulator. After the automatic BPR, the stream flows to a custom made Gas-Liquid separator, at this point, the liquid samples are collected and flow rates measured using a volumetric flask and stopwatch . The gas stream flows to a three way valve, which allows the gas stream to be initially directed to a customised gas bubble flow meter to measure its flow rate using a stop watch, and then to the six way valve loop, which feeds into the online gas chromatograph (GC).

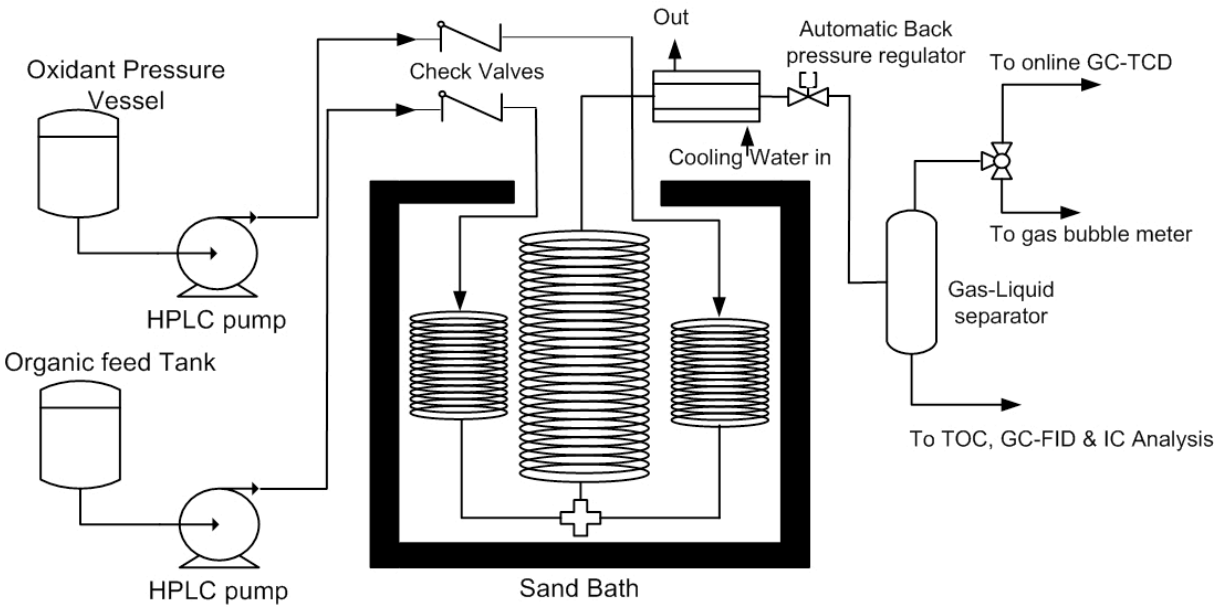

Figure 3.4 SCWO System

3.4.2 Experimental Procedure

3.4.2.1 Reagent Preparation

The DBU (Sigma, 99% purity) feed solution was prepared by dilution with distilled-dionised water to the required concentration, and then deoxygenated by purging with Helium gas for one hour. A liquid sample of the feed was collected for analysis.

A 2L solution of Hydrogen Peroxide was prepared by diluting 50 ml of Hydrogen Peroxide (Sigma Aldrich 99% purity, 30% w/w) with distilled-dionised water. 50 ml was chosen as the maximum volume for dilution because using a larger volume, was found to react and vapourise before reaching the pump, thereby giving inaccurate oxidant flow rates. The prepared solution was then poured into a pressure vessel (Taiatsu Techno) and pressurised with helium gas.

3.4.2.2 Reactor Operation

At the start of every experiment, the sand bath and automatic back pressure regulator were set to the reaction temperature and pressure and the GC-TCD started. The system temperature and pressure were raised using distilled water as feed from both HPLC pumps, at low flow rates (1 ml/min). When the temperature and pressure were stable at desired conditions, the water was switched to DBU and H_2O_2 at the desired flow rates. The system took approximately 30 - 40 minutes to stabilise. Liquid flow rates were then measured at 3 consecutive times using a stop watch and a volumetric flask, to ensure steady state operation. The gas flow rate was also measured at 3 consecutive times using a stop watch and the bubble flow meter, to ensure steady state. Consistency of both liquid and gas flow rates indicated steady state conditions had been achieved in the reactor.

During the experimental run, the temperatures at the reactor entrance and exit were monitored, and had a ± 3 ºC deviation. The pressure at the automatic back pressure regulator

was also monitored and had a ± 0.2 MPa deviation. For each experimental point two gas samples were analysed and five liquid samples were collected, three for HPLC and IC analysis and two for TOC analysis. The liquid samples were refrigerated once collected. Once all the necessary samples had been collected, reactions conditions (flow rates) could be changed or the reactor could be shutdown.

The feed solutions were heated to reaction temperature in their respective preheaters, and then mixed in a cross piece fitting at the reactor inlet. Oxygen was obtained by the complete decomposition of the aqueous hydrogen peroxide solution fed into the preheating line.

The reaction temperature was controlled within a 3 °C deviation, using a fluidised sand bath (Techne) equipped with temperature controller. The reaction temperature was continuously monitored by using two K-type thermocouples at the reactor inlet and outlet.
The reaction pressure was controlled by using an automatic back-pressure regulator (JASCO). The effluent stream was rapidly cooled with water, the pressure reduced to atmospheric pressure via the back pressure regulator, and then separated in a gas-liquid separator. The separator was connected to a direct injection loop for a gas chromatograph and to a bubble flow meter to measure the gas flow rate, while the liquid effluent was collected for analysis. The liquid flow rate was also measured for two purposes: the estimation of the residence time in the reactor and calculation of the carbon balance.

The gas flow rates were measured using a stop watch and a bubble flow meter, the liquid flow rates at the exit were measured using a stop watch and volumetric flask.

3.5 Analytical Methods for SCWO

The different techniques used to evaluate the oxidation efficiency of the SCWO process are described here.

3.5.1 Liquid Phase Analysis

3.5.1.1 High Performance Liquid Chromatography (HPLC)

DBU collected in the liquid samples was analysed by a Jasco high performance liquid chromatograph in isocratic mode with a Finepak Sil C8-10 column (Jasco). The eluent mixture was 30% acetonitrile - 70% water (Fisher Scientific) with 0.05% w/w TFA added. The flowrate was 1 ml/min, the detector wavelength was 230 nm and column temperature was 50 ºC. A calibration curve was developed for the organic compound and used to evaluate the experimental data.

3.5.1.2 Total Organic Carbon Analyser (TOC)

A Shimadzu TOC 5050A with an ASI-5000A auto sampler is used for TOC monitoring. Results are expressed in form of Total Carbon (TC), Inorganic Carbon (IC) and Total Organic Carbon (TOC).

3.5.1.3 Ion Chromatography

Ammonia production in the liquid samples was quantified by using an Ion chromatograph (JASCO with CD-5 detector). A 20 mmol/L solution of Nitric acid (HNO3) was used as eluent at a flowrate of 1 ml/min.

3.5.1.4 Gas Chromatography with Mass Spectrometer (GC-MS)

Identification of the reaction products was accomplished by GC-MS (Hewlett Packard 5900). Prior to the analysis, the liquid samples were extracted with dichloromethane in a 1:1 volume ratio. Both phases were then used in the analysis.

3.5.2 Gas Phase Analysis

3.5.2.1 Chromatography with Thermal Conductivity Detector (GC-TCD)

Gas phase analysis was performed by using gas chromatogram with thermal conductivity detector (Shimadzu) linked to a plotter (Shimadzu). Propak Q and Haysep C columns were used for the separation and identification of carbon monoxide (CO), carbon dioxide (CO_2), methane (CH_4) and nitrous oxide (N_2O).

Prior to each experimental run, standard gases of known composition and concentration were analysed on the GC-TCD to obtain specific areas for the gases of interest. These areas were then used to calculate the concentration of the gas phase effluent.

RESULTS AND DISCUSSION

The experimental results are presented in 3 chapters, which comprise the Results and Discussion section. Each chapter is dedicated to a particular process. Chapter 4 deals with the effect of WAO system operating variables on DBU oxidation. Chapter 5 investigates the CWAO of DBU using Ruthenium pellets as catalyst. Chapter 6 investigates the SCWO of DBU.

CHAPTER 4 - WET AIR OXIDATION OF DBU

This chapter presents the results and discussion of experiments performed to study the Wet Air Oxidation of DBU. The aim of the study was to investigate the effect of operating variables on the complete oxidation of DBU. Kinetic analysis and modeling are also presented in this chapter.

4.1 Screening Study

The capital cost, operational cost and problems associated with WAO technology, have limited its wider use as a preferred treatment method of toxic waste water. The aim of this study was to investigate the effect of various operating variables, namely temperature, pressure and initial organic concentration.

Preliminary studies were undertaken to initially screen the range of operating conditions. As this was a preliminary study, the subsequent results are displayed as TOC values in Figure 4.1.

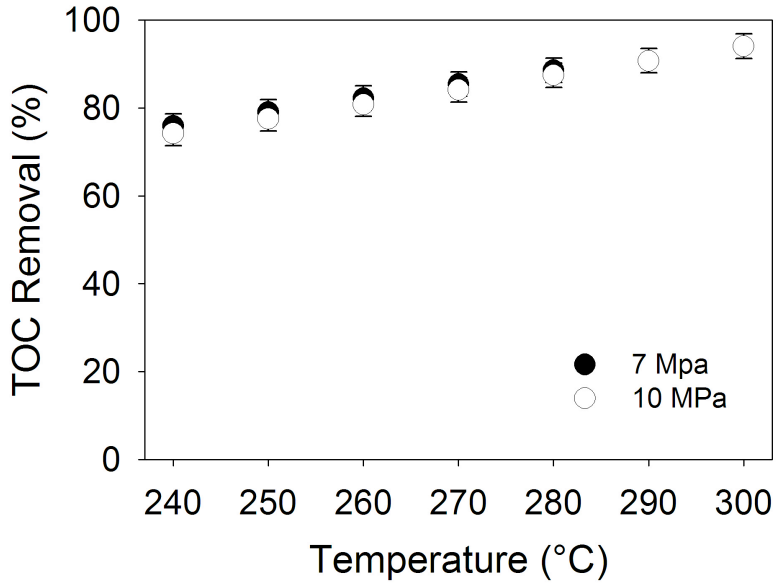

Figure 4.1 Preliminary Study on the effect of process parameters on TOC Removal.

Figure 4.1 clearly shows that above 240 ºC, there is a minimum TOC removal of 75% after 90 minutes and the effect of pressure change is not pronounced. The value of TOC removal is high and could potentially mask the effect of any catalyst used, hence lower temperatures were selected for study.

Parameter	Range	Fixed Conditions
Temperature	170 - 240ºC	Concentration = 6 mM Pressure = 4 & 7 Mpa O2 FlowRate = 0.4 L/min
Pressure	4 & 7 MPa	Temperature = 170 - 240 ºC Concentration = 6 mM O2 FlowRate = 0.4 L/min
Concentration	6-18 mM	Temperature = 240 ºC Pressure = 7 Mpa O2 FlowRate = 0.4 L/min
Oxygen Flowrate	0 - 1 L/min	Temperature = 240 ºC Pressure = 7 Mpa Concentration = 6 mM

Table 4.1 Summary of WAO experiments

Table 4.1 summarises the various operating conditions investigated in this work for WAO. All concentration values refer to the stock solution, the molar concentration of prepared solution at ambient conditions. The selected concentration of DBU in the reaction mixture was in the range of 1000 - 3000 mg L^{-1}, which is representative of concentrations found in industrial waste waters. This was also done to simulate a situation where upon initial breakdown of DBU, there would be a variety of initial intermediates to be further oxidised. The maximum residence time of 90 minutes used in all runs, was based on data obtained from previous works, which showed that after 90 minutes the removal of DBU is minimal and plateaus.

The need for the reaction to operate as a gas-liquid system, i.e. water remains in the liquid phase and does not evaporate at higher temperatures, governed the minimum system pressure of the experiments. It should be noted that for the temperature and pressure range investigated the change in density of water is negligible, as shown in Figure 4.2, where the circles represent the experimental runs done.

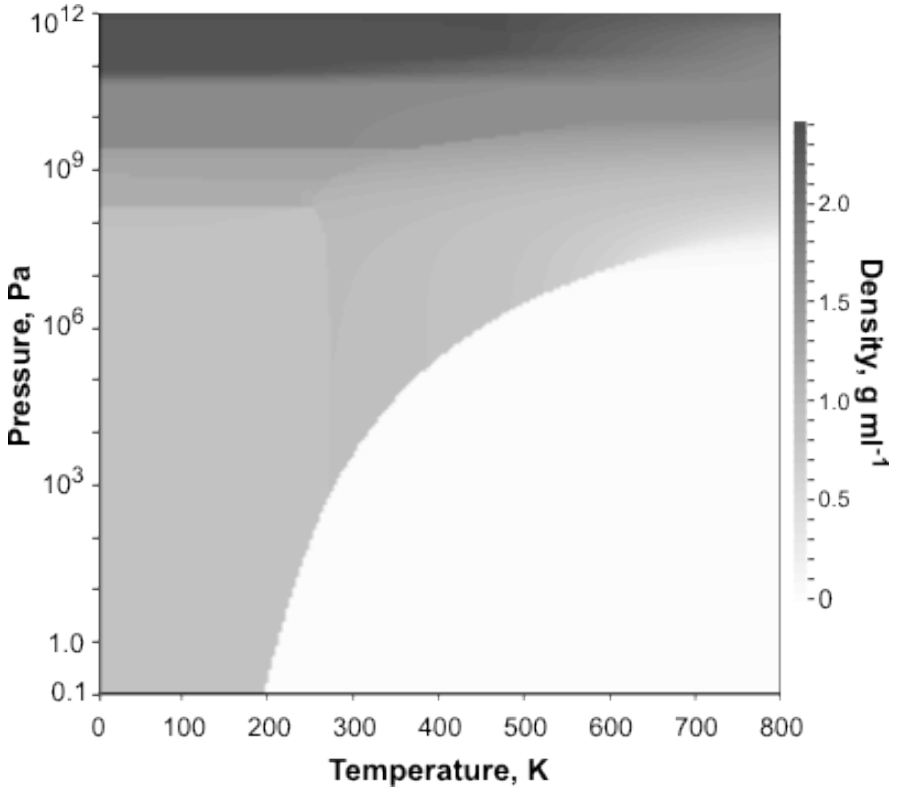

Figure 4.2. Temperature and pressures studied, shown on temperature-pressure diagram for water.

4.2 Mass Transfer and Solubility

The overall oxidation process is controlled by two steps: (i) mass transfer of oxygen from the gas phase to the liquid phase; and (ii) reaction between the dissolved oxygen and DBU.

Joglekar et al. (1991) showed the resistance of the first step (mass transfer) can be eliminated by manipulating the agitation speed. Runs were performed to verify this and it was found that in those experiments, the oxidation rate was independent of the agitation speed above 500 rpm or more, as shown in Figure 4.3. Indicating that above this speed the reaction is not mass transfer limited.

Reynolds numbers calculations were also done using equation 4.1 (Harnby *et al.*, 1992), to confirm that the flow pattern in the vessel above this speed was fully turbulent (> 10^4) and not laminar, where D is the agitator diameter (m), N is the rotational speed per second, is the fluid density (kg/m3), and is the fluid viscosity (kg/ m s)

$$\mathrm{Re} = \frac{D^2 N \rho}{\mu} \tag{4.1}$$

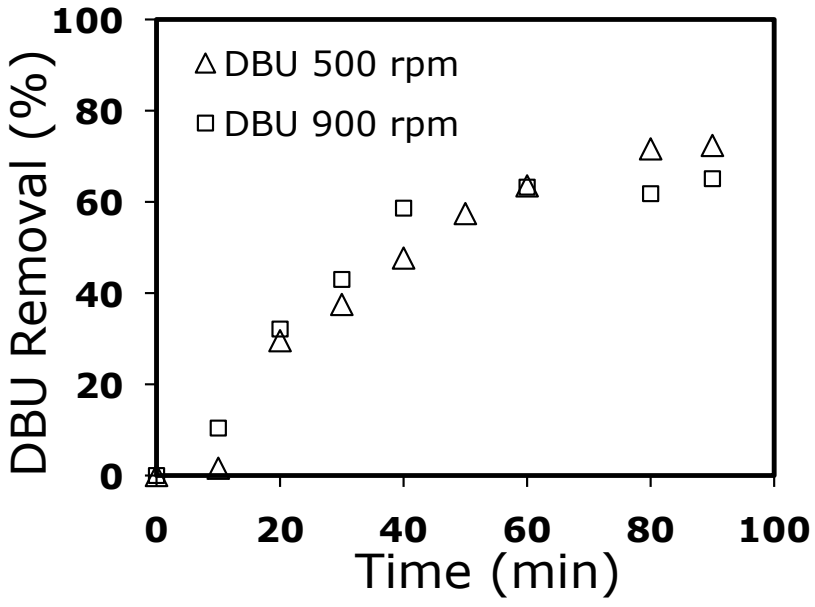

Figure 4.3 Effect of varying impeller speed at 240 ºC and 7MPa

The solubility of dissolved oxygen in the liquid phase was estimated by extrapolating data obtained by Pray *et al.,* (1952), based on Henry's law and experimental data they obtained for the solubility of pure gases in water.

They found that the solubility of oxygen in water in a high temperature and pressure range, similar to that investigated in this work; exhibits a linear relationship with pressure, follows Henry's law and can be predicted within limits of engineering accuracy. This is shown in Figure 4.4, where the circle represents, the region of interest for this work. O_2 partial pressures were calculated from the concentration of oxygen in analysed gas samples (see Appendix 1).

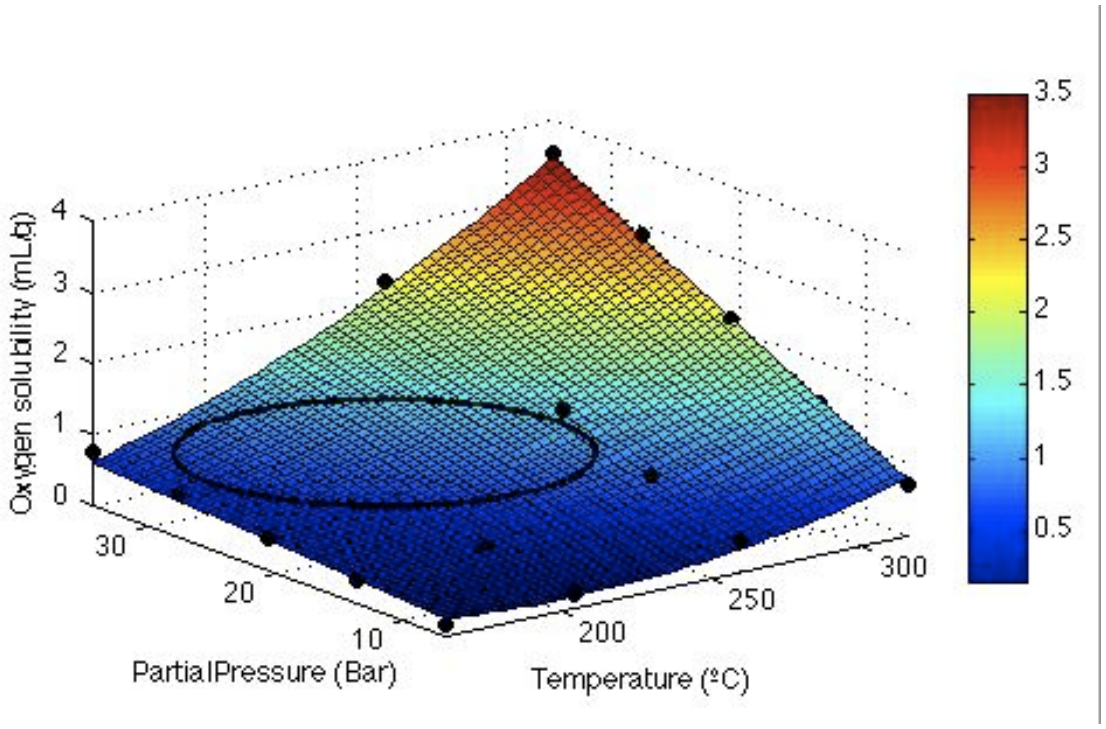

Figure 4.4 Oxygen solubility as a function of system temperature and oxygen partial pressure

Tromans (2001) used thermodynamically based analysis to show that the equilibrium concentration of molecular oxygen dissolved in the aqueous phase of pure water, can be represented by the following equation over a wide range of temperatures and pressures

$$\frac{C_{aq}}{P_{O_2}} = k \tag{4.2}$$

where C_{aq} is the concentration of molecular oxygen in pure water (mol O_2 / kg H_2O)

P_{O2} is the partial pressure of oxygen gas (MPa)

k is the equilibrium constant (mol O_2 / kg H_2O) (MPa^{-1})

k, the equilibrium constant is a temperature dependent function and is given by

$$\mathrm{k} = 9.8692\exp\left(\frac{0.046T^2 + 203.35T\ln\left(\frac{T}{298}\right) - (299.378 + 0.092T)(T - 298) - \left(20.591\times 10^3\right)}{(8.3144)T}\right) \tag{4.3}$$

Tromans (2001) showed that the above equation is satisfactorily valid for oxygen partial pressures up to 6 MPa, (which is greater than the range of oxygen partial pressures in this study), and compared well with published values by Cramer (1980) for oxygen solubility in water at high temperatures and pressures. Panayiotou (1997) found that the increase in solubility as temperature increases is largely due to a reduction in the hydrogen-bonding propensity of water, reflected by its hydrogen bonding solubility parameter component δH.

To summarise, it is assumed that at ambient conditions (or a high pressure system with low temperature), even after a turbulent flow pattern is attained, the reaction rate of the organic compound in solution and oxygen is very slow, due to the low solubility of oxygen in water. Therefore, by increasing the reaction temperature, not only does this directly increase the chemical reaction rate, but the concentration of dissolved oxygen in solution also increases, further enhancing the rate of reaction.

4.3 Thermal decomposition of DBU

It was noticed for all experiments undertaken, that the concentration of DBU at time t = 0 min, was approximately 50% of the initial concentration of DBU charged into the autoclave. In contrast, the concentration of TOC was unchanged.

To evaluate the extent of thermal decomposition that occurred while heating the reactor, an experimental run was performed at 240°C and 70 bar, in the absence of oxygen. Figure 4.5 shows the result of the thermal decomposition experiment. The concentration of DBU continued to decrease, resulting in a 30% reduction between time t = 0 min and t = 90 min.

TOC concentration was unchanged, indicating that DBU removal is due to its thermal decomposition into lower weight organic compounds, which then polymerise, thereby not changing the TOC concentration. These lower weight organic compounds and the subsequent polymerised compounds are not oxidised in the absence of oxygen.

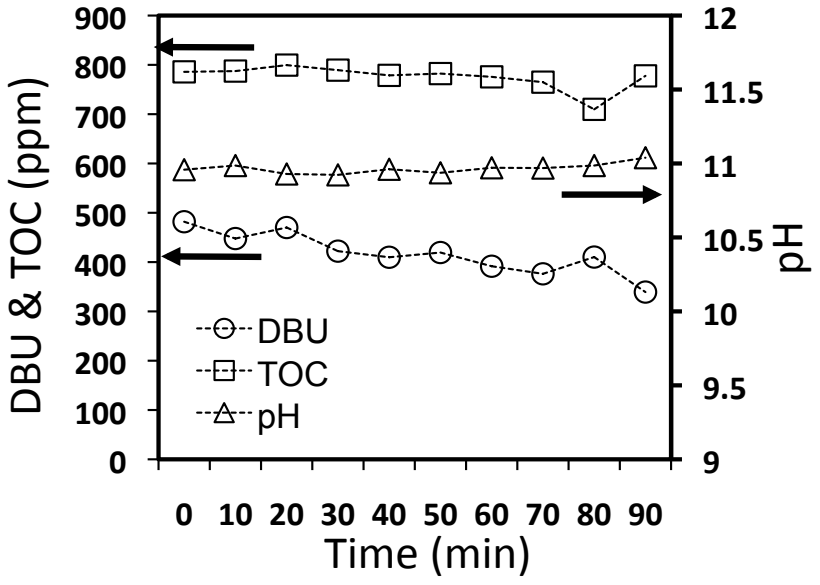

Figure 4.5 Removal of DBU and TOC by thermal decomposition at 240 °C, 7 MPa, 0.0 L/min O_2.

The solution pH dropped slightly from 11.9 to 10.9 during heating indicating the decomposition of DBU into lower molecular weight acids. The constant pH of the solution

during the experimental run further confirmed that no oxidation reaction occurred, as this would characterised by the formation of carboxylic acids (Portela *et al.*, 1997) (Suárez-Ojeda *et al.*, 2007) , which would lower the pH even further.

This is explained by Shriner and Neumanw (1944) , who showed that upon heating amidines in water (aqueous solution) in the absence of oxygen, its decomposition is either by i) hydrolysis or ii) pyrolysis. If hydrolysis occurs, an amide and amine of DBU would be formed. The amide would then be decomposed into an acid and another amine, depending on the hydrolytic conditions. If pyrolysis occurs, DBU would decompose into ammonia and a corresponding nitrile. The nitrile would then polymerise to yield additional products.

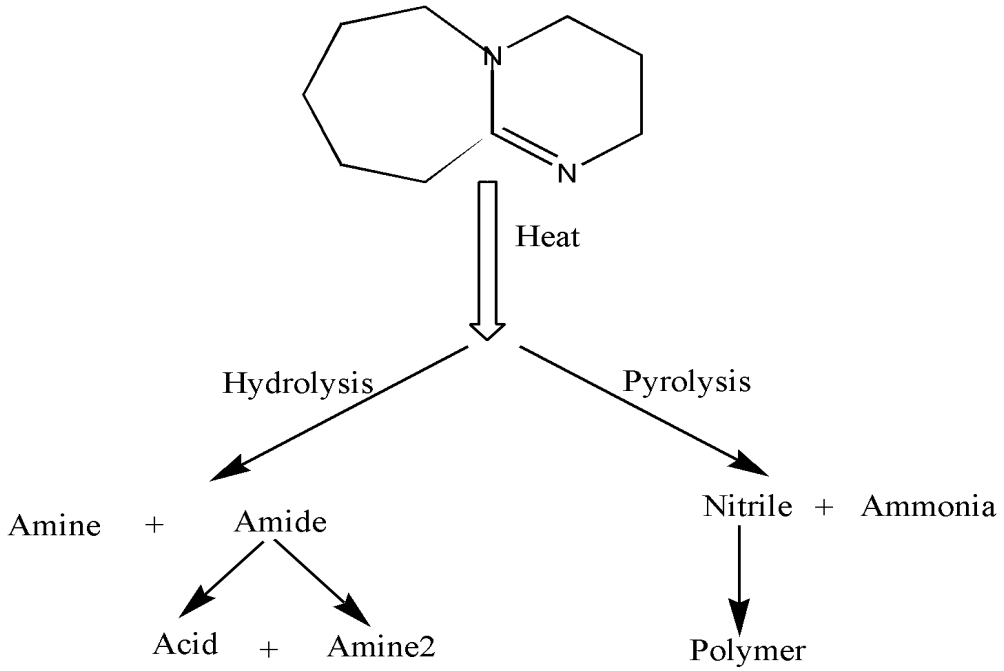

Figure 4.6 Thermal decomposition mechanism of DBU

Based on the findings of Shriner and my experimental results of no further change in pH after the heating up period and the detection of ammonia in the sample collected, it can be deduced that DBU decomposes by pyrolysis. Therefore, it is assumed that during the experimental runs (addition of oxygen) there are two reactions occurring: direct oxidation and pyrolysis.

4.4 Effect of System Temperature

The effect of temperature on DBU and TOC removal is shown in Figure 4.7a after a reaction time of 90 minutes, at a pressure of 7 MPa, DBU initial concentration of 6 mM, and a flow rate of 0.4 L/min of Oxygen. (At an oxygen flow rate of 0.4 L/min, the oxygen partial pressure was calculated as 2 MPa at 240 ºC and increased to 3 MPa at 170 ºC)

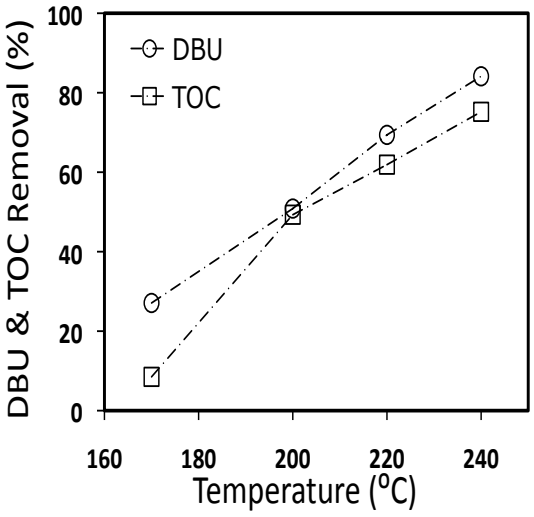

Figure 4.7a Effect of varying temperature on DBU and TOC removal at 7 MPa, 0.4L/ min O_2

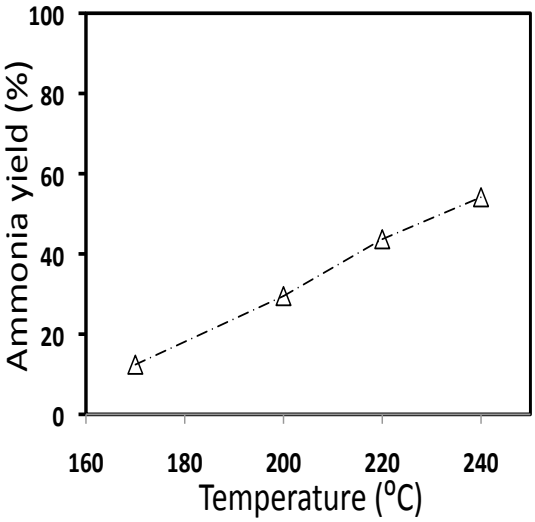

Figure 4.7b Effect of varying temperature on ammonia yield at 7 MPa and 0.4L/min O_2

DBU and TOC removal increased with temperature in a linear fashion, confirming that the reaction temperature is the most important parameter in the oxidation of DBU.

DBU and TOC removal were calculated using equation (4.4) and ammonia yield was calculated using equation (4.5)

$$DBU\ \&\ TOC\ removal(\%) = \frac{C_0 - C}{C_0} \times 100 \tag{4.4}$$

where C_o is the initial concentration of DBU and TOC; C is the concentration of DBU and TOC at time t.

$$Ammonia\ yield(\%) = \frac{C_{NH_3}}{C_{N_{in}}} \times 100 \tag{4.5}$$

where C_{NH3} is the molar concentration of nitrogen atoms in ammonia after 90 minutes, and C_{Nin} is the molar concentration of nitrogen atoms in the feed.

The value of DBU removal of increased from 27% to 87% as the temperature increased from 170 to 240 ºC, similarly TOC removal increased from 8.5% to 76%. At all temperatures investigated, DBU removal is higher than TOC removal, indicating that some DBU had been partially oxidised into other organic compounds. At the lowest temperature investigated 170 ºC, there is no fast reaction phase, just a continuous induction phase. This trend was also found by Chen *et al*., (2003) for COD values at 150 ºC during the WAO of printing and dyeing wastewater.

Figure 4.7b also shows that there is also a linear relationship between operating temperature and the yield of ammonia from DBU. The yield of ammonia increased from 12% (26 mg/L) to 55% (119 mg/L), as the temperature increased. These are high concentrations of ammonia, which is an undesirable and refractory intermediate of the process. Grosjean *et al*., (2010) also found ammonia as a refractory intermediate and dominant nitrogen containing compound in the wet air oxidation of DMF; In their study ammonia concentration increased with increased temperature.

Cocero *et al*., (2000a) also found a general trend of ammonia yield increasing with temperature, Bermejo *et al*., (2008) have suggested that a temperature of 700 ºC, is needed to completely oxidise ammonia.

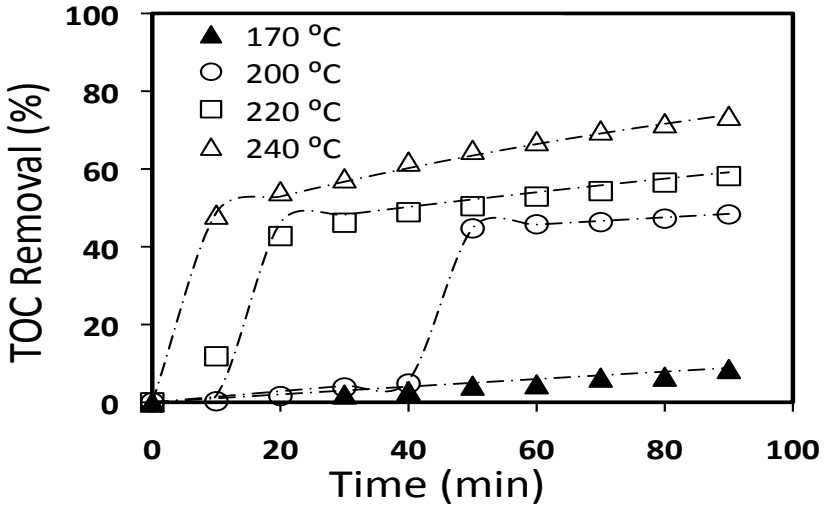

Figure 4.7c Effect of varying temperature on TOC removal at 7 MPa, 0.4L/min O_2 for 90 mins

The three step phases (induction, fast, slow) and their sigmoid profile seen in Figure 4.7c are typical of autocatalytic reactions. In autocatalytic reactions, one or more of the products formed is also a reactant (IUPAC, 1997). The reaction proceeds slowly at the start shown by the induction phase because, initially there is a low concentration of the of the reactant formed. In this case the concentration of the reactant increased until there was a sufficient amount for rapid oxidation. After the phase of fast oxidation, the reactant concentration has been depleted. Rate equations for autocatalytic reactions are fundamentally nonlinear and accurately modeling requires the identification and quantification of the reactant formed (Winterbottom and King, 1999).

To confirm the effect of temperature on the removal of DBU and TOC, and verify the reproducibility of the experimental results, a number of repeat experiments were done at the same experimental conditions and the standard deviation calculated.

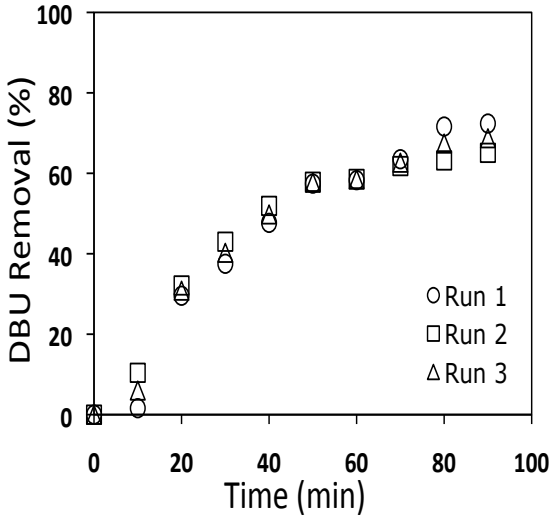

Figure 4.8a Repeated experiments to verify reproducibility at 240 ºC, 7 MPa and 0.4 L/min O_2

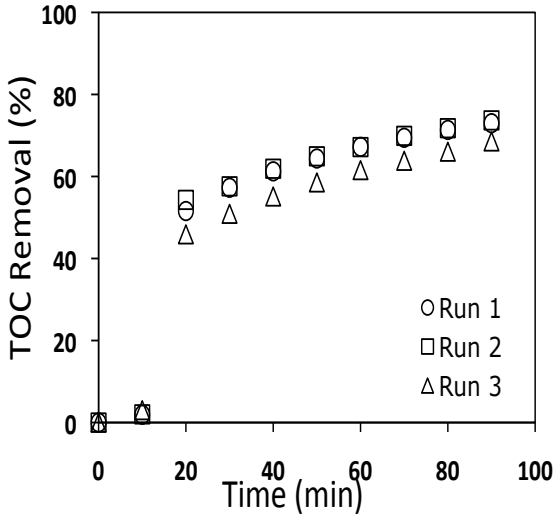

Figure 4.8b Repeated experiments to verify reproducibility at 240 ºC, 7 MPa and 0.4 L/min O_2

The curves in Figures 4.8a and 4.8b, show DBU and TOC removal at 240 ºC and 7 MPa is reproducible and a standard deviation of 4.4% and 4.3% was obtained for DBU and TOC respectively. Error bars are omitted from all experimental graphs for clarity.

Figure 4.9 shows the effect of temperature on the gas composition in the samples taken at t = 90 mins. Nitrogen and carbon dioxide gas are detected and show a general trend of increasing as the temperature increased, but no carbon monoxide is detected at 170 ºC. The values are low because the gas phase of the system is oxygen rich, and oxygen accounts for a significant percentage of the sampled gas.

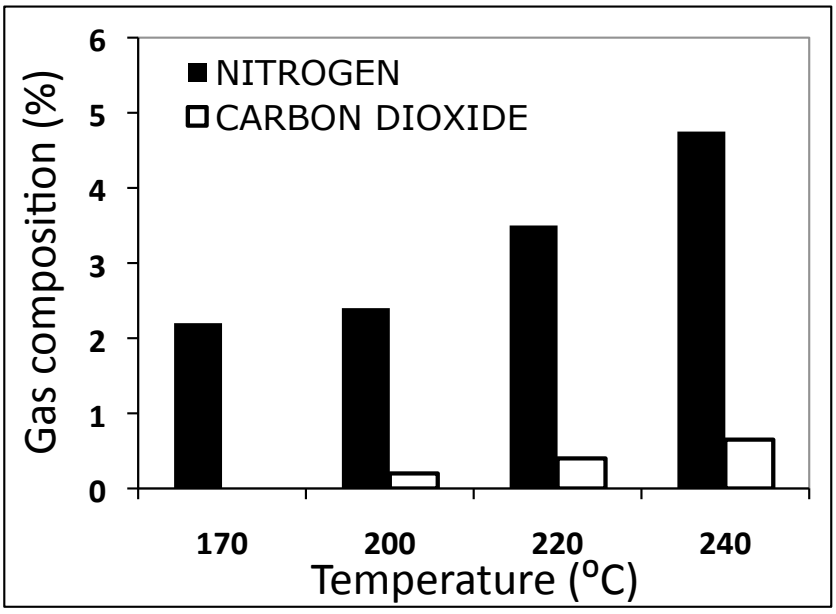

Figure 4.9 Effect of operating temperature on the gas sample composition at 7 MPa

4.5 Kinetics

The objectives of the present kinetic analysis were to determine the reaction rate constant (k), its associated Arrhenius parameters, and the reaction order for DBU.

According to a second order irreversible reaction, the kinetic expression obtained by applying the integral method of kinetic data analysis can be approximated to the following pseudo first order equation (Levenspiel, 1972):

$$-r_{DBU} = \frac{-dC_{DBU}}{dt} = k\left[C_{DBU}\right] \tag{4.6}$$

where $k = A\exp\left(\frac{E_a}{RT}\right)$

The above approximation assumes the oxygen concentration is in stoichiometric excess during the reaction, which is presumed to be valid because there was always an excess of oxygen present approximately 21 mM.

Separating and integrating equation (4.6), equation (4.7) is obtained

$$-\ln\frac{C_{DBU}}{C_{DBU_0}} = kt \tag{4.7}$$

Assuming that the rate constant *k* has Arrhenius behaviour, it was calculated for the various temperatures studied by plotting the negative natural logarithm of DBU at any time, t, divided by the initial DBU concentration versus the residence time in the reactor (Equation 4.7). As shown in Figure 4.10. The rate constant *k* was obtained from the slope of the linear fit in Figure 4.10. Table 4.2 shows a summary of the *k* values for the temperatures and pressures studied.

The rate constant *k* is the pseudo first order rate constant for the disappearance of DBU, which is the sum of pyrolysis and direct oxidation first order rate constant.

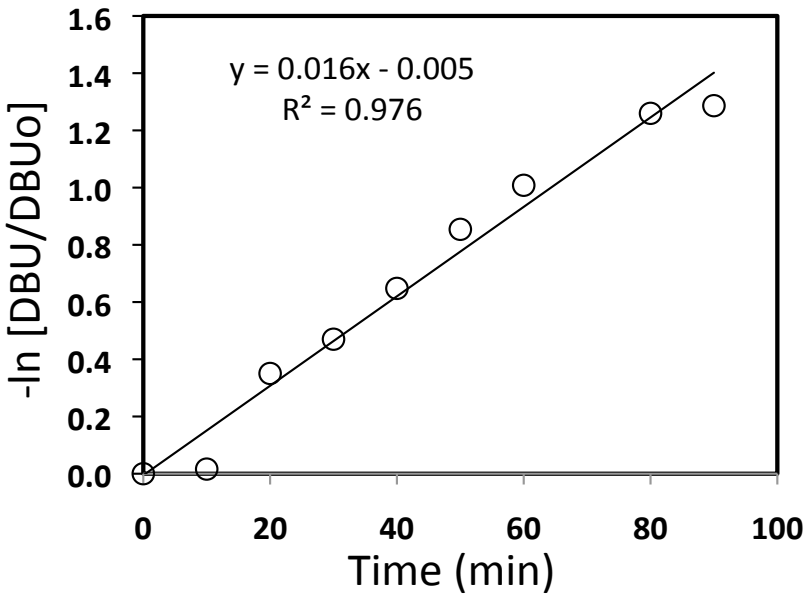

Figure 4.10 Natural log of DBU concentration versus time at 240 ºC, 7 MPa and 0.4 L/min O_2

Temperature (°C)	Pressure (MPa)	k_{DBU} x 10^{-3} (min^{-1})
200	7	3.3
220	7	7.5
240	7	15.7
200	4	1.6
220	4	4.9
240	4	6.7

Table 4.2 Pseudo first order rate constants for selected conditions

The pre-exponential, A and the activation energy, Ea, were calculated by performing a linear fit of ln k versus 1000/T as shown in Figure 4.11.

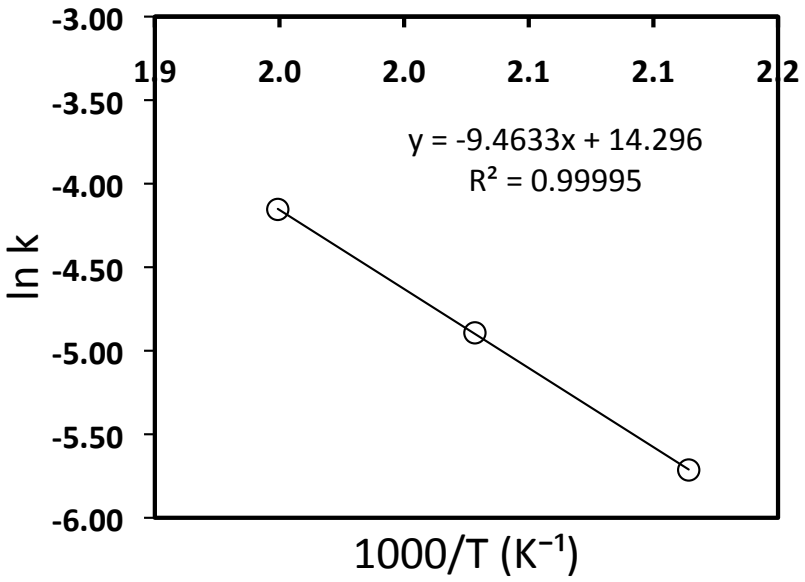

Figure 4.11 Arrhenius graph for DBU oxidation at 7 MPa

The activation energy for DBU under subcritical conditions had a value of 78.7 kJ mol^{-1} and the pre exponential factor was 1.62×10^6 min^{-1}.

The resulting pseudo first order rate expression for the oxidation of DBU for the temperature range investigated and at 7 MPa is given by:

$$-r_{DBU} = 1.62 \times 10^6 \text{ min}^{-1} \text{e}\left(-\frac{78700 J\ mol^{-1}}{RT}\right)[C_{DBU}] \quad (4.8)$$

Using the values of k at 4 MPa shown in Table 4.2 and the method outlined above, the pseudo first order rate expression of DBU at 4 MPa for the temperatures investigated is given by:

$$-r_{DBU} = 1.94 \times 10^5 \text{ min}^{-1} \text{e}\left(-\frac{72740 J\ mol^{-1}}{RT}\right)[C_{DBU}] \quad (4.9)$$

The values of Ea at 4 and 7 MPa are very similar, which shows that temperature is the most important parameter in the WAO of DBU and gives a sense of the accuracy of the experimental data. The rate expressions given above are compared against the experimental

results in Figures 4.12 and 4.13. They clearly illustrate that there is good agreement between the experimental data and the fitted rate expression.

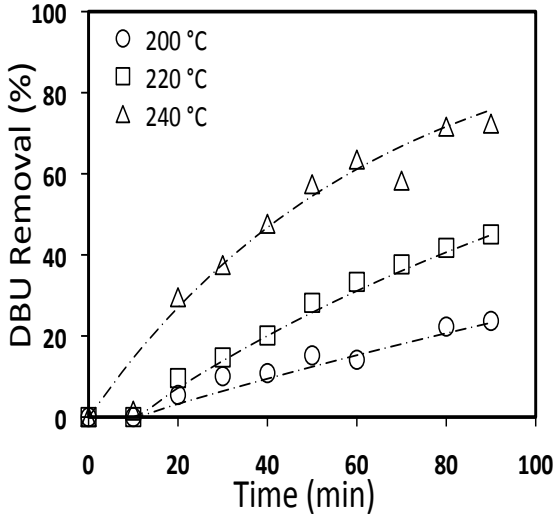

Figure 4.12a WAO DBU conversion plotted versus residence time for several temperatures at 7 MPa and 0.4 L/min O_2. Symbols represent experimental data and lines denote kinetic model fitting.

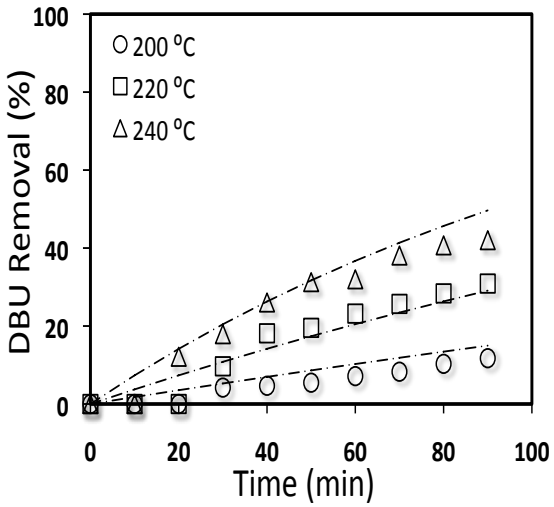

Figure 4.13 WAO DBU conversion plotted versus residence time for several temperatures at 4 MPa and 0.4 L/min O_2. Symbols represent experimental data and lines denote kinetic model fitting.

4.6 Effect of System Pressure

A comparative set of experiments at a lower pressure, 4 MPa were investigated to determine the effect of system pressure on DBU and TOC removal. The temperature was varied from 170 to 240 ºC, with an initial DBU concentration of 6 mM, and a flow-rate of 0.4 L/min of Oxygen. Figure 4.14 and 4.15 show the effect of system pressure on the removal of DBU and TOC.

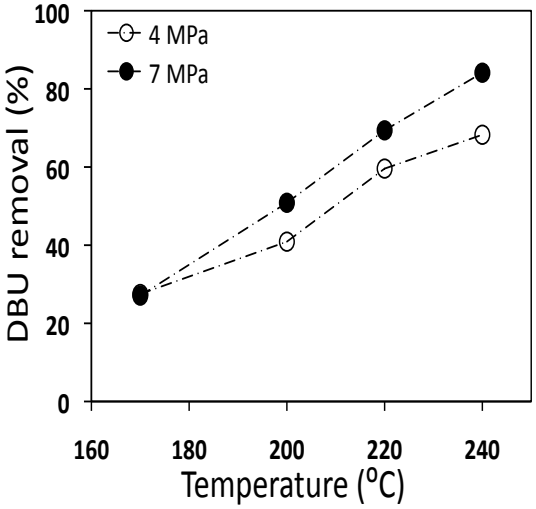

Figure 4.14 Effect of System Pressure on DBU removal at varying temperatures after 90 min.

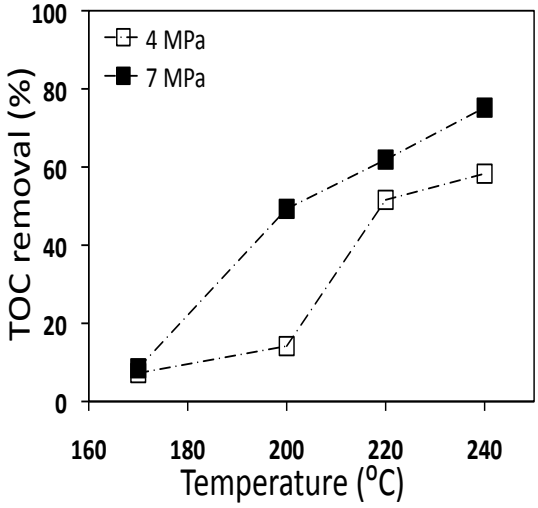

Figure 4.15 Effect of System Pressure on TOC removal at varying temperatures after 90 min.

At the 4 MPa, the removal of DBU, followed a similar linear trend to that seen at 7 MPa. TOC removal had a large increase in value as the temperature increases from 200 to 220 ºC. This shows that below a certain system condition (220 ºC and 4 MPa), there is not a sufficient buildup of free radicals to initiate the total oxidation of DBU intermediates. DBU and TOC removal increased from 27% to 65% and 7% to 58% respectively as temperature increased. At all temperatures investigated at 4 MPa, the value of DBU removal is always higher than TOC removal, indicating that some DBU is converted into refractory compounds.

DBU removal values varied at both pressures, with the difference being 0% at the lowest temperature studied and increasing to 16% at the highest temperature. TOC removal values also varied at both pressures, with a 1% increase at the lowest temperature studied,

increasing to 35% at 200 ºC, and then decreasing to 17% at 240 ºC. This shows that the operating temperature is the main parameter that influences DBU and TOC removal, but the system pressure also mildly enhances DBU and TOC removal. A mild enhancement of phenol and TOC removal by system pressure was also found by Portela (1997) in the WAO of phenol. The trends observed can be explained by Tromans solubility equation (4.3), discussed earlier in this chapter, where at a given temperature, increasing the system pressure would also increase the partial pressure of oxygen in the system and therefore enhance the solubility of oxygen in water and concentration of oxygen available for reaction in the aqueous phase.

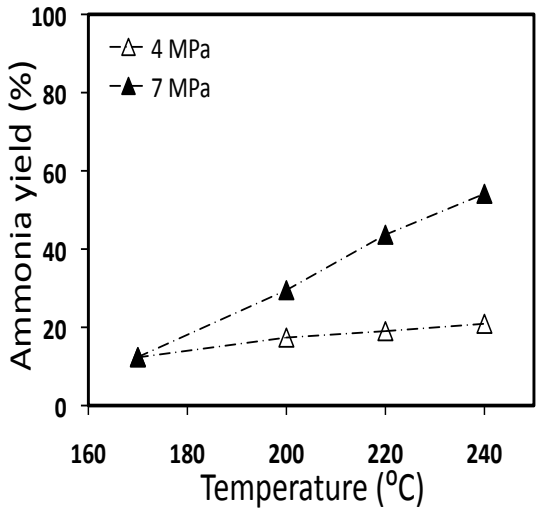

Figure 4.16 Effect of system pressure on the yield of ammonia at varying temperatures after 90 min.

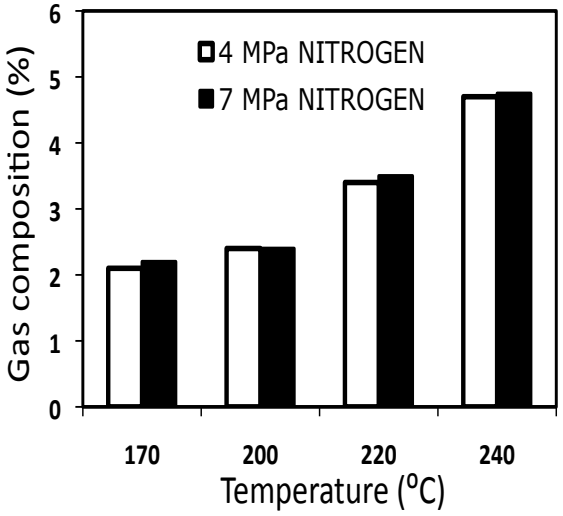

Figure 4.17 Effect of system pressure on gas composition at varying temperatures after 90 min.

Figure 4.16 illustrates the effect of system pressure on the yield of ammonia, it clearly shows that a lower the system pressure results in a reduced ammonia. The ammonia yields obtained at 4 MPa increase from 12% (24 mg/L) to 21% (54 mg/L), in the temperature range studied. Therefore operating the system at lower pressures favours a lower yield of ammonia but lowers the removal of DBU and TOC.

Figure 4.17 shows that reducing the system pressure from 7 MPa to 4 MPa did not affect the percentage of nitrogen in the gas sample, no carbon dioxide was detected in the gas sample and followed a general trend of increasing as the temperature increased.

4.7 Effect of Initial DBU Concentration

These experimental runs were undertaken to evaluate the effect of initial DBU concentration on DBU and TOC removal, and ammonia yield. The runs were undertaken at 240 ºC, 7 MPa, 0.4 L/min of oxygen. The initial concentrations investigated were 6 mM, 12 mM and 18 mM. Figures 4.18a and 4.18b show the effect of varying the initial concentration.

There is no marked increase in overall DBU removal as the initial concentration increased, Figure 4.19 shows that at all concentrations investigated the rate of DBU removal for each concentration is in the same range. This indicates that the oxidation of DBU is strongly influenced by the system temperature and the effect of initial concentration is hidden / masked by this. To verify this, the same initial concentrations were repeated at a lower temperature, 200 ºC, there was also no marked increase in the overall DBU removal as the initial concentration increased. Ashraf-Ball (2005) also found that above an initial DBU concentration of 6 mM, the increase in DBU removal is minimal, in the study of DBU oxidation, at a concentration range between 1 and 9 mM.

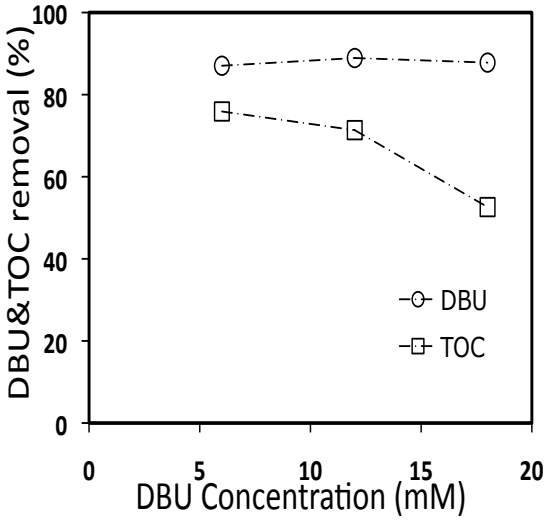

Figure 4.18a Effect of initial concentration on the removal of DBU and TOC at 240 ºC, 7 MPa and 0.4 L/min^{-1}

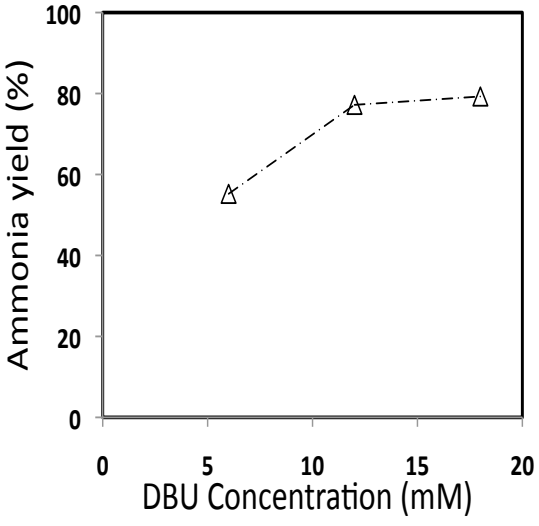

Figure 4.18b Effect of initial concentration on ammonia yield at 240 ºC, 7 MPa and 0.4 L/min^{-1}

TOC removal decreased from 76% to 53% as the initial DBU concentration increased, Figure 4.20 illustrates the TOC removal versus time for the three initial concentrations. It is of interest to note that there was no induction phase seen as the concentration increased, indicating that free radicals are readily generated for the reaction to proceed. It might be assumed that the reduction in TOC removal might be due to the system operating in an oxygen lean atmosphere, although the reduction in TOC removal is more likely due to the greater concentration of slightly recalcitrant intermediates formed as the initial DBU concentration increased, which are oxidised over a longer time greater than the residence time used in this study. This is illustrated by the graph of 12 mM initial concentration in Figure 4.20, where the value of TOC removal rose steadily, but is less than that of 6 mM, until time t = 80, where it experienced a sharp rise to a final value closer to that of 6 mM. If the residence time were increased there is good reasoning to suggest that TOC removal of the 18 mM initial concentration graph would increase to a value closer to the lower concentrations.

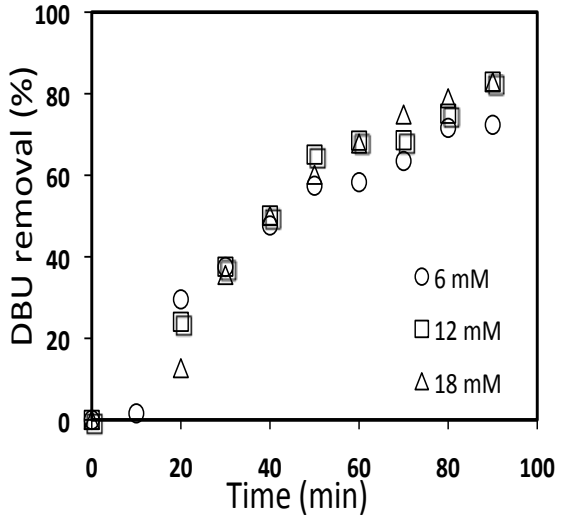

Figure 4.19 DBU removal for varying DBU initial concentrations at 240 ºC, 7 MPa, 0.4 L/min O_2

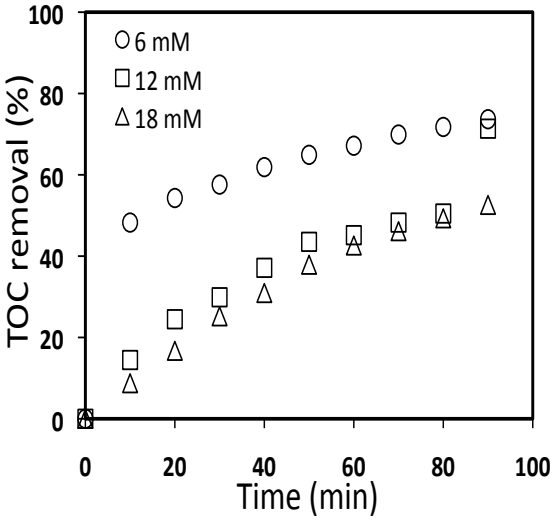

Figure 4.20 TOC removal for varying DBU initial concentrations at 240 ºC, 7 MPa, 0.4 L/min O_2

The yield of ammonia increased as the initial from 55% to 79% as the initial DBU concentration increased. The yield rose sharply from 6 mM to 12 mM, and then plateaued till 18 mM.

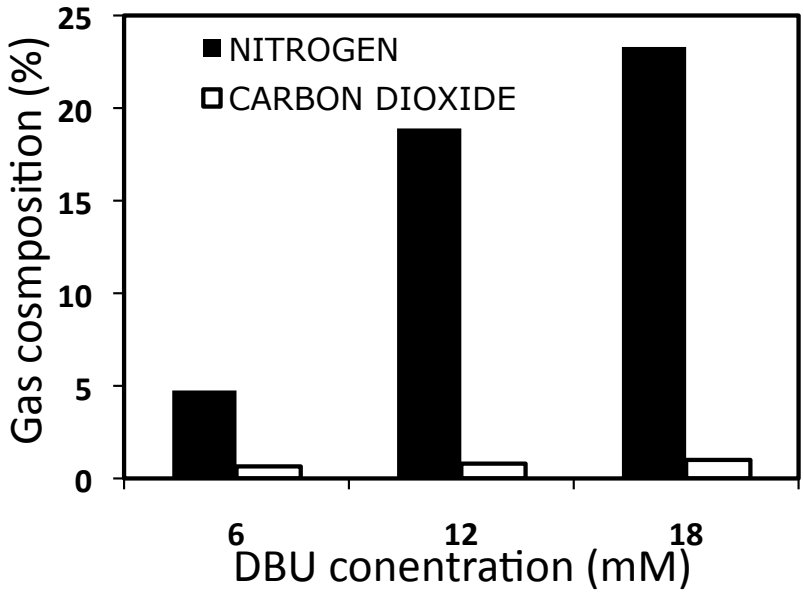

Figure 4.21 Effect of varying DBU initial concentration on the gas composition at 240 ºC, 7 MPa, 0.4 L/min O_2.

The percentage of nitrogen in the gas sample increased with initial concentration, which is inline with the trend seen in this work, where increased ammonia yield also result in increased nitrogen in the gas. The change in the percentage of carbon dioxide was minimal as the initial concentration increased, it was expected that there would be a larger increase, but the lower TOC removal values indicate that less organic carbon in the system would be oxidised to carbon dioxide.

4.8 Effect of Oxygen Flow rate

These experimental runs were undertaken to evaluate the effect of oxygen flow rate on DBU and TOC removal, and ammonia yield. The runs were undertaken at 240 ºC, 7 MPa, and an initial DBU concentration of 6 mM. The oxygen flow rate was varied between 0 - 1.0 L/ min. Figures 4.22a and 4.22b show the effect of varying the oxygen flow rate.

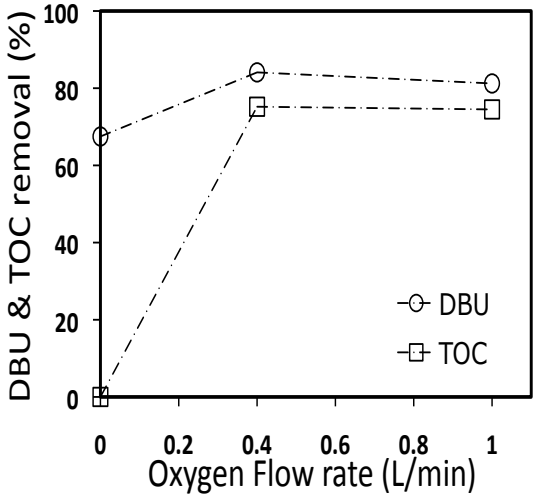

Figure 4.22a The effect of oxygen flow rate on DBU and TOC removal at 240 ºC and 7 MPa

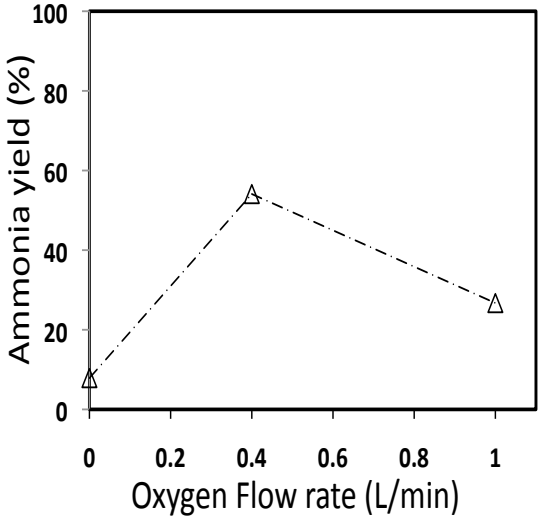

Figure 4.22b The effect of oxygen flow rate on ammonia yield at 240 ºC and 7 MPa

In the absence of oxygen flow, 0.0 L/min, there was 68% DBU removal, 0% TOC removal and an 8% (19 mg/L) yield of ammonia. These results are due to pyrolysis occurring, as explained in section 4.1.3, the DBU removed was not oxidised but was converted into polymers, smaller organic compounds and ammonia. The increase in oxygen flow rate to 0.4 L/min resulted in increased DBU removal by 16% to 84%, the DBU removal at this flow rate is due to oxidation and is confirmed by the increase in TOC removal to 75%. Ammonia yield also increased to 54% (124 mg/L). Increased oxygen flow rate, resulted in no further removal of DBU and TOC removal, but it reduced the yield of ammonia to 27% (71 mg/L). This result suggests the increased concentration of oxygen due to increased partial pressure (2.7 MPa) at 1.0 L/min did not react primarily with DBU or other organic compounds, but was involved in the oxidation of ammonia. of nitrogen, therefore the increased formation of nitrogen above

0.4 L/min indicates that ammonia is a recalcitrant intermediate in nitrogen formation. Increased oxygen flow rate above 0.4 L/min did not affect the formation of carbon dioxide.

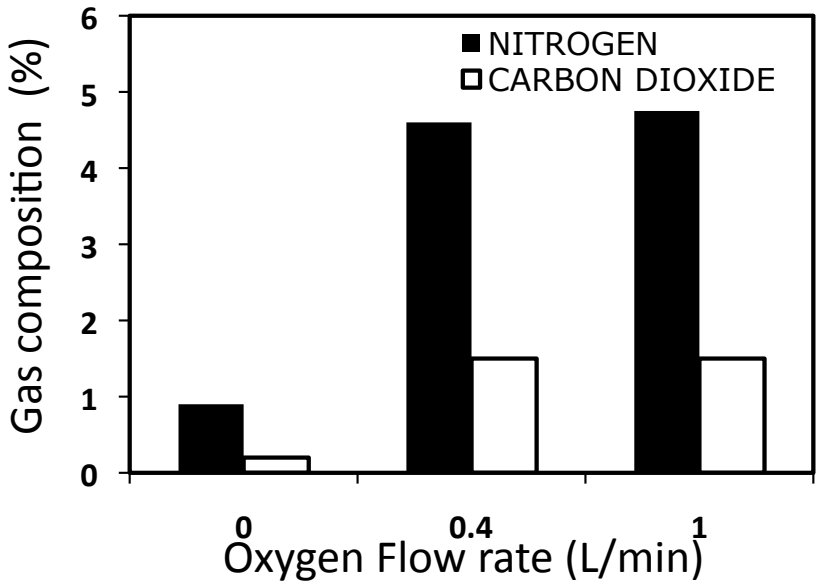

Figure 4.23 The effect of oxygen flow rate on the gas composition at 240 ºC and 7 MPa

4.9 Summary

The current results show that good removal of DBU and TOC, with values between 27% - 84% and 7% - 75% respectively, is possible for the temperature and pressure ranges investigated, but at these conditions, there tends to be a high yield of ammonia, an undesirable intermediate. The yield of ammonia ranged from 12% (24 mg/L) to 54% (119 mg/L), this is far above the permitted amount of ammonia in water set by environmental regulators, which should be less than 10 mg/L. Effluent from the above process has ammonia concentration ten times more than that in environmental regulations and would therefore require either, a further treatment step, Increased temperature and pressure, or the use of a catalyst to achieve the regulations.

Increasing the initial DBU concentration did not influence DBU removal but reduced TOC removal and increased ammonia yield for the residence time, t = 90 min.

The oxidation kinetics of DBU solutions were investigated at 4 MPa, 7 MPa and 170 - 240 ºC. A pseudo first order rate expression was used to satisfactorily fit the oxidation of DBU at 4 and 7 MPa, with an activation energy of 72.7 kJ mol^{-1} and 78.7 kJ mol^{-1} and pre-exponential factor of 1.94 x 10^5 min^{-1} and 1.62 x 10^6 min^{-1} at 4 MPa and 7MPa respectively.

CHAPTER 5 - CATALYTIC WET AIR OXIDATION OF DBU

This section presents the results and discussion of experiments performed to study the catalytic wet air oxidation of DBU. The aim of the study was to investigate the effect of catalysts to enhance complete oxidation of DBU under milder conditions compared to a non-catalytic system, and to determine the effect of various operating variables in order to establish optimised conditions necessary to achieve complete oxidation. Kinetic analysis and modeling are also presented in this chapter.

5.1 Catalyst Screening

Various catalysts have been tested for the oxidation of organic hydrocarbon pollutants, and a general consensus is, that their choice of catalyst was influenced by the nature of the organic pollutant (Imamura, 1999, Luck, 1996, Rivas *et al.*, 1998, Gomes *et al.*, 2005, Ukropec *et al.*, 1999, Oliviero *et al.*, 2000, Aymonier *et al.*, 2000, Imamura *et al.*, 1982, Pintar and Levec, 1994, Takayama *et al.*, 1999, Chang *et al.*, 1995, Zhang and Chuang, 1998). It was decided to screen a selection of catalysts, which had been successfully used in the oxidation of organic hydrocarbons. All catalysts were screened at the same reaction conditions (240 ºC, 7 MPa, 0.4 L/min O2 and 500 rpm) and the subsequent results after 90 minutes are displayed as TOC values in Figure 5.1.

From Figure 5.1, only 3% and 0.5% ruthenium supported on alumina (Ru/Al_2O_3) pellets enhanced TOC removal, while other catalysts screened were not active for TOC removal. This is line with the findings of Imamura (1999). Ruthenium on various supports was found to be active for the oxidation of morpholine (a nitrogen containing compound) by

Gunale and Mahajani (2008b), Oliviero *et al*.,(2003) found that Ru was more active than Pt, Pd and CeO_2 for the oxidation of Aniline.

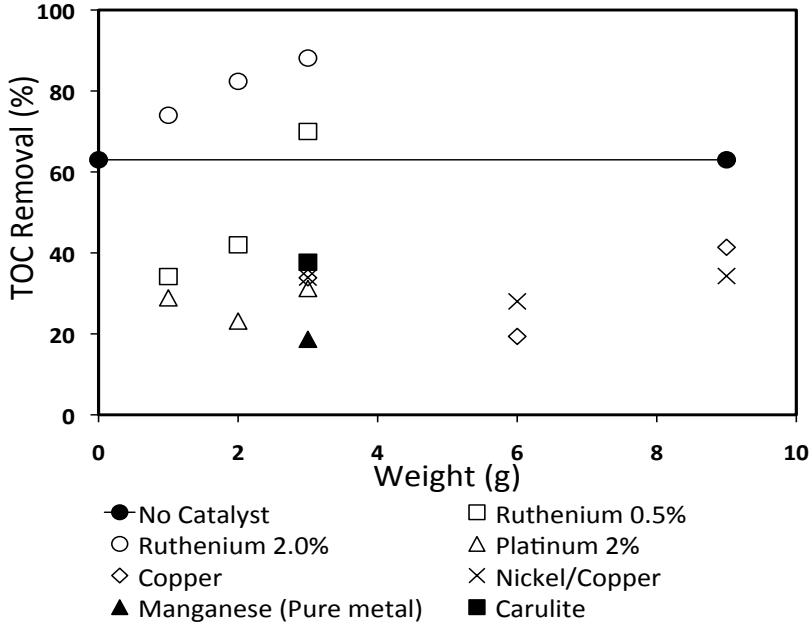

Figure 5.1 Catalyst screening to evaluate activity for TOC removal.

It is assumed that the non-active catalysts interfered with the reaction mechanism such as formation of free radicals that initiate oxidation, by converting them into less active forms or removing them from the reaction (Satterfield, 1980).

This is in line with findings by Imamura (1999), who found Ruthenium supported on Ceria (Ru/CeO_2) to be more active than Manganese supported on Ceria (Mn/CeO_2) and Copper catalysts for the oxidation polyethylene glycols, n-butylamine and pyridine. Therefore ruthenium supported on alumina (Ru/Al_2O_3) pellets were selected as the catalyst for further investigation. Based on the screening results, commercially available 3% Ru/Al_2O_3 pellets were selected for further investigation, and in specific experiments 0.5% Ru/Al_2O_3 pellets were used.

In all experiments the actual weight of catalyst used was: 1 g for 3.0% Ru/Al_2O_3 and 3 g for 0.5% Ru/Al_2O_3, unless stated otherwise. The specific weights were selected based on

TOC removal values. For 0.5% Ru/Al_2O_3, 3 g was the only weight that enhanced TOC removal, and for 3.0% Ru/Al_2O_3, 1 g gave an increased TOC removal and was more economical for further investigation.

5.2 External Mass Transfer

As discussed in chapter 4.1.2, the elimination of mass transfer resistance is important. Runs were performed at different impeller speeds to verify this and it was also found that above 500 rpm, the oxidation rate was independent of the impeller speed, thus the reaction is not mass transfer limited. This is shown in Figure 5.2. These runs were carried out under the following experimental conditions: 240 ºC, 7 MPa, 6 mM DBU, 0.4 L/min O_2, 3 g of 0.5% Ru/Al_2O_3.

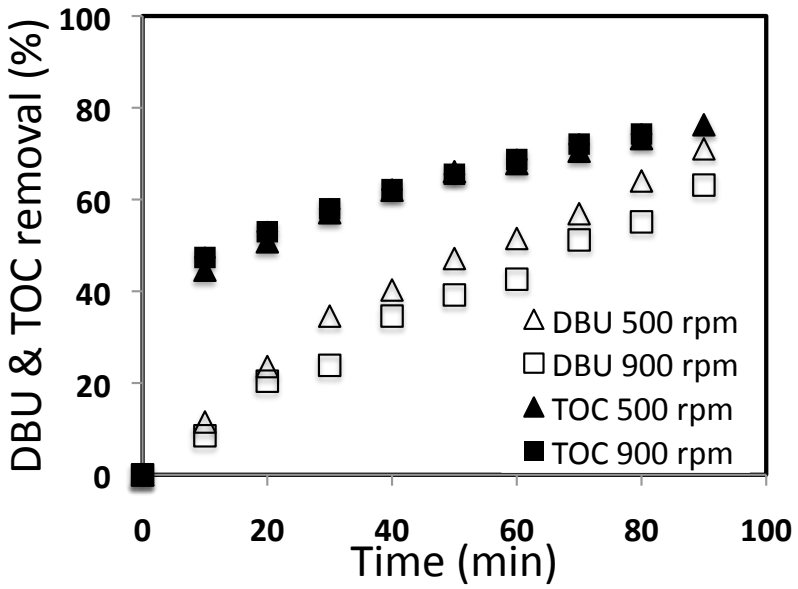

Figure 5.2 Effect of varying impeller speed on DBU and TOC removal at 240 ºC and 7 MPa

5.3 Catalyst Characterisation

The selected Ruthenium catalysts were characterised by different analytical techniques as described in Chapter 3. Results of the various characterisations are summarised here.

Figure 5.3 shows the adsorption and desorption isotherm for the Ru/Al_2O_3 catalyst obtained using BET analysis, the isotherm is classed as a type IV isotherm (Bond, 1987), the hysteresis loop present indicates open-ended cylindrical pores are predominant for the catalyst. The change in adsorption and desorption path is called a hysteresis loop, which is because the evaporation (desorption) of condensed gas in the fine pores does not occur as easily as its condensation (adsorption).

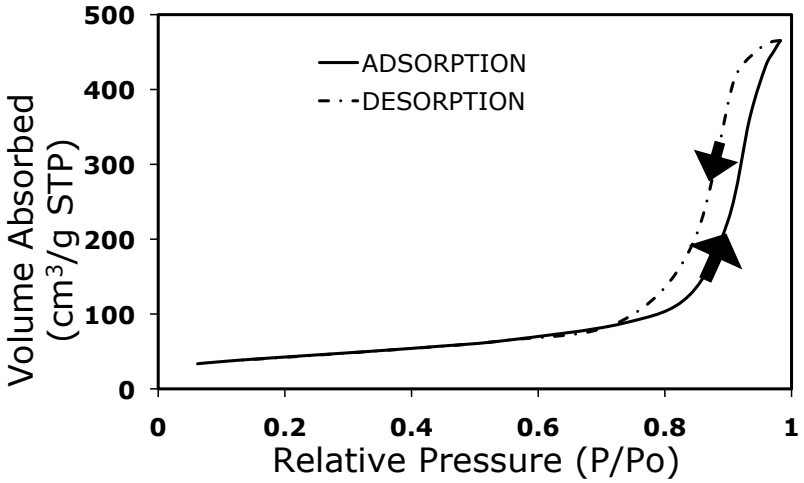

Figure 5.3 BET Adsorption and desorption isotherm for 3% Ru/Al_2O_3 catalyst

Metal loading (%)	BET Surface Area (m^2/g)	External Surface Area (m^2/g)	Micropore Volume ($cm^3/g \times 10^{-3}$)	Average Pore Diameter (nm)
0.5	80	77.2	3.94	10.98
3.0	153	135	6.85	18.62

Table 5.1 Characterisation of Ru/Al_2O_3 catalyst

Figure 5.4 shows a cross-sectional vertical slice of the Ru/Al_2O_3 catalyst as analysed using X-ray micro-tomography. It can be seen that the catalyst has 2 distinct regions, a non porous Al_2O_3 core, highlighted in blue, and an outer ruthenium metal layer highlighted in green. This suggests that all reactions that would occur using Ru/Al_2O_3 catalysts would be primarily surface catalysed reactions, which is confirmed by the high total surface area values as determined by BET analysis (Table 5.1). The average pore diameter for both catalysts is also in the mesopore region (2-50 nm), which is usually representative of surface catalysed reactions on non porous catalysts (Lopes *et al.*, 2007). Figure 5.5 shows an SEM of the catalyst surface morphology.

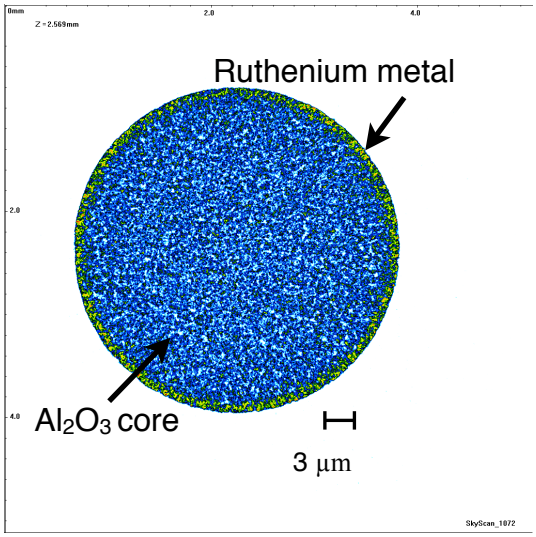

Figure 5.4 A vertical slice of the catalyst obtained used X-ray micro tomography.

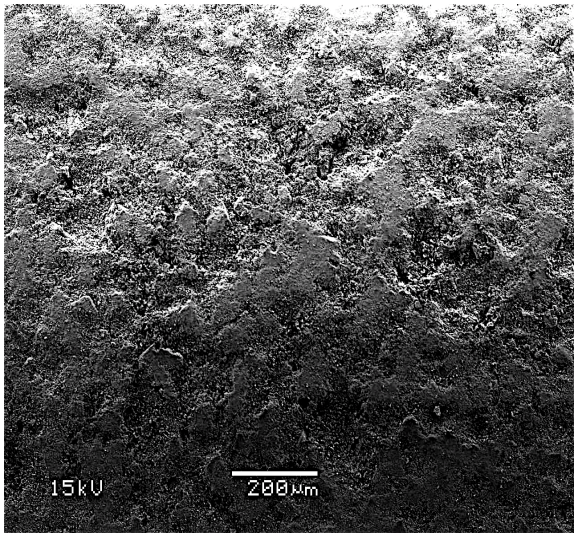

Figure 5.5 Catalyst surface at 95x magnification

5.4 Effect of System Temperature

The effect of temperature on DBU removal is shown in Figure 5.6 after a reaction time of 90 minutes, at a pressure of 7 MPa, DBU initial concentration of 6 mM, and an oxygen flow rate of 0.4 L/min.

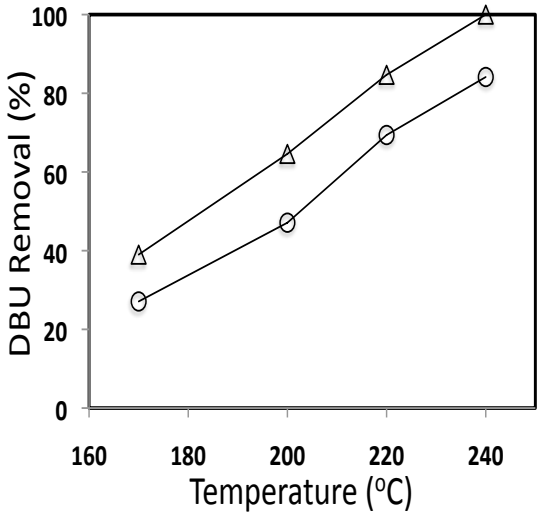

Figure 5.6 Effect of operating temperature on DBU removal at 7 MPa after 90 min residence time. WAO (◯), 3.0% Ru/Al_2O_3 (△)

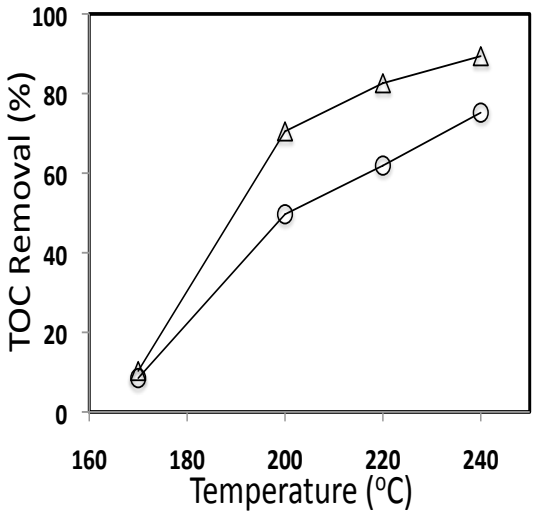

Figure 5.7 Effect of operating temperature on TOC removal at 7 MPa after 90 min residence time. WAO (◯), 3.0% Ru/Al_2O_3 (△)

DBU removal increased with increased temperature using 3% Ru/Al_2O_3 pellets. At all temperatures investigated the use of catalyst enhanced DBU removal when compared to WAO. 100% DBU removal was achieved at 240 ºC using the 3.0% Ru/Al_2O_3 catalyst, while 39% DBU removal is achieved at 170ºC.

Using 3% Ru/Al_2O_3 pellets at a lower temperature, DBU removal values in a similar range to WAO at a higher temperature were achieved. For example, 43% DBU removal is achieved at 200 ºC without a catalyst, while 39% DBU removal is achieved at 170 ºC using 3% Ru/Al_2O_3 pellets. This trend continues with increased temperature.

TOC removal increased with temperature using 3% Ru/Al_2O_3 pellets with a maximum TOC removal of 89% at 240 ºC. 3% Ru/Al_2O_3 pellets enhanced TOC removal when compared to WAO. Using 3% Ru/Al_2O_3 pellets at a lower temperature, TOC removal values in a similar range to WAO at a higher temperature was achieved. 75% TOC removal is achieved at 240 ºC without a catalyst, while 71% TOC removal is achieved at 200 ºC using 3% Ru/Al_2O_3 pellets. This showed that similar TOC removal can be achieved 3% Ru/Al_2O_3 pellets at milder temperatures with up to a 40 ºC reduction in system temperature. DBU removal is higher than TOC removal using the 3% Ru/Al_2O_3 pellets, indicating that some DBU was oxidised into other organic compounds.

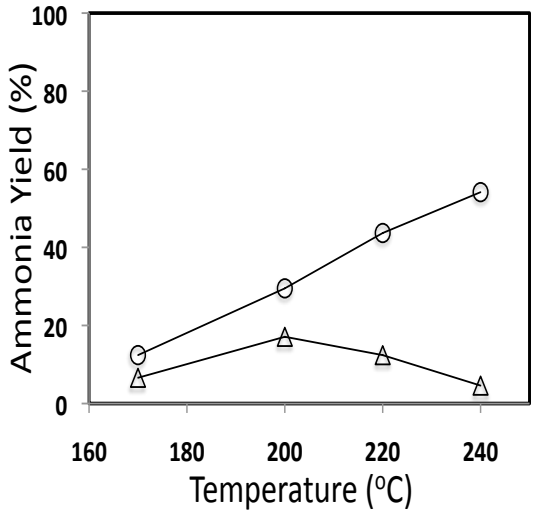

Figure 5.8 Effect of operating temperature on Ammonia yield at 7 MPa after 90 min residence time. WAO (◯), 3.0% Ru/Al_2O_3 (△)

3% Ru/Al_2O_3 pellets showed a significant decrease in the yield of ammonia, compared to WAO at all temperatures investigated. The ammonia yield initially increased from 6.6% to 17.1%, then decreased to a final value of 4.6% as the temperature increased. At the highest temperature investigated, 240ºC, the yield of ammonia was reduced from 54.1% (WAO) to 4.6% (3.0% Ru/Al_2O_3 pellets). A significant decrease of 49.5% was obtained using the 3.0% catalyst. This shows that Ruthenium supported on Alumina is very active for ammonia oxidation. The above result agrees with Qin and Aika(1998), who found that Ru/Al_2O_3 exhibited an ammonia removal efficiency of 99% at 230 ºC in the oxidation of ammonia by various noble metals. Gunale and Mahajani (2010) also found that ammonia yield decreased by up to 20% as temperature increased in their investigation of Ru/TiO_2 catalysed oxidation of N-ethylethanolamine. They

attributed this to ammonia being oxidised by O_2 adsorbed on the Ru actives sites. Lee (2003) confimred that ammonia catalysed by a ruthenium catalyst (Ru/TiO_2) progressed via the following reaction mechanism:

$$O_2(aq) + 2* \rightleftarrows 2O* \quad (5.1)$$

$$NH_3(aq) + O* \rightarrow NH* + H_2O \quad (5.2)$$

$$NH* + O* \rightleftarrows NHO* + * \quad (5.3)$$

$$NHO* + O* \rightarrow HNO_2 + 2* \quad (5.4)$$

$$HNO_2 \rightleftarrows H^+ + NO^-_2 \quad (5.5)$$

$$NH_3(aq) + H^+ \rightleftarrows NH^+_4 \quad (5.6)$$

$$NO^-_2 + NH^+_4 \rightarrow N_2 + 2H_2O \quad (5.7)$$

where, * represents a catalytic active site at a vacant state. Initially dissolved oxygen is adsorbed onto two active sites in close proximity, dissociating into two activated oxygen species. The oxygen species then react with ammonia, resulting in the formation of nitrous acid, HNO_2, which dissociates to form a nitrite ion and a proton. The formation of protons, shifts the reaction equilibrum favouring the formation of ammonium ions, NH^+_4. The subsequent reaction between ammonium and nitrous ions results in N_2 formation.

The above mechanism can be applied to Ru/Al_2O_3 catalysts, because Gunale and Mahajani (2008a), found that the metal-support interaction of ruthenium on varying supports (TiO_2, Al_2O_3, SiO_2 and CeO_2) was negligible on the conversion of morpholine and to the increased formation of N2 using 3% Ru/Al_2O_3 pellets.

Figures 5.9 and 5.10 show the effect of temperature on the gas composition in the samples at t = 90 mins. N_2 and CO_2 formation increased with temperature. For all temperatures investigated the CWAO runs gave increased amounts of N_2 and CO_2 compared to WAO, due with the increased TOC removal and decreased ammonia yield. 3% Ru/Al_2O_3 pellets enhanced selectivity to N_2 and CO_2, similar results were found by Grosjean *et al*., (2010) in their study of DMF oxidation using supported Ru catalysts.

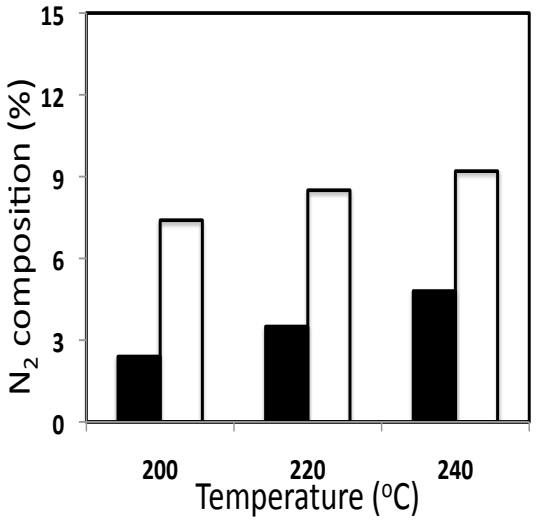

Figure 5.9 Effect of temperature on N_2 formation at 7 MPa after 90 min residence time. WAO(■), 3.0% Ru/Al_2O_3 (□)

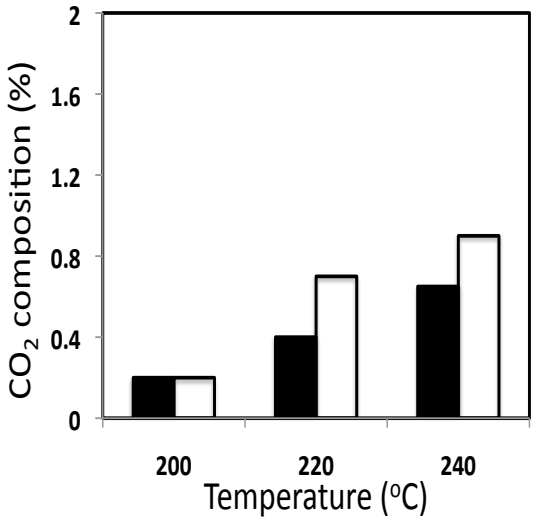

Figure 5.10 Effect of temperature on CO_2 formation at 7 MPa after 90 min residence time. WAO(■), 3.0% Ru/Al_2O_3 (□)

5.5 Kinetic Study

The objective of the present kinetic analysis is to determine the reaction rate constant (k), its associated Arrhenius parameters, and the reaction order for DBU for the Global Power Law rate equation. (Levenspiel, 1972)

$$-r_{DBU} = \frac{-dC_{DBU}}{dt} = k\left[DBU\right]^{m} \tag{5.8}$$

Shende and Mahajani (1994) and Klinghoffer *et al*.,(1998), showed that catalytic experimental data can be assessed using power law kinetic expression, where the pseudo first order rate constant is replaced by an Arrhenius dependence on temperature as shown in (5.9). In the global power law evaluation for CWAO, the reaction order of the organic compound (in terms of actual concentration or TOC) is reported as having a value of 1 or close to 1 (Eftaxias *et al.*, 2001, Stuber *et al.*, 2005, Shende and Mahajani, 1994)

$$-r_{DBU} = \frac{-dC_{DBU}}{dt} = A\exp\left(-\frac{Ea}{RT}\right)\left[DBU\right] \tag{5.9}$$

$-r_{DBU}$ *has units of* $\frac{mol_{DBU}}{g_{cat}\,\min}$

The above psuedo first order approximation assumes a constant stoichiometric excess of oxygen in the liquid phase. The oxygen term is lumped into the apparent pseudo first order rate constant (*k*). Pintar and Levec (1994) and Vaidya and Mahajani (2002) found experimentally that the reaction order for oxygen in CWAO systems ranged between 0 - 0.5. Separating and integrating equation (5.8), equation (5.10) is obtained

$$-\ln\frac{C_{DBU}}{C_{DBU_0}} = kt \tag{5.10}$$

The values of *k* are obtained from a plot of the natural logarithm of DBU concentration divided by initial DBU concentration versus residence time as shown in Figure 5.11

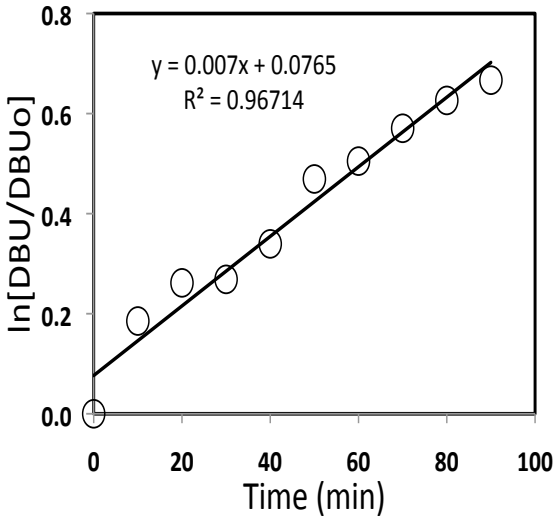

Figure 5.11 Natural log of DBU concentration versus time at 240 ºC and 7 MPa

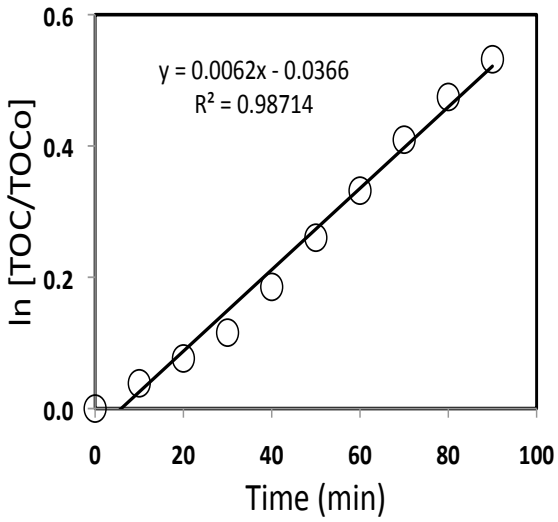

Figure 5.12 Natural log of TOC concentration versus time at 240 ºC and 7 MPa

k was then evaluated for all experimental runs. The *k* values obtained for CWAO and WAO are shown in Table 5.2.

Temperature (°C)	Pressure (MPa)	Catalyst metal loading (%)	Weight of catalyst (g)	k_{DBU}x10^{-3} (min^{-1})
200	7	-	-	3.3
220	7	-	-	7.5
240	7	-	-	15.7
200	7	3	1	7
220	7	3	1	12.7
240	7	3	1	17.9

Table 5.2 DBU First order rate constants for WAO and CWAO (3.0% Ru/Al_2O_3) at 7 MPa

The first order rate constants for WAO and CWAO are shown in Table 5.2. At 200 ºC, the pseudo first order rate constant doubles from 3.3 x 10^{-3} min^{-1} to 7 x 10^{-3} min^{-1} when the catalyst is used.This enhancement of the pseudo first order rate constant is also seen at 220 ºC

and 240 ºC. Gunale and Mahajani (2008b) found a similar result during the oxidation of morpholine using a Ru/TiO_2 catalyst. The rate of p-nitrophenol oxidation was also enhanced by the addition of a catalyst (Kayan and Gizir, 2005)

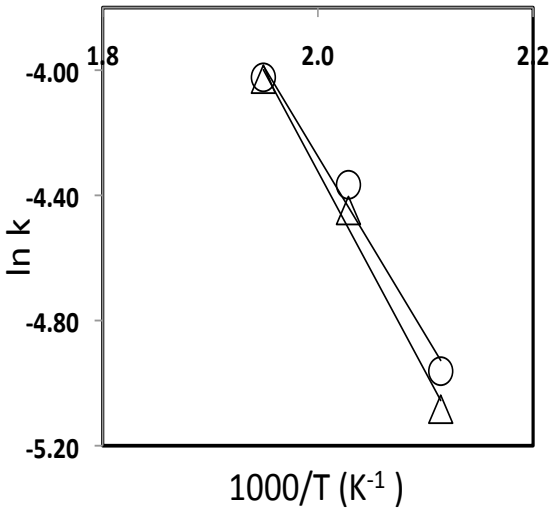

Figure 5.13 Arrhenius graph for DBU and TOC oxidation at 7 MPa using 3% Ru/Al_2O_3; DBU(△), TOC (◯).

The pre-exponential constant, A and the activation energy, Ea, for each set of temperatures were calculated by performing a linear fit of ln *k* versus 1000/T as shown in Figure 5.13.

The values of *Ea* and A calculated are shown in Table 4.3. The value of *Ea* and A at 7 MPa were 47.5 kJ mol^{-1} and 1.27 x 10^3 min^{-1} respectively. As such, the resulting pseudo first order rate expression for the oxidation of DBU in the temperature range investigated at a pressure of 7 MPa is given by:

$$-r_A = 1.27 \text{ x } 10^3 \text{ min}^{-1} \text{e}\left(-\frac{47500 J\ mol^{-1}}{RT}\right)[C_{DBU}] \qquad (5.11)$$

Pressure (MPa)	Catalyst metal loading (%)	Weight of catalyst (g)	*Ea* (kJ mol^{-1})	A (min^{-1})
4	-	-	72.7	1.94 x 10^5
4	3	1	50.1	1.03 x 10^3
7	-	-	78.7	1.62 x 10^6
7	3	1	47.5	1.27 x 10^3

Table 5.3 DBU Activation energy and pre-exponential constant for WAO and CWAO

The value of *Ea* and A at 4 MPa were 50.1 kJ mol^{-1} and 1.03 x 10^3 min^{-1} respectively. As such, the resulting pseudo first order rate expression for the oxidation of DBU in the temperature range investigated at a pressure of 4 MPa is given by:

$$-r_A = 1.03 \text{ x } 10^3 \text{ min}^{-1} \text{e}\left(-\frac{50100 J\ mol^{-1}}{RT}\right)[C_{DBU}] \qquad (5.12)$$

3.0% Ru/Al_2O_3 pellets reduced the activation energy required for the oxidation of DBU by 31 kJ mol^{-1} at 7 MPa and 22 kJ mol^{-1} at 4 MPa. The activation energy for 3.0% Ru/Al_2O_3 pellets at 4 and 7 MPa are in the same range, signifying the effect of pressure on the activation energy of DBU is negligible.

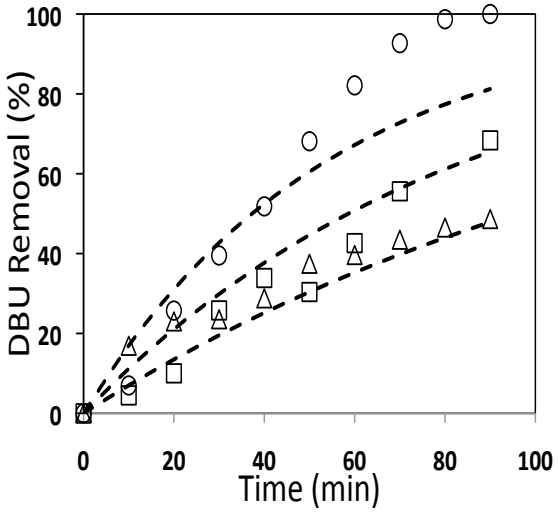

Figure 5.14 DBU removal against residence time for several temperatures at 7 MPa.Symbols represent experimental data and the lines denote first order model predictions.
240ºC (○), 220ºC (□), 200ºC (△)

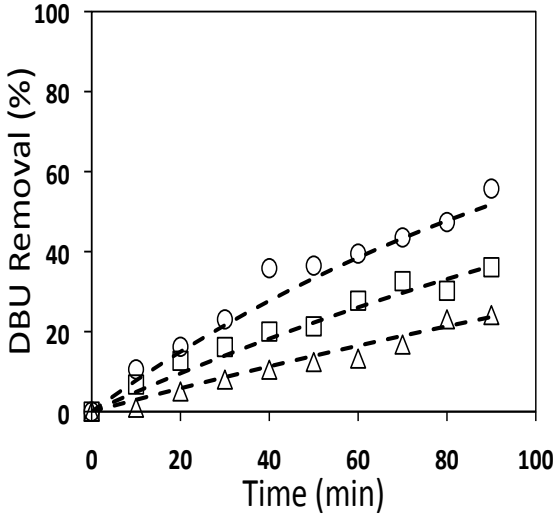

Figure 5.15 DBU removal against residence time for several temperatures at 4 MPa.Symbols represent experimental data and the lines denote first order model predictions.
240ºC (○), 220ºC (□), 200ºC (△)

The pseudo first order rate expressions given by equations 5.9 and 5.10 are compared against experimental data in Figures 5.14 and 5.15. There is good correlation between the experimental data and the fitted rate expressions for all data at 4 and 7 MPa. Although the rate

expression under-predicts DBU removal at 240 ºC and 7 MPa, due to an sharp increase in the reaction rate.

The pseudo first order rate constants were calculated for TOC at 7 MPa as shown in Figure 5.12 and Table 5.4. The Arrhenius parameters calculated as shown in Figure 5.13.

Temperature (°C)	Pressure (MPa)	Catalyst metal loading (%)	Weight of catalyst (g)	$k_{TOC}x10^3$ (min^{-1})
200	7	3	1	6.2
220	7	3	1	11.7
240	7	3	1	17.8

Table 5.4 TOC First order rate constants for CWAO (3.0% Ru/Al_2O_3) at 7 MPa

The value of *Ea* and A at 7 MPa for TOC were 53.3 kJ mol^{-1} and 4.92 x 10^3 min^{-1} respectively. As such, the resulting pseudo first order rate expression for the oxidation of TOC in the temperature range investigated at a pressure of 7 MPa is given by:

$$-r_A = 4.92 \text{ x } 10^3 \text{ min}^{-1} \text{e}\left(-\frac{53300 J\ mol^{-1}}{RT}\right)[C_{TOC}] \qquad (5.13)$$

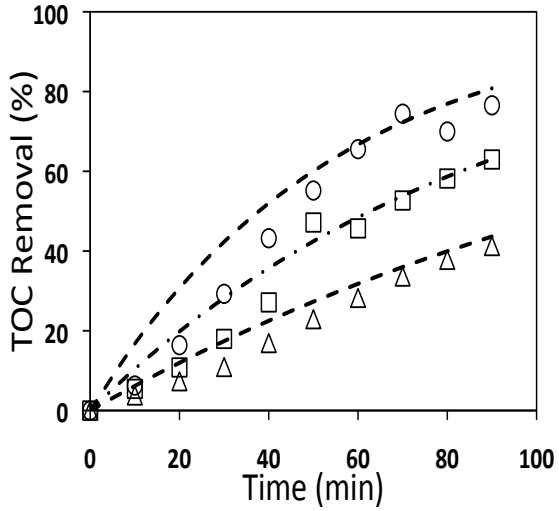

Figure 5.16 TOC removal against residence time for several temperatures at 7 MPa. Symbols represent experimental data and the lines denote first order model predictions.
240ºC (○), 220ºC (□), 200ºC (△)

The pseudo first order rate expression for TOC above, was compared against experimental results in Figure 5.16. There is a good agreement between the experimental data and the fitted rate expression.

5.6 Effect of System Pressure

A comparative set of experiments were investigated to determine the effect of system pressure on DBU removal, TOC removal and Ammonia yield. 4 and 7 MPa were the pressures investigated, with an initial DBU concentration of 6 mM, and an oxygen flow rate of 0.4 L/min, using 1 g of 3% Ru/Al_2O_3 pellets.

Figures 5.17 and 5.18 show the effect of system pressure on DBU and TOC removal. At 220 ºC DBU removal is enhanced by 30%, this pressure enhancement is slightly reduced at other temperatures. TOC removal was enhanced by 15% as the temperature increased. Increased DBU and TOC removal with increased pressure is due to the enhanced solubility of oxygen in water and increased concentration of oxygen available for reaction in the aqueous phase (Chapter 4.1.2). Silva *et al*., (2003) found a similar trend of TOC removal increasing as they increased the partial pressure of oxygen from 1 MPa to 3.5 MPa for the catalytic wet air oxidation of formaldehyde.

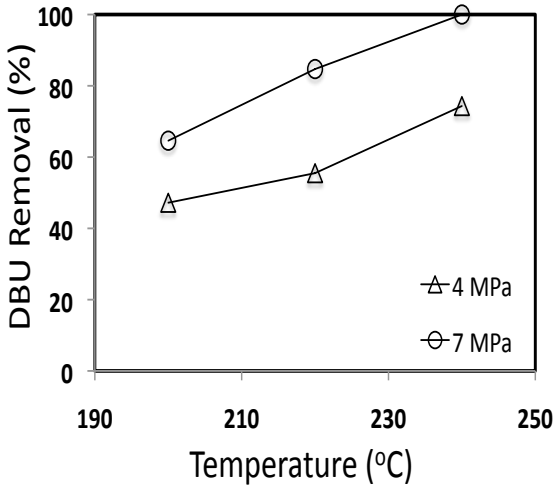

Figure 5.17 Effect of system pressure on DBU removal after 90 min residence time using 3.0% Ru/Al_2O_3 pellets.

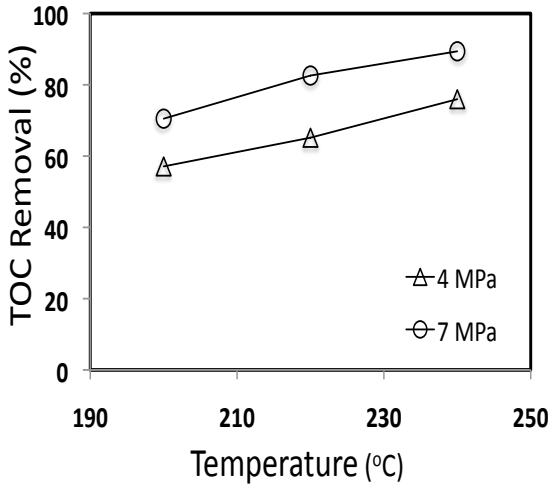

Figure 5.18 Effect of system pressure on TOC removal after 90 min residence time using 3.0% Ru/Al_2O_3 pellets.

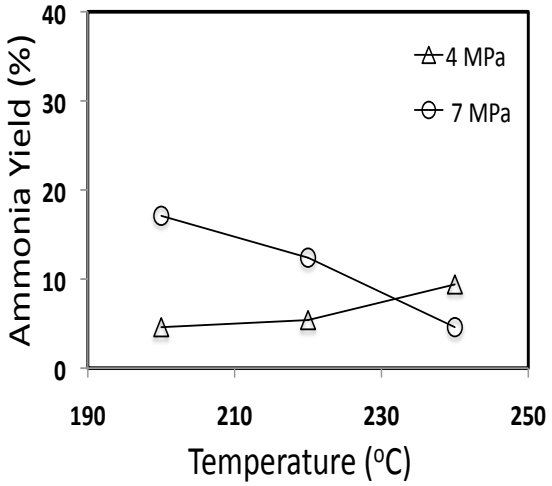

Figure 5.19 Effect of system pressure on ammonia yield after 90 min residence time using 3.0% Ru/Al_2O_3 pellets.

Initially ammonia yield increased with pressure apart from at 240 ºC, where it decreased from 11.7% to 4.6%. This difference indicates different reaction mechanism for the formation and oxidation of ammonia with increased pressure. N_2 and CO_2 formation increased with pressure as shown in Figures 5.20 and 5.21. This is due to increased TOC removal and decreased ammonia yield.

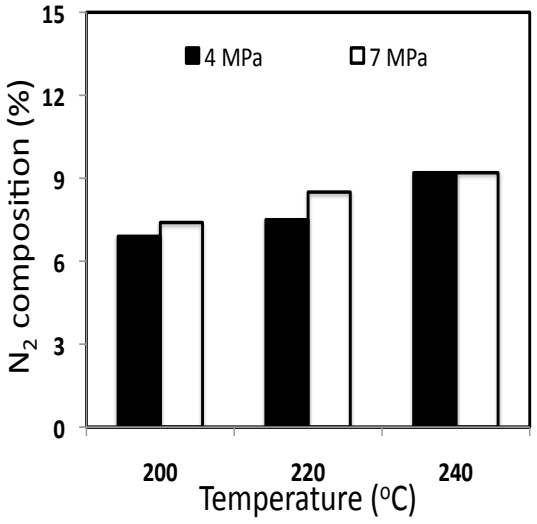

Figure 5.20 Effect of system pressure on N_2 formation after 90 min residence time using 3.0% Ru/Al_2O_3 pellets.

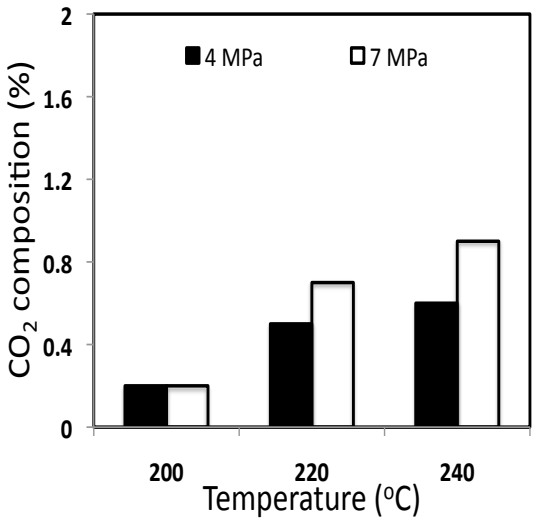

Figure 5.21 Effect of system pressure on CO_2 formation after 90 min residence time using 3.0% Ru/Al_2O_3 pellets.

5.7 Effect of Initial DBU concentration

These experimental runs were undertaken to evaluate the effect of initial DBU concentration on DBU and TOC removal and ammonia yield under CWAO conditions. The runs were undertaken at 240 ºC, 7 MPa, oxygen flow rate of 0.4 L/min and using 1 g of 3.0% Ru/Al_2O_3 catalyst. The initial concentrations investigated were 6 mM, 12 mM and 18 mM.

DBU removal showed a slight decrease from 100% to 82% as the initial concentration increased from 6 to 18 mM, TOC removal decreased from 89% to 53% as the initial DBU concentration increased. The initial rate of DBU removal is similar for the various concentrations of DBU but then decreased with increased DBU concentration as shown in Figure 5.23.

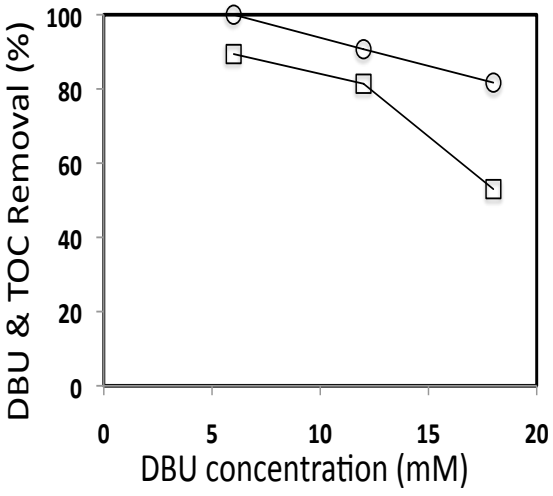

Figure 5.22 Effect of initial DBU concentration on DBU and TOC removal at 7 MPa, after 90 min residence time using 3.0% Ru/Al_2O_3. DBU (◯), TOC (□)

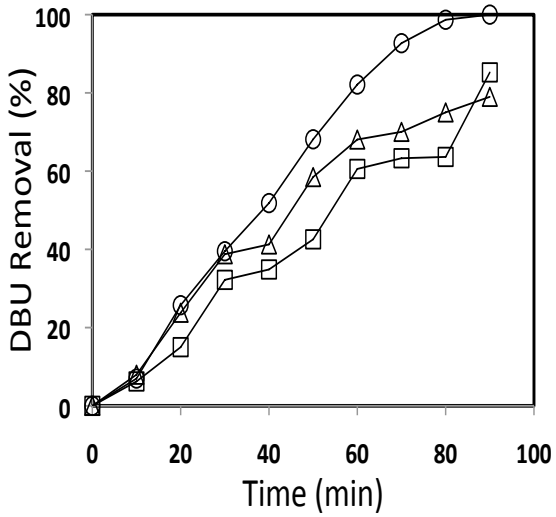

Figure 5.23 DBU removal against time at varying initial concentrations at 7 MPa using 3.0% Ru/Al_2O_3. 6 mM (◯), 12 mM (□), 18 mM (△)

It is was reported (Rebrov *et al.*, 2002) that noble metals, in this case Ruthenium, catalysed oxidations by adsorbing oxygen unto their active sites and then the adsorbed oxygen further reacts with the compound. Conversely it has been shown that DBU readily forms an metallo-organic complex with Ruthenium (Barker and Kilner, 1994), and this would be the first step

in the oxidation of DBU, followed by the chemisorption of oxygen and then the subsequent reactions. It is possible to assume that as the concentration of DBU increases, that more DBU molecules occupy a greater number of active sites that should be available for oxygen adsorption, thereby hindering the subsequent oxidation of DBU and removal of TOC. The reduction in TOC removal could also be due to the greater concentration of recalcitrant intermediates formed as the initial DBU concentration increased.

The yield of ammonia using 3.0% Ru/Al_2O_3 pellets (Figure 5.24) increased from 5% to 28% as the initial DBU concentration increased, with a sharp rise seen as the concentration increased from 12 mM to 18 mM. This can be explained based on the observations of Barker and Kilner (1994). It is likely that as more DBU or intermediate molecules are strongly adsorbed unto the active sites required for oxygen absorption hindering the adsorption of ammonia onto the catalyst surface for oxidation leading to higher yields.

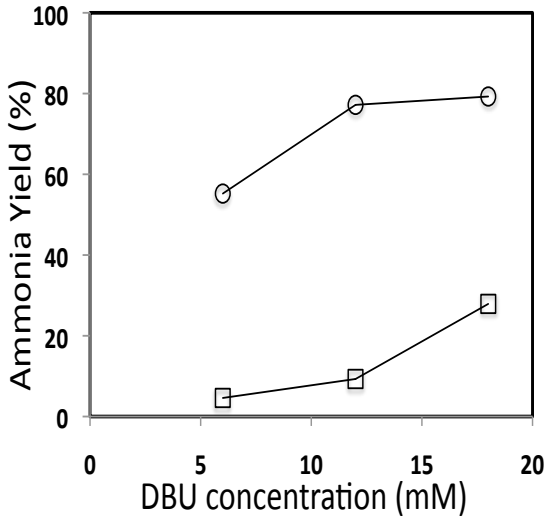

Figure 5.24 Effect of initial DBU concentration on Ammonia yield at 7 MPa after 90 min residence time.
WAO (○), 3.0% Ru/Al_2O_3 (□)

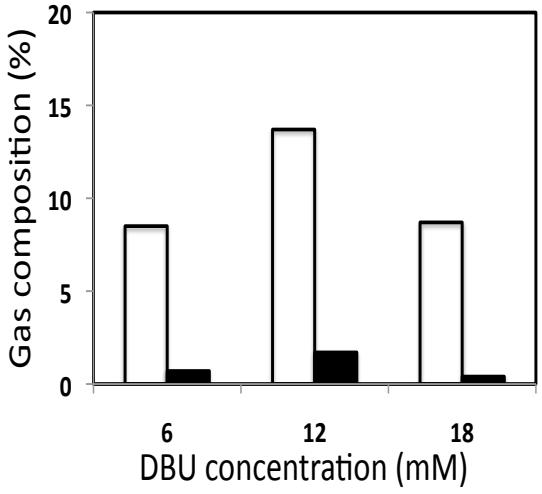

Figure 5.25 Effect of initial DBU concentration on N_2 and CO_2 formation at 7 MPa after 90 min residence time.
N_2(□), CO_2(■)

There is a significant decrease in the yield of ammonia under CWAO conditions, at 6 mM the difference in ammonia yield between WAO and CWAO was 51%, the difference then increased to 68% at 12 mM and then decreased back to 51% at 18 mM.

The percentage of nitrogen gas in the sample increased with initial concentration and then decreased after 12 mM, due to the increased ammonia yield at 18 mM, suggesting that the further oxidation of ammonia to nitrogen is hindered at high initial concentrations of DBU. The percentage of carbon dioxide increased slightly then decreased at 18 mM, this was due to decreased TOC removal.

5.8 Effect of Catalyst Metal Loading

Metal loading on the catalyst surface is a parameter that has been investigated by researchers (Gunale and Mahajani, 2008b, Minh *et al.*, 2007). In their studies increased metal loading, increased the oxidation rate or was more selective towards specific end products. They also found the required metal loading that enhanced oxidation rate or conversion, changed as the organic pollutant changed.

The metal loading on the Ru/Al_2O_3 was decreased from 3.0% to 0.5% and all other reaction conditions were kept constant. DBU removal decreased as the metal loading decreased for all temperatures as shown in Figures 5.26. 100% DBU removal was achieved using 3.0% Ru/Al_2O_3 while 78% DBU removal was achieved using 0.5% Ru/Al_2O_3 at 240 ºC.

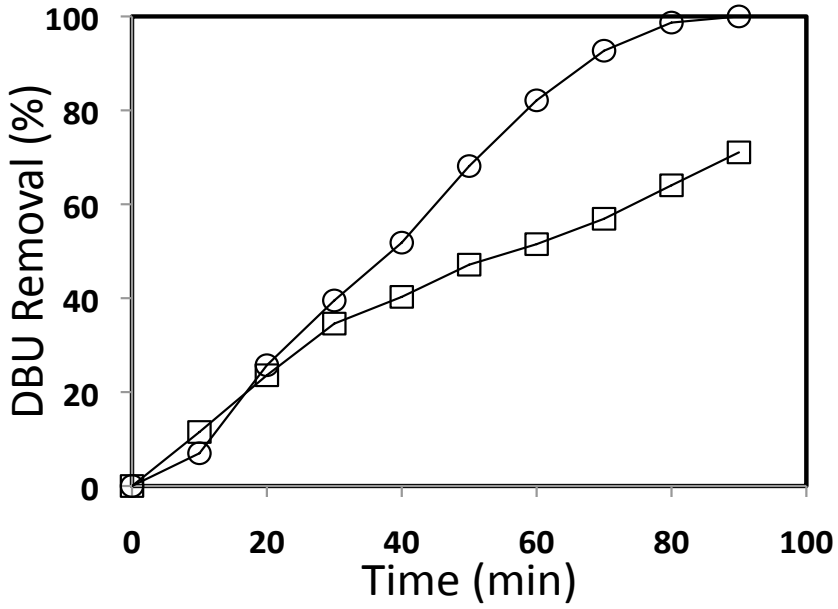

Figure 5.26 DBU removal using varying metal loadings at 240 ºC and 7 MPa. 3.0% Ru/Al_2O_3 (○), 0.5% Ru/Al_2O_3 (□)

The 3.0% Ru/Al_2O_3 catalyst TOC profiles show an S-shaped increase with time, whereas the 0.5% Ru/Al_2O_3 catalyst profiles clearly exhibit 3 distinct phases except at 240 ºC (induction, fast and slow oxidation), similar to that seen for WAO conditions. This induction phase is the time required to generate a sufficient concentration of free radicals need to

initialise the reaction, similar to WAO or due to the strong adsorption of DBU onto the catalyst surface, which then forms less strongly absorbed products as oxygen is added, freeing more active sites for oxygen chemisorption(Satterfield, 1980, Bond, 1987).

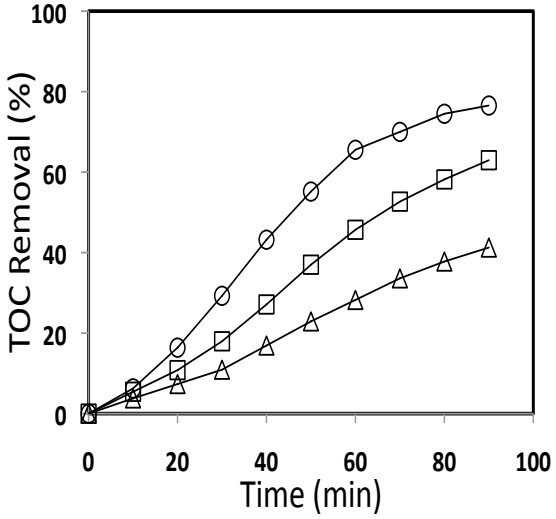

Figure 5.27 TOC removal against residence time for several temperatures at 7 MPa using 3.0% Ru/Al_2O_3. 240ºC (◯), 220ºC (□), 200ºC (△)

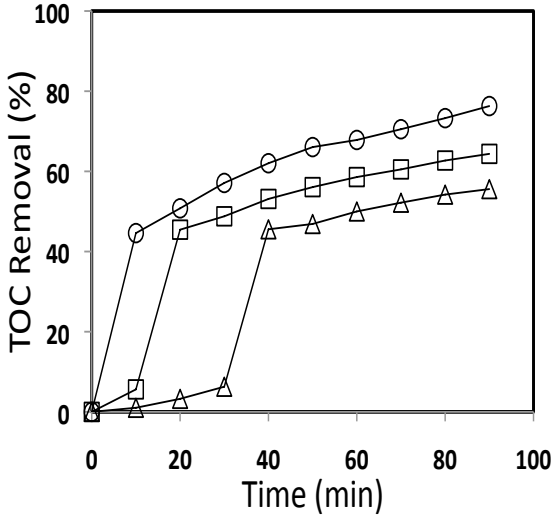

Figure 5.28 TOC removal against residence time for several temperatures at 7 MPa using 0.5% Ru/Al_2O_3. 240ºC (◯), 220ºC (□), 200ºC (△)

Rebrov et al(2002) have also suggested that increased metal loading, results in increased metal cluster size, facilitating the formation of more favorable configurations for the formation of surface intermediates. Minh *et al.,* (2007) also found that changing the loading of ruthenium on the support from 1% to 3% enhanced conversion. They attributed this to increased average particle of the metal on the support and the homogenous distribution of the metal particles on the support.

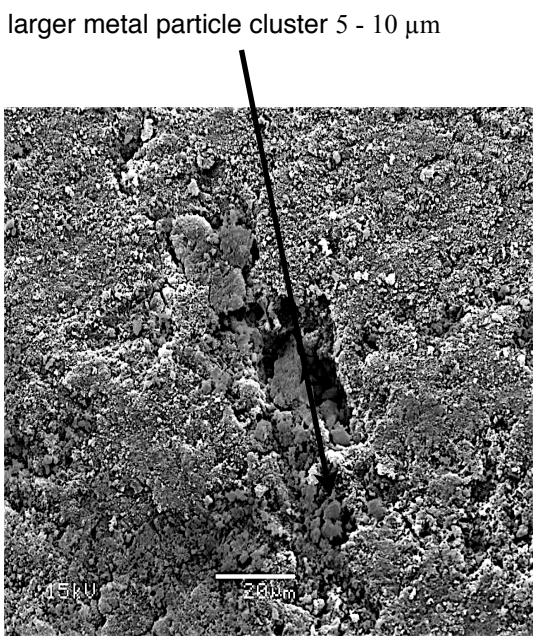

Figure 5.29 SEM Image for 3% Ru/Al_2O_3 at 550x magnification

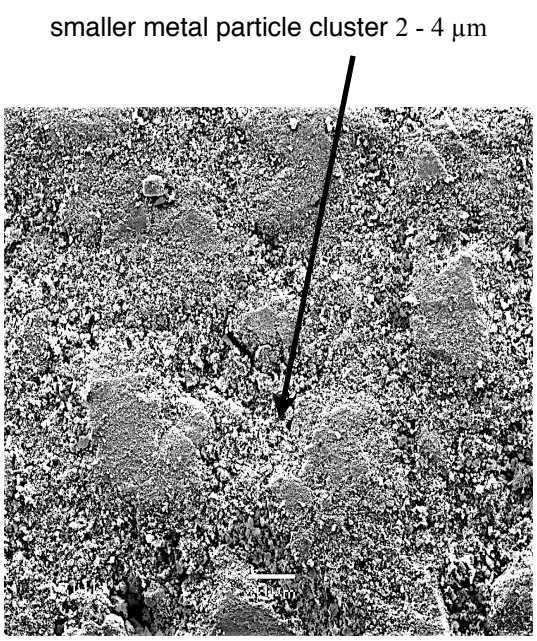

Figure 5.30 SEM Image for 0.5% Ru/Al_2O_3 at 550x magnification

Figures 5.29 and 5.30 show the surface of 0.5% and 3% Ru/Al_2O_3 catalysts at 550x magnification, for the 0.5% metal loading the metal particle cluster that have a size range of approximately 2 - 4 μm, while the 3% metal loading surface has metal particle clusters that have a size range of approximately 5 - 10 μm, which support the findings of Rebrov *et al.,* (2002) and Minh *et al.,*(2007).

5.9 Effect of catalyst weight

These experiments were undertaken to evaluate the effect of catalyst weight on DBU and TOC removal, and ammonia yield. The runs were undertaken using 3% Ru/Al_2O_3 at 240 ºC, 7 MPa, 6 mM and 0.4 L/min of oxygen. The catalyst weights investigated were 1 g, 2 g and 3 g.

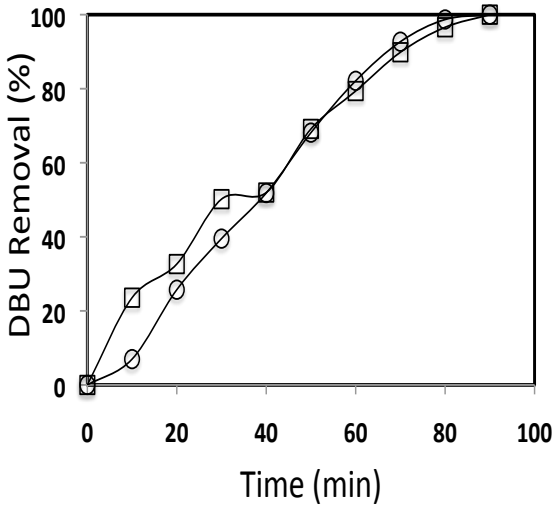

Figure 5.31 DBU removal against residence time for 2 catalyst weights at 240 ºC and 7 MPa using 3.0% Ru/Al_2O_3. 1 g (○), 3 g (□)

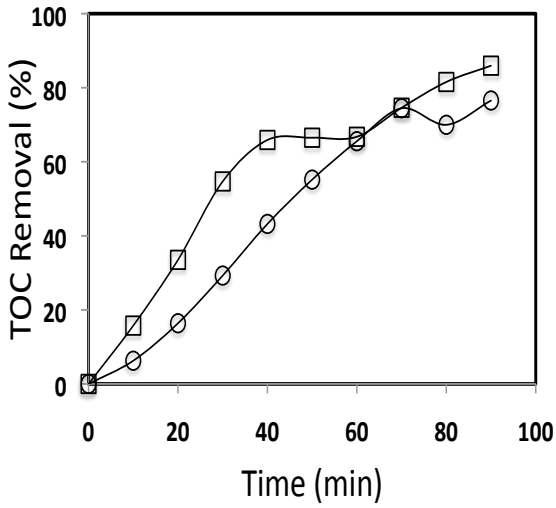

Figure 5.32 TOC removal against residence time for 2 catalyst weights at 240 ºC and 7 MPa using 3.0% Ru/Al_2O_3. 1 g (○), 3 g (□)

It was found that DBU removal differed slightly, while TOC removal increased marginally with catalyst weight. The initial reaction rate increased with increased catalyst weight, but then reverted to a rate similar to 1 g as shown in Figure 5.31. Increased catalyst weight corresponds to larger catalyst surface and more active sites for DBU adsorption and oxidation to occur, giving an increased DBU removal rate.

Ammonia yield decreased with increased catalyst weight and N_2 formation increased with catalyst weight, signifying greater selectivity to N_2, CO_2 formation remained constant. Lee (2003) found similar results for ammonia oxidation using 3% Ru/TiO_2, he found that ammonia in solution is mainly converted to N_2, 90% of ammonia is converted to N_2, also Increased catalyst weight increased ammonia removal and yield of N_2. Gunale and Mahajani

(2008a) also observed that increased catalyst weight resulted in reduced ammonia yield during the ruthenium catalysed oxidation of morpholine.

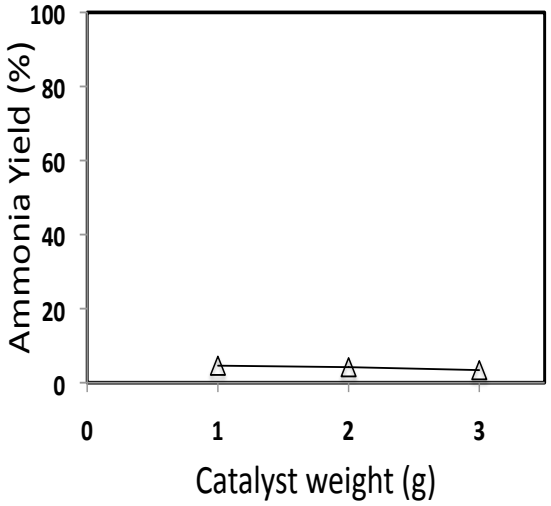

Figure 5.33 Effect of catalyst weight on ammonia yield at 240 ºC and 7 MPa, after 90 min residence time.

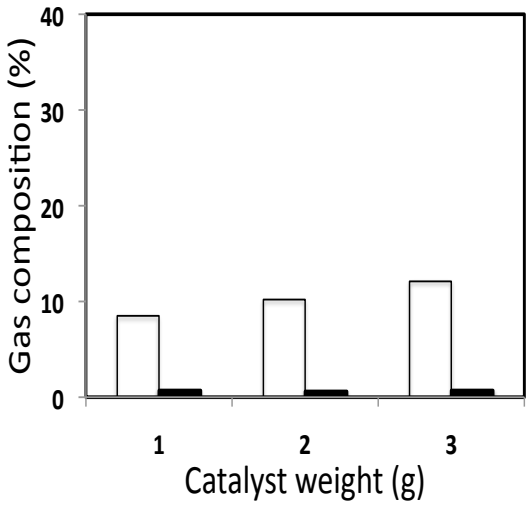

Figure 5.34 Effect of catalyst weight on N_2 and CO_2 formation at 240 ºC and 7 MPa after 90 min residence time. N_2 (□), CO_2 (■)

5.10 Catalyst stability

To determine the stability of the catalyst under reaction conditions, a series of experimental runs were undertaken. The same catalyst was used for the runs and dried overnight before reuse. These runs were performed using 1 g of 3% Ru/Al_2O_3 catalyst at 240 ºC, 7 MPa, 6 mM DBU and 0.4 L/min of oxygen. Figures 5.35 and 5.36 show the DBU and TOC removal for the runs respectively. Data relating to the catalysts runs are shown in Table 5.5.

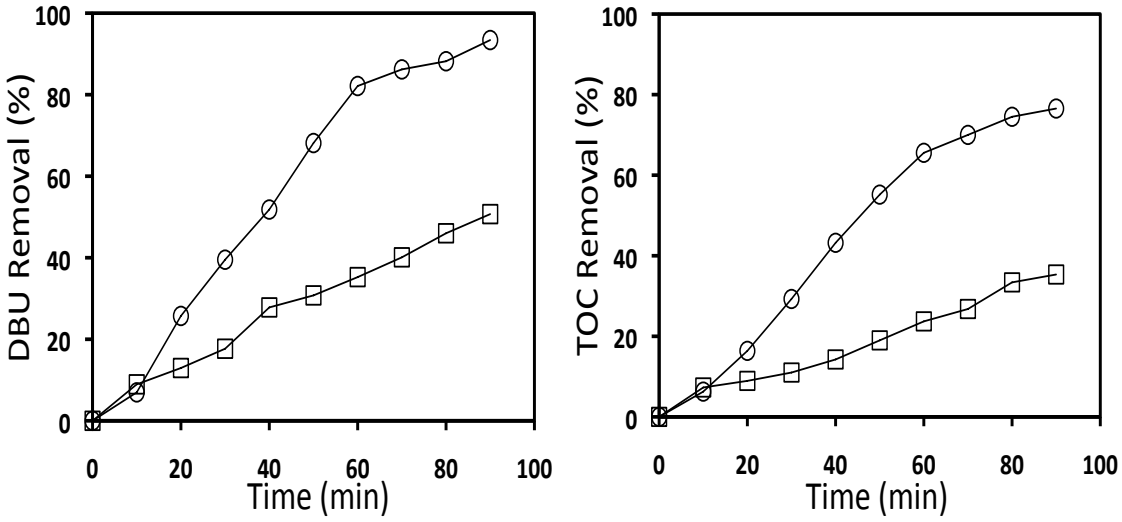

Figure 5.35 DBU removal for reuse of catalyst at 240 ºC and 7 MPa. first run (○), second run (□)

Figure 5.36 TOC removal for reuse of catalyst at 240 ºC and 7 MPa. first run (○), second run (□)

The rate, and overall value of DBU and TOC removal are significantly reduced for the second run, due to the change in the physical properties of the catalyst as shown in Table 5.6. The second run also gave an increased yield of ammonia yield, however this yield was lower than the yield under WAO conditions.

The number of runs were limited to two because after the second run, the catalyst pellets had become fragile and began to crumble. For reasons of safety, any further runs were decided against to prevent potential blockage of inlet and outlet lines, which could lead to dangerous pressure build up in the reactor.

Catalyst Run number	DBU removal (%)	TOC removal (%)	Ammonia Yield (%)
1	93.4	89.4	4.6
2	68.6	69.8	9.8

Table 5.5 Table showing the DBU and TOC removal and ammonia yield for catalyst reuse

The SEM images in Figures 5.37 a and b show the significant surface structure changes after two consecutive runs using the same catalyst. At the higher magnifications, visible erosion and break up of the catalyst is visible. Using Inductively Coupled Plasma (ICP) analysis, the concentration of Ru metal found in the liquid sample after experimental run 2 was found to be 5 mg/L.

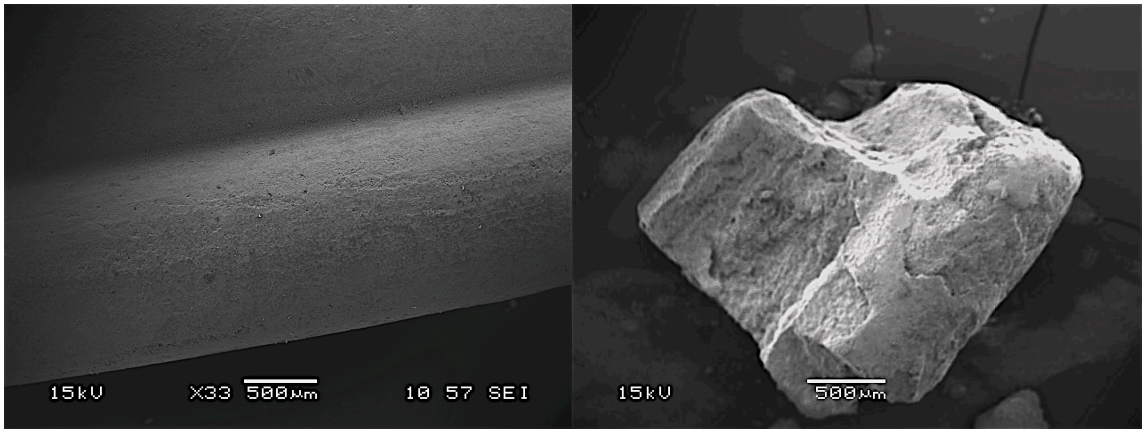

(a-1) fresh, 35x (b-1) 2 runs, 35x

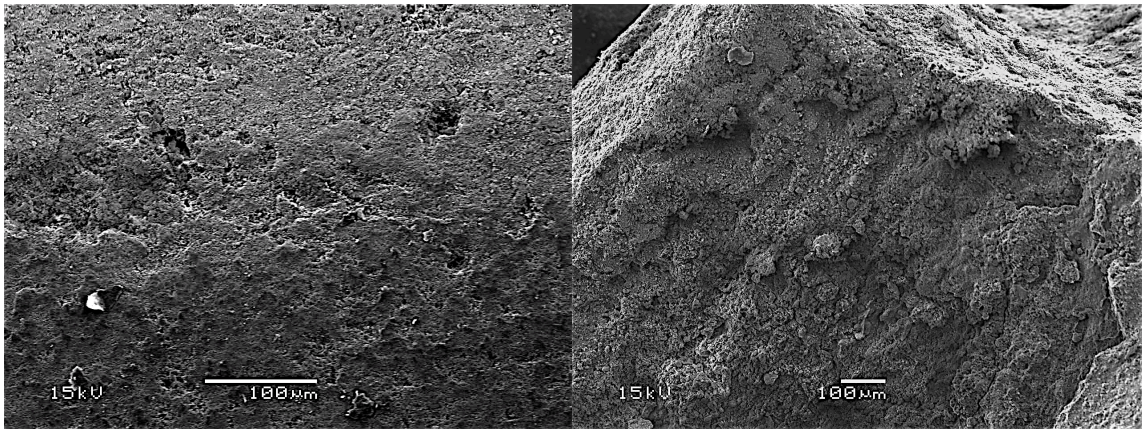

(a-2) fresh, 250x (b-2) 2 runs, 250x

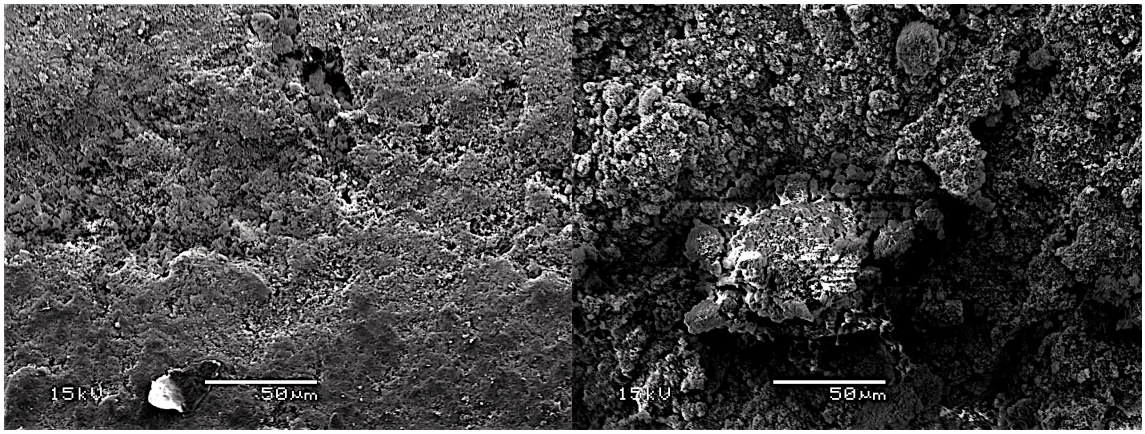

(a-3) fresh, 500x (b-3) 2 runs, 500x

Figure 5.37 SEM image of fresh and used catalyst. (a-1) fresh, 35x; (a-2) fresh, 250x; (a-3) fresh, 500x. (b-1) 2 runs, 35x; (b-2) 2 runs, 250x; (b-3) 2 runs, 500x.

BET results in Table 5.6 show a large reduction in the surface area of the catalyst, but of note is the similar average pore diameter values for the fresh and used catalyst, showing that mesopores are still the predominant pores.

Catalyst Status	BET Surface Area (m^2/g)	External Surface Area (m^2/g)	Micropore Volume ($cm^3/g \times 10^{-3}$)	Average Pore Diameter (nm)
Fresh	153	135	6.85	18.62
Used	25.7	17.6	3.64	15.21

Table 5.6 Characterisation of fresh and used Ru/Al_2O_3 catalyst

5.11 Industrial Effluent Treatment

Ultimately the aim of this work is to show that enhanced degradation of wastewater consisting of nitrogenous organic compounds is enhanced by heterogeneous catalysis. Therefore, industrial effluent consisting of a mixture of nitrogenous organic compounds was obtained from a wastewater treatment company (Severn Trent, U.K). The industrial effluent was classified as hazardous by the company because it was irritating to the skin, eyes, respiratory system and harmful by ingestion.

The effluent was analysed to determine its initial TOC and ammonia concentration, these were found to be 100 mg/L and 35.4 mg/L respectively. The effluent was then treated by WAO and CWAO processes under the following conditions: 240 ºC, 7 MPa, 0.4 L/min O_2, and 1 g of 3% Ru/Al_2O_3 for CWAO.

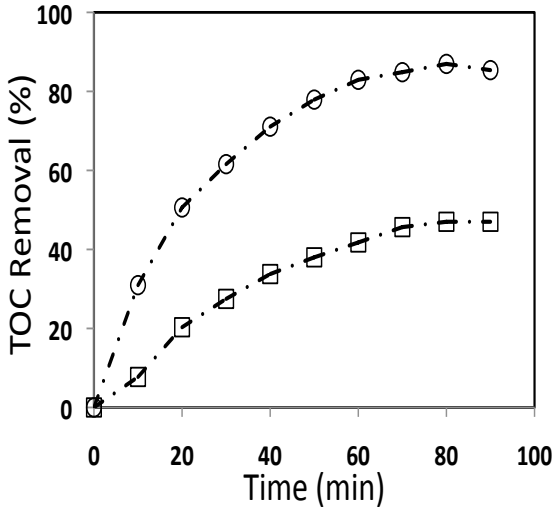

Figure 5.38 TOC removal against time of real waste at 240 ºC and 7 MPa. WAO (□), 3% Ru/Al_2O_3(○)

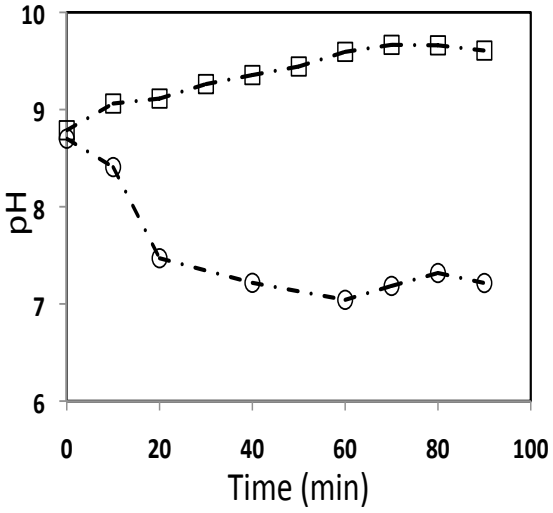

Figure 5.39 pH profile of real waste at 240 ºC and 7 MPa.WAO (□), 3% Ru/Al_2O_3(○)

3% Ru/Al_2O_3 enhanced TOC removal by 40% as shown in Figure 5.38. TOC removal was 47% and 87% for WAO and CWAO respectively. The initial ammonia concentration decreased by 18.4 mg/L to 27 mg/L for WAO and no ammonia was detected after 90 minutes reaction time for CWAO. This highlighted that 3% Ru/Al_2O_3 is active for ammonia oxidation. It also confirms that it would be especially suitable for the treatment of industrial effluents containing a variety of nitrogenous compounds, as ammonia has been shown to be a highly refractory compound(Qin and Aika, 1997, Grosjean *et al.*, 2010).

Figure 5.39 shows the pH profile for WAO and CWAO of the industrial effluent; for WAO the pH increased from an initial value of 8.7 to 9.6, while for CWAO it decreased to 7.2, this would be due to the oxidation of ammonia to nitrogen (Lee *et al.*, 2005) and the formation of simple carboxylic acids(Imamura, 1999).

	Initial	**WAO**	**3% Ru/Al_2O_3**
Ammonia Concentration (mg/L)	35.4	27.0	0.0

Table 5.7 Industrial effluent ammonia concentration before and after treatment by WAO and 3% Ru/Al_2O_3.240 ºC, 7 MPa and 0.4 L/min O_2

5.12 Reticulated Foam Monolith

Based on the findings from 5.10, that 3% Ru/Al_2O_3 pellet was only stable for 2 runs. It was decided to investigate other heterogeneous catalyst delivery methods into the reactor. Cybulski (2007) reviewed the different types of CWAO reactors used experimentally and industrially and found that monolith reactors have shown potential for application in CWAO.

Reticulated foam monoliths are a family of materials whose light weight, flow through properties can be easily fabricated to meet design requirements of reactor catalyst support. They exhibit a three dimensional pore structure with versatility of shape, pore size, permeability, surface area and chemistry. A desirable property of reticulated foams is their thermal resistance and stability (Matatov-Meytal and Sheintuch, 1998), which makes them suitable for high temperatures. In addition, and unlike honeycomb monoliths, reticulated

foam monoliths have a tortuous pore structure which gives higher surface areas and enhanced mixing and mass transfer.

The aim of this work is to compare the efficiency of Ruthenium coated reticulated foams with the Ru/Al_2O_3 pellets and perform an initial evaluation of the use of reticulated foam monoliths as an improved, more stable heterogeneous catalyst delivery method to the reactor, instead of pellets. The reticulated foam was designed to replace the catalyst basket in the CWAO experimental procedure, which is shown in chapter 3. The reticulated foam was fabricated by Vesuvius, UK according to those specifications.

Figure 5.40 a and b show pictures of the uncoated and coated reticulated foam respectively. Figure 5.41 is an SEM micrograph of a selected area showing the unique pore structure of a 15 Pores Per Inch (PPI), 99.5 wt.% α-Al_2O_3 uncoated Reticulated Foam Monolith. The spray coating undertaken by Johnson Matthey, UK resulted in specified uniform wash coat loading, as indicated by visual and microscopic analysis.

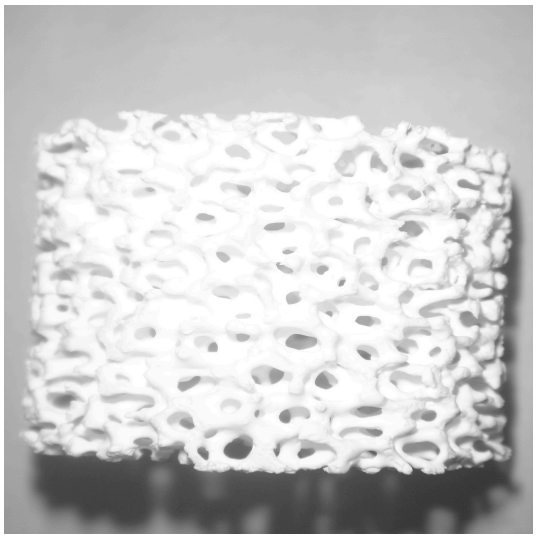

Figure 5.40a Uncoated reticulated foam.

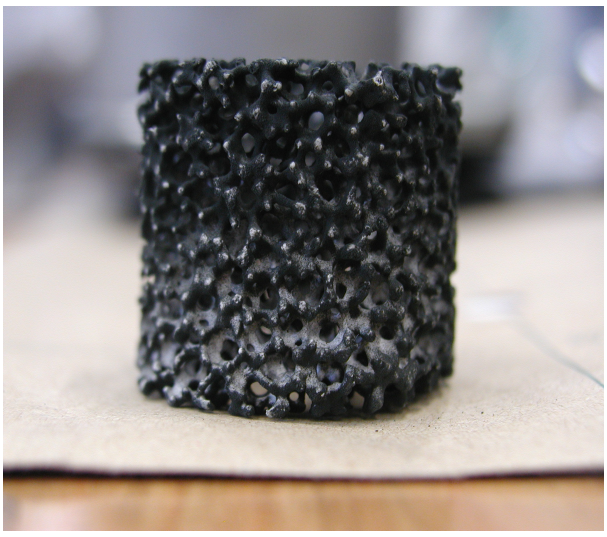

Figure 5.40b Reticulated foam monolith coated with 0.03 g of Ruthenium metal.

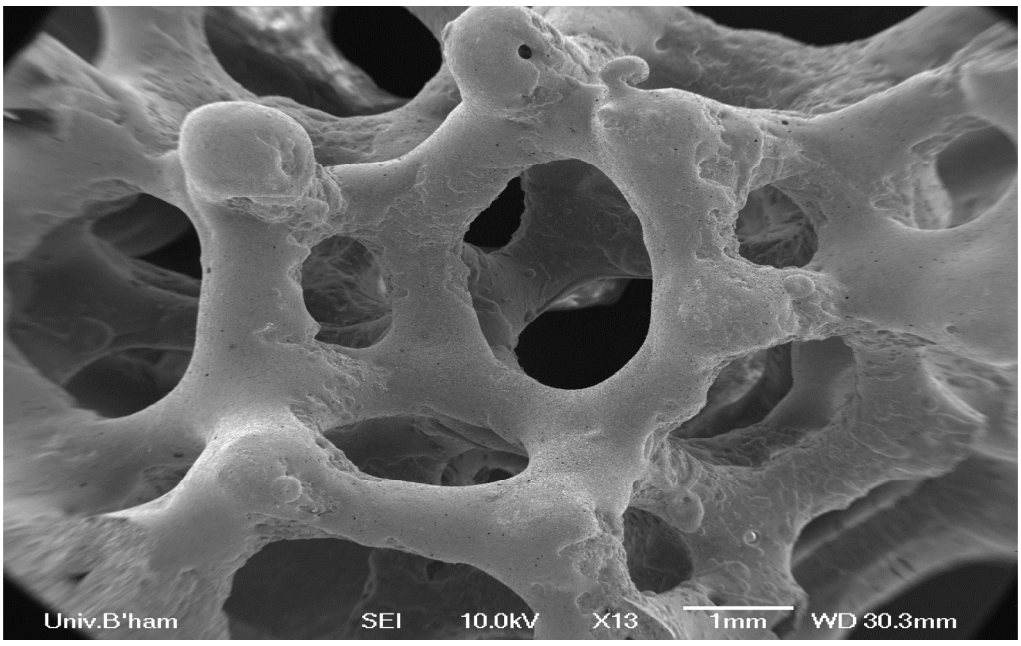

Figure 5.41 SEM showing the unique pore structures of a 15 PPI, 99.5 wt.% α-Al_2O_3 uncoated Reticulated Foam Monolith.

5.12.1 Comparing Pellet and Reticulated foam reactions

To evaluate the efficiency of the ruthenium coated reticulated foams, experimental runs were carried out at the same reaction conditions using 1 g of 3% Ru/Al_2O_3 pellets and a weight equivalent of ruthenium metal (0.03 g) on the reticulated foam. These results are illustrated in Figures 5.42 and 5.43.

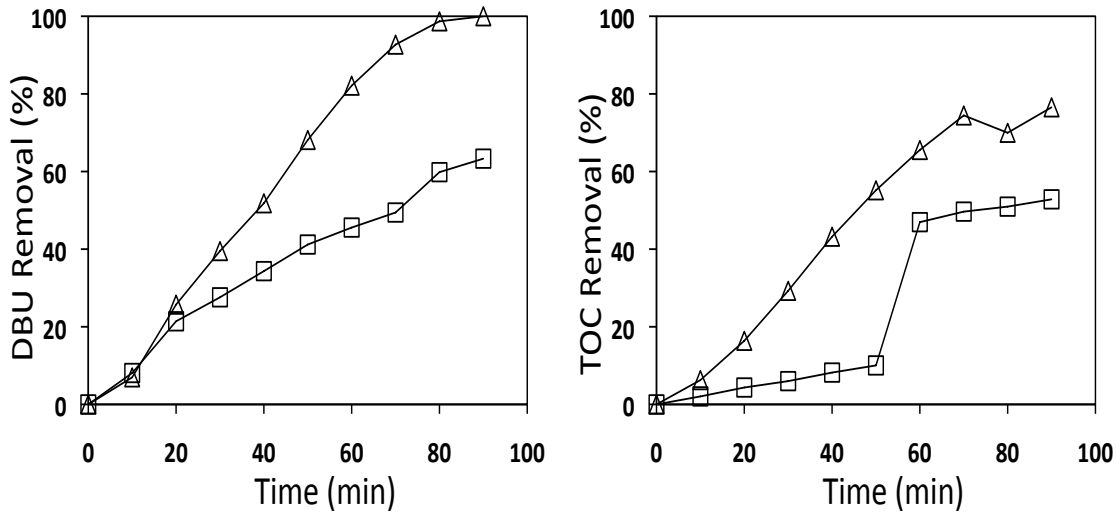

Figure 5.42 DBU removal against time for 3% Ru/Al_2O_3 pellets and Ru coated reticulated foam monolith at 240 ºC and 7 MPa.
0.03g Reticulated foam (□), 3% Ru/Al_2O_3 pellets

Figure 5.43 TOC removal against time for 3% Ru/Al_2O_3 pellets and Ru coated reticulated foam monolith at 240 ºC and 7 MPa.
0.03g Reticulated foam (□), 3% Ru/Al_2O_3 pellets

100% DBU removal was achieved using 1g of 3% Ru/Al_2O_3 pellets compared to the 63% DBU removal using 0.03g Ru-coated reticulated foam monolith. Also TOC removal was 77% and 53% for 1g of 3% Ru/Al_2O_3 pellets and 0.03g Ru-coated reticulated foam monolith respectively, this is contrary to the results of Schutt and Abraham (2004) who found that a palladium coated monolith was more effective than palladium pellets for cellulose conversion; they attributed this to reduced mass transfer between the gas and solid phase. The TOC removal profile for 0.03g Ru-coated reticulated foam monolith (Figure 5.43) clearly shows an induction period, in which the generation of free radicals is poor and then a fast oxidation rate, when an adequate concentration of free radicals has been attained. It was assumed the induction period was seen for the reticulated foam monolith because, the weight of ruthenium metal on the reticulated foam monolith was not sufficient, as this has been shown to be an important factor in catalytic reactions (Pintar and Levec, 1994).

Catalyst type	Reticulated foam	3% Ru/Al_2O_3
Ammonia yield (%)	16.7	4.6

Table 5.8 Ammonia yield for the reticulated foam monolith and 3% Ru/Al_2O_3 pellets.

Ammonia yields of 4.6 % and16.7% were achieved for 1 g of 3% Ru/Al_2O_3 pellets and 0.03g Ruthenium-coated reticulated foam monolith respectively as shown in Table 5.8. The Ru/Al_2O_3 pellets is more selective towards reduced ammonia yield than the reticulated foam

monolith. The difference in performance between the coated reticulated foam monolith and pellets could be due to the method of catalyst preparation (Klinghoffer *et al.*, 1998) or a non-optimal weight of Ru coating on the reticulated foam monolith (Pintar and Levec, 1994).

To assess the coating weight effect, two reticulated foam monoliths of similar dimensions were coated with 0.015 g and 0.09 g of Ru and their removal efficiency tested at 240 ºC, 7 MPa and 0.4 L/min O_2. DBU removal was in the same range (63%) for all coating weights (Figure 5.44), while TOC removal increased from 52% to 66% with increased metal coating weight (Figure 5.45). The induction time also decreased with increased metal coating weight, confirming that metal coating weight on the reticulated foam monolith needs to be optimised for enhanced system performance. Ammonia yield decreased from 18.6% to 8.7% with increased metal coating as shown in Table 5.9.

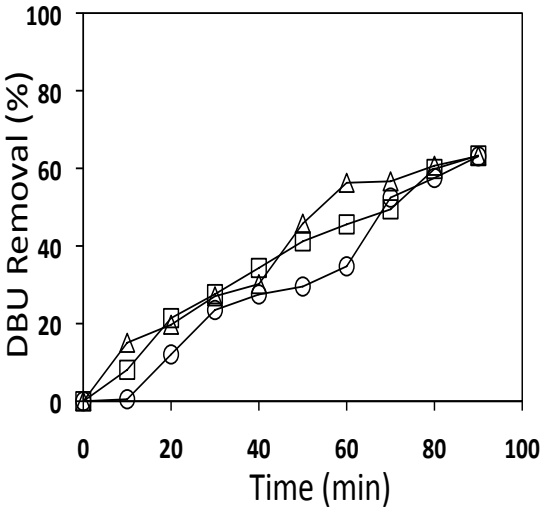

Figure 5.44 DBU removal against time for varying Ruthenium metal loading on the reticulated foam at 240 ºC and 7 MPa.
0.015 g (○), 0.03 g (□), 0.09 g (△)

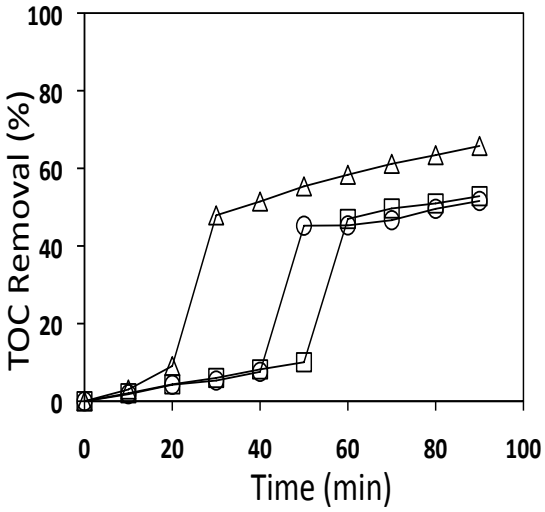

Figure 5.45 TOC removal against time for varying Ruthenium metal loading on the reticulated foam at 240 ºC and 7 MPa.
0.015 g (○), 0.03 g (□), 0.09 g (△)

Weight (g)	0.015	0.03	0.09
Ammonia yield (%)	18.6	16.7	8.7

Table 5.9 Ammonia yield for different Ruthenium metal loadings on the reticulated foam. 240 ºC, 7 MPa and 0.4 L/min O_2

An advantage of using the reticulated foam is the increased lifetime of the catalyst. The reticulated foam monolith was found to maintain its activity for up to 4 experimental runs, while the activity of the pellets reduced significantly after one experimental run due to catalyst disintegration from support erosion as discussed in chapter 5.10.

5.12 Summary

Similar temperature and pressure ranges that were investigated for WAO, were investigated for CWAO using two Ru/Al_2O_3 catalysts. The results for CWAO of DBU showed higher values than those for WAO for the removal of DBU and TOC, these values are highest using the higher catalyst loading of 3% Ru/Al_2O_3. It was found that using the 3% Ru/Al_2O_3 pellets at lower temperatures resulted in DBu and TOC removal values achieved at higher temperatures. The yield of ammonia was significantly reduced when compared to WAO and results with ammonia concentrations below the environmentally permitted discharge levels (10 mg/L) were achieved.

The oxidation kinetics for CWAO were described using a global power rate law, which satisfactorily modeled the oxidation of DBU at 4 and 7 MPa and TOC removal at 7 MPa.

CHAPTER 6 - SUPERCRITICAL WATER OXIDATION OF DBU

6.1 Introduction

This section presents the results and discussion of experiments performed to study the supercritical water oxidation of DBU. The mineralisation of DBU was studied by varying specific operating conditions, namely the operating temperature and the initial DBU concentration. The system pressure was kept constant at 25 MPa for all experiments, because in the temperature range investigated, increasing the system pressure above 25 MPa results in negligible increase in conversion.

Previous work has shown that above 1.2 times stoichiometric oxidant excess, the oxidant ratio stops being a key a parameter in the in the SCWO process. Based on this, it was decided to use a 25% excess volumetric flow of H_2O_2.

The stoichiometric equation for the complete oxidation of DBU is given by:

$$C_9H_{16}N_2 + 13\,O_2 \rightarrow 8H_2O + 9CO_2 + N_2$$

and H_2O_2 decomposes via the following global reaction producing water and oxygen:

$$2H_2O_2 \rightarrow 2H_2O + O_2$$

The temperature range investigated was in the range between 400 and 450 ºC. The initial concentration of DBU was in the range of 6 to 18 mM to correspond to the concentrations investigated in the previous chapters. Table 6.1 shows the range of conditions. The residence times used in the experiments were based upon the liquid flowrates required to maintain a turbulent flow regime, and the accuracy of determining the residence times.

Parameter	Range	Fixed Conditions	Residence Time Range
		Concentration = 6 mM	
Temperature	400 - 450ºC	Pressure = 25 Mpa	2 - 7 s
		Oxidant Flowrate =1.25 SR	
		Temperature = 400 ºC	
Concentration	6 - 18 mM	Pressure = 25 Mpa	2 - 7 s
		Oxidant Flowrate = 1.25 SR	

Table 6.1 Summary of the SCWO experiments

Conversion and Yield Calculations

DBU and TOC conversion (X_{DBU} and X_{TOC}) at a particular location was calculated from the concentration C at that location and the initial concentration C_{in} of the species of interest:

$$X = \frac{C_{in} - C}{C_{in}} \times 100 \qquad (6.1)$$

Yields (Y) of CO, CO_2 and CH_4 were calculated as the molar flow rate of CO, CO_2 and CH_4 divided by the Total Carbon (TC) molar flow rate in the feed (Vera Perez *et al.*, 2004), (Savage *et al.*, 1984). For N_2O, the molar flow rate of N_2O is divided by twice the molar flow rate of nitrogen atoms in the feed, where $\dot{n}$ represents the molar flow rate of the species of interest:

$$Y_{CO_2} = \frac{\dot{n}_{CO_2}}{\dot{n}_{TC_{in}}} \tag{6.2}$$

$$Y_{N_2O} = \frac{\dot{n}_{N_2O}}{2\dot{n}_{N_{in}}} \tag{6.3}$$

Gas compositions were given as plotted areas. These areas were then related to areas obtained from a known standard gas mixture. Therefore the molar flow rates of gases were calculated as:

$$\dot{n}_{CO_2} = \frac{CO_2\ Area\ from\ sample}{CO_2\ Area\ from\ s\tan dard} \times CO_2\%\ in\ s\tan dard \times flowrate\ of\ sample \tag{6.4}$$

The molar flows of TC or N in the feed were given by their corresponding concentrations in the feed, in g/l multiplied by the total liquid feed flow rate in l/min and divided by their respective molecular weight. For example:

$$\dot{n}_{TC} = \frac{C_{TC_{in}} \dot{m}_{liquid}}{12} \tag{6.5}$$

The quality and acceptance of the data for all experiments were verified by a carbon balance closure. Most experiments provided carbon balance closures between 90 and 110%, indicating that most carbon has been accounted for in the detected products or as unreacted reagent.

Table 6.2 shows a summary of the experimental results obtained from this work.

Concentration (mmol/L)	Residence time (s)	DBU conversion X (%)	TOC conversion X_{TOC} (%)	Yield (%)				
DBU				NH_3	N_2O	CO	CO_2	CH_4
EXP 1		Reaction Temperature = 400°C						
6.8	2.0	91.4	48.1	2.2	0.0	0.3	0.0	0.0
6.8	3.0	95.6	48.8	2.2	0.0	0.6	0.0	0.0
6.8	4.0	97.0	48.9		0.0	1.0	0.0	0.0
6.8	5.1	99.0	50.3	4.0	0.0	1.5	0.0	0.0
6.8	6.0	99.5	51.5	6.1	0.0	2.7	0.5	0.0
6.8	7.0	99.9	54.2	7.0	0.0	3.8	2.1	0.0
EXP 2		Reaction Temperature = 425°C						
6.8	1.2	95.9	58.7	-	0.0	3.9	0.0	0.0
6.8	2.0	98.1	63.6	-	0.0	4.8	1.8	0.0
6.8	3.0	98.6	65.8	-	0.0	7.8	4.3	0.0
6.8	5.1	99.6	72.3	-	0.3	11.7	7.6	0.1
EXP 3		Reaction Temperature = 450°C						
6.8	1.1	97.9	67.0	4.9	0.9	5.5	1.9	0.0
6.8	2.0	99.7	72.9	7.2	0.9	9.9	6.5	0.1
6.8	3.0	99.9	77.2	8.4	0.9	6.5	1.3	0.2
6.8	4.0	100.0	80.8	9.3	1.0	14.5	11.0	0.3
6.8	5.1	100.0	83.1	10.1	1.0	15.4	12.3	0.4
EXP 4		Reaction Temperature = 400°C						
12.0	2.0	97.2	66.7	2.1	0.0	0.9	0.0	0.0
12.0	3.0	97.4	68.8	2.7	0.0	1.4	0.1	0.0
12.0	4.0	97.7	69.9	4.0	0.0	2.6	0.4	0.0
12.0	5.1	98.6	73.5	4.9	0.0	3.8	1.9	0.0
12.0	6.0	99.3	75.5	5.8	0.3	4.6	3.1	0.0
12.0	7.0	99.6	77.4	6.3	0.3	5.0	4.0	0.0
EXP 5		Reaction Temperature = 400°C						
18.00	3.0	98.3	78.0	2.9	0.0	2.9	0.1	0.0
18.00	4.0	99.1	79.5	3.8	0.0	5.3	2.0	0.0
18.00	5.1	99.5	82.0	4.4	0.0	6.8	4.4	0.0
18.00	6.0	99.8	83.1	5.1	0.7	8.2	6.7	0.0
18.00	7.0	99.9	84.5	5.6	0.8	9.7	7.9	0.0

Table 6.2 SCWO of DBU Experiments at 400 - 450 °C and 25 MPa

6.2 Effect of System Temperature

The effect of temperature on DBU and TOC removal, and Ammonia yield at a residence time of 3 seconds is shown in Figure 6.1.

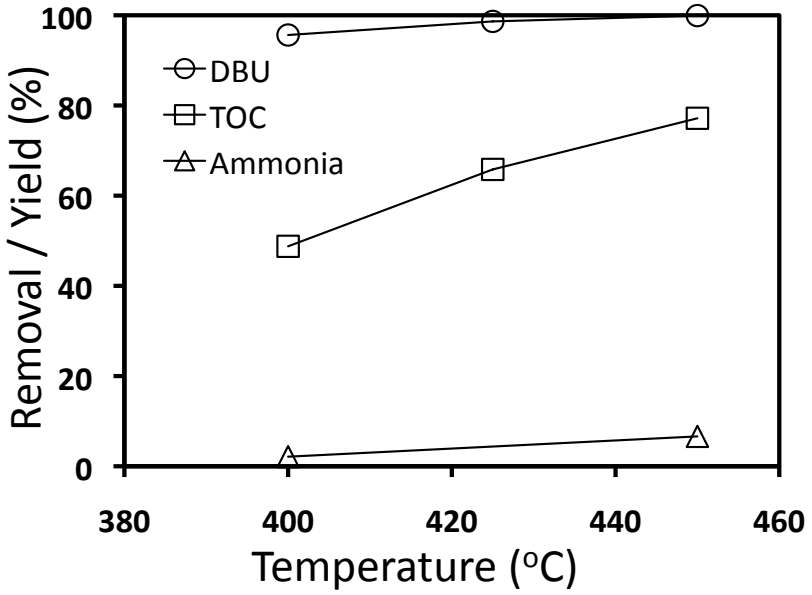

Figure 6.1 Effect of operating temperature on the removal of DBU, TOC and the yield of Ammonia at 25 MPa and 3 s residence time.

DBU and TOC removal increased with temperature, and were calculated as shown in equation (4.4).DBU removal increased from 96% to 100% as the temperature increased, indicating that the SCWO is very active and rapid for the complete breakdown of the DBU molecule. Although DBU was completely oxidised at 450ºC, TOC was not, indicating that DBU was partially oxidised into other organic compounds. TOC removal increased from 49%

to 77% as the temperature increased. The partially oxidised compounds formed are mainly organic, with approximately 10 - 15% represented as Inorganic Carbon (IC).

The yield of ammonia increased from 2% to 7% as the temperature increased, indicating the scission of the C-N bond in DBU is facilitated at higher temperatures. This in agreement with Cocero *et al*., (2000a), who observed a similar trend for ammonia yield from N-containing compounds such as aniline and acetonitrile. In the supercritical water oxidation of quinoline, it was observed that ammonia yield increased with temperature till 550ºC and then began to decrease (Pinto *et al.*, 2006). At temperatures higher than those investigated in this study, it is expected that ammonia yield would continue to increase until a sufficiently high temperature was attained, which would result in a decrease in the yield of ammonia and then complete breakdown. Webley et al.,(2004), showed in their work that temperatures in excess of 650ºC would be necessary to completely break down ammonia.

Figure 6.2 shows the yield of gaseous products with temperature, and that carbon monoxide and carbon dioxide are the primary gaseous products of DBU oxidation. The gas yield increased for all gases as the temperature increased. There was no evolution of gas at the 400ºC, except for slight formation (0.5%) of carbon monoxide. At all temperatures the yield of carbon monoxide was slightly higher than carbon dioxide (~2%). Aymonier *et al.* (2000), found that carbon dioxide was the major gas product, with smaller amounts of carbon dioxide and nitrogen present in the SCWO of fenuron.

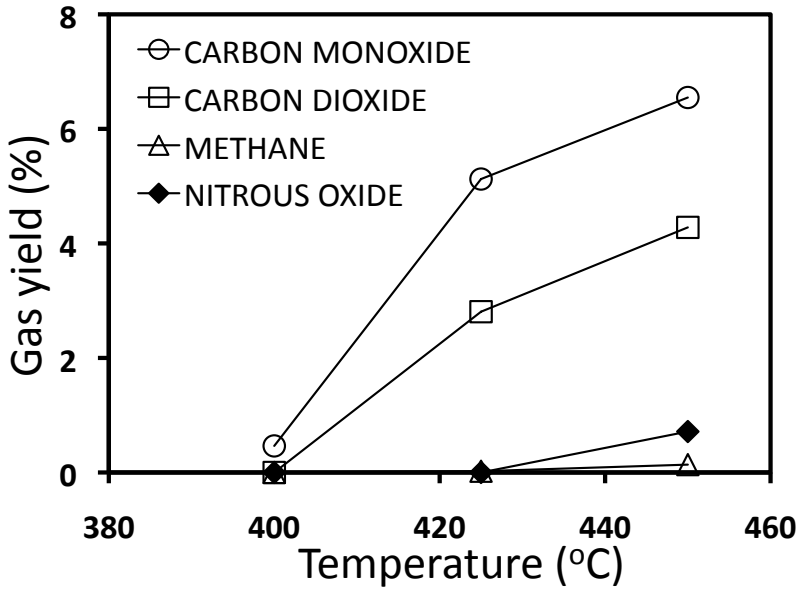

Figure 6.2 Effect of operating temperature on gas yield at at 25 MPa and 3 s residence time.

The presence of nitrous oxide (N_2O) in the gaseous stream can be seen as possible evidence of the reactor wall acting as a mild catalyst, during the oxidation of ammonia. This was suggested by Suwa *et a*l.(1961), who found that in the presence of a manganese dioxide-bismuth oxide catalyst, ammonia is oxidised as shown in below:

$$2HN_3 + 2O_2 \rightarrow N_2O + 3H_2O$$

As the yield of nitrous oxide is low, and the direct oxidation of ammonia is known to primarily evolve nitrogen gas and water, it is assumed that the catalytic effect of the wall is minimal. This would have be confirmed by nitrogen gas analysis.This is in agreement with Segond *et al.*(2002), who found that the yield of nitrous oxide was less than 1% during the SCWO of ammonia, even at a 600ºC. Li and Oshima.,(2005), using a similar experimental setup to that used for the SCWO, found that in the oxidation of methyl amine, the formation of nitrogen was favoured over nitrous oxide, and the yield of nitrogen was on average 10 times greater than that of nitrous oxide.

Above 425ºC, methane is detected in very low amounts, < 0.2% as a product in the gas. This would be as a direct result of the incomplete oxidation of some organics.

Figure 6.3 to Figure 6.6b show in more detail the effect of varying temperature on DBU removal, TOC removal, ammonia yield and gas yield.

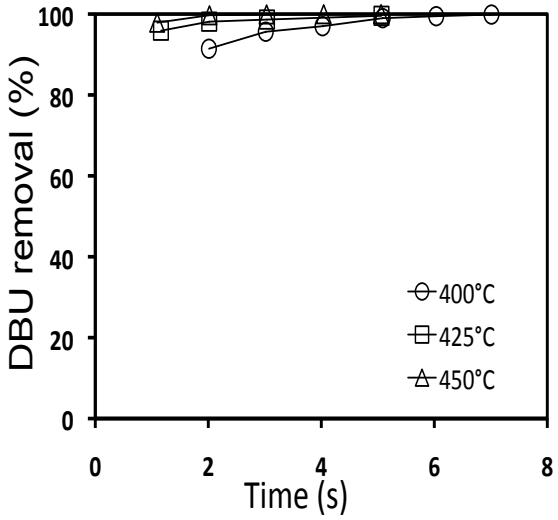

Figure 6.3 Effect of varying temperature on DBU removal at 25 MPa

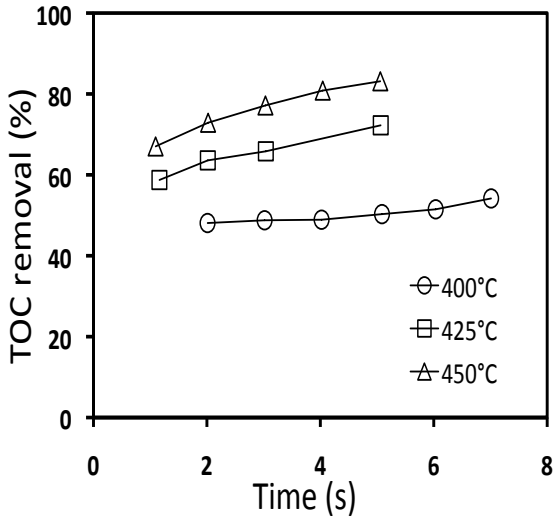

Figure 6.4 Effect of varying temperature on TOC removal at 25 MPa

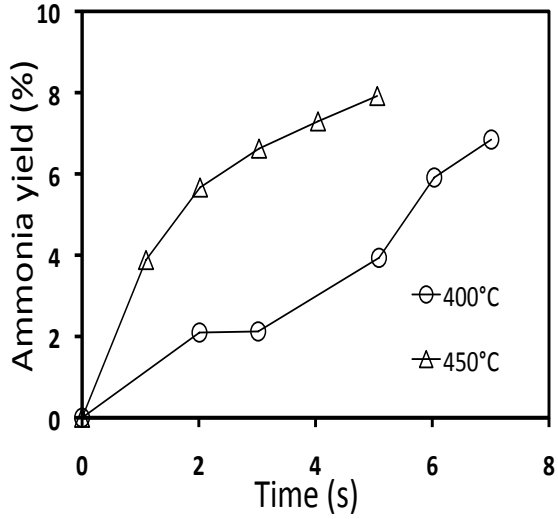

Figure 6.5 Effect of varying temperature on ammonia yield at 25 MPa

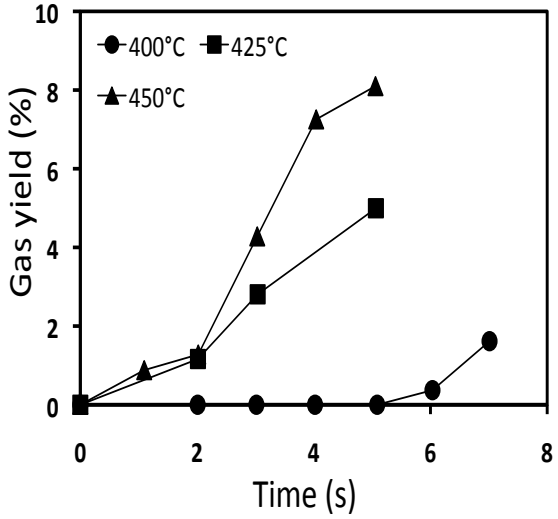

Figure 6.6 Effect of varying temperature on carbon dioxide yield at 25 MPa

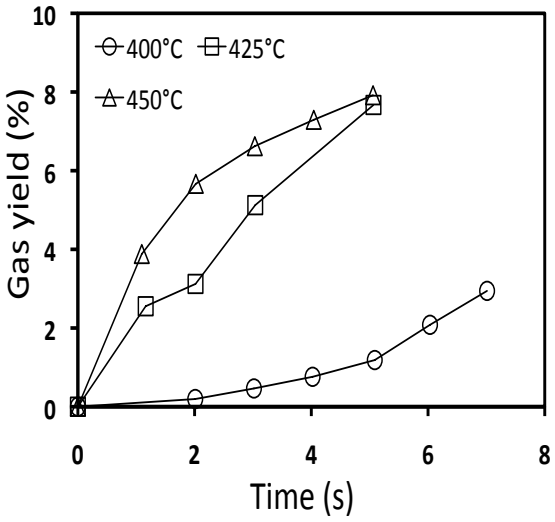

Figure 6.6b Effect of varying temperature on carbon monoxide yield at 25 MPa

6.3 Kinetics

The objectives of the present kinetic analysis were to determine the reaction rate constant (k), its associated Arrhenius parameters, and the reaction order for DBU. The global power rate law for the SCWO of DBU can be expressed as shown in equation (6.6)

$$-r_{DBU} = \frac{d[DBU]}{dt} = A\exp\left(\frac{-E_a}{RT}\right)[DBU]^a[O_2]^b[H_2O]^c \qquad (6.6)$$

As the reaction medium consists of more than 99% water, it is generally accepted by many researchers (Lee *et al.*, 1997) (Anikeev *et al.*, 2005) that its impact on DBU oxidation rate might be hidden; because it is present in such excess, its concentration is assumed to be

virtually constant. Therefore the water concentration effect is absorbed into the rate constant, and the reaction order of water is considered to be zero.

Many researchers describe the global kinetics for SCWO of organic compounds by a pseudo first order expression, attributing a value of 1 to the organic compound reaction order and a value of zero to the oxygen reaction order (Thomsen, 1998) . This was used as a good initial approximation in this work, because oxygen (oxidant) was used in excess to the stoichiometric flowrate (greater than 13 times the molar flow rate of DBU) needed to completely oxidise DBU and ideal plug flow conditions (i.e. turbulent flow regime) were also observed.

The rate constant k was calculated as shown in Figure 6.7, k is the slope of the linear fit. The process was repeated for other temperatures to obtain their respective k values. Similar to the analysis of TOC data for WAO (Chapter 4.1.5), it was also found that the oxidation of TOC exhibited two distinct phases (fast and slow oxidation) and they showed Arrhenius behaviour. *k* was calculated for these two phases.

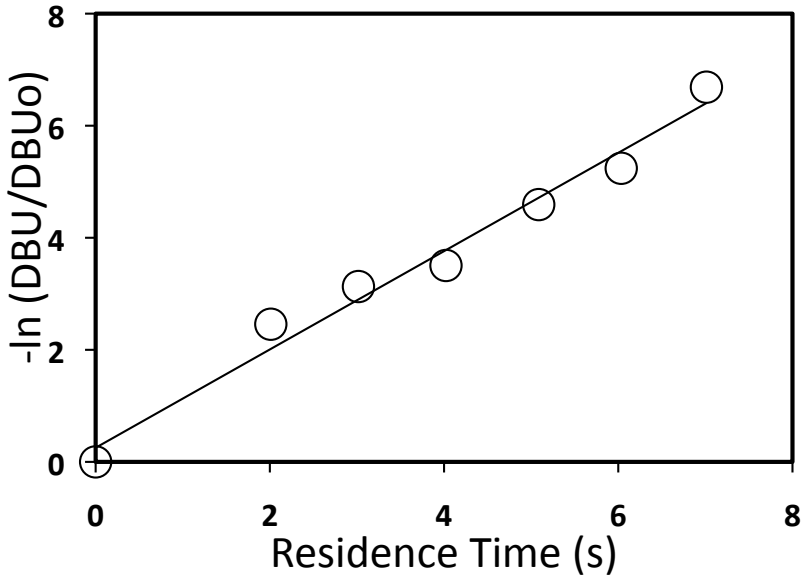

Figure 6.7 Natural log of DBU concentration versus time at 450ºC and 25 MPa

The rate constants were naturally higher than those found for the WAO oxidation of DBU and as expected an increase in temperature resulted in a higher rate constant.

The pre-exponential, A and the activation energy, Ea, were calculated for DBU and TOC by performing a linear fit of ln k versus 1000/T as shown in Figure 6.8.

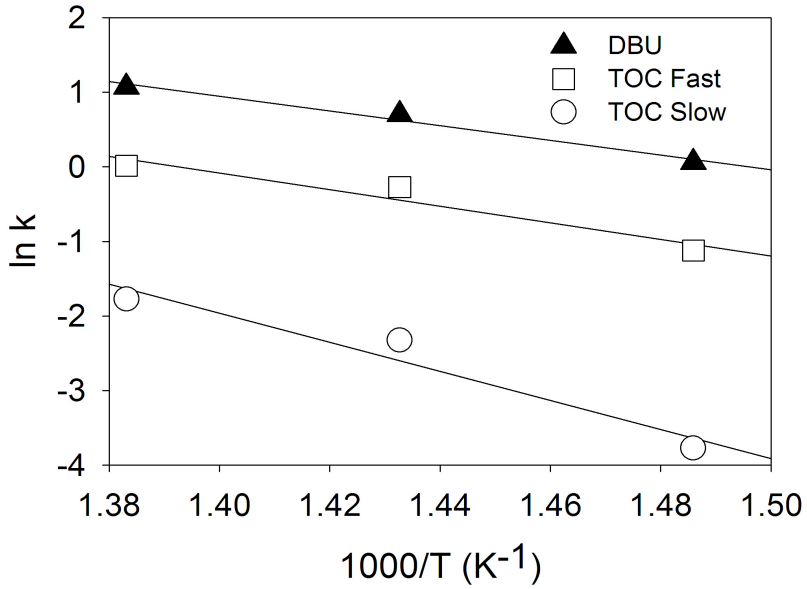

Figure 6.8 Arrhenius graph for DBU oxidation at 7 MPa

The activation energy, *Ea*, for DBU had a value of 82 kJmol^{-1} and the pre exponential factor, A, had a value of 2.5 x 10^{6} s^{-1}. The resulting pseudo-first order reaction rate expression for the oxidation of DBU between 400 – 450°C, at a constant pressure of 25 MPa is given by:

$$-r_A = 2.5\ x\ 10^6\ s^{-1} \exp\left(-\frac{81888\ Jmol^{-1}}{RT}\right)[C_{DBU}] \qquad (6.7)$$

The above expression was modelled against the experimental data for comparison as shown in Figure 6.9.

The activation energy, *Ea*, and the pre-exponential factor, A, for TOC had the following values for both phases:

Fast phase Ea = 92.3 kJ mol^{-1} A = 5.1 x 10^{6} s^{-1}

Slow phase Ea = 162.1 kJ mol^{-1} A= 9.9 x 10^{10} s^{-1}

These were modelled by using a modified pseudo first order kinetic equation, whose integrated form is:

$$\ln \frac{C_{TOC}}{C_{TOC_o}} = k_f t_f + k_s t_s \qquad (6.8)$$

Equation 6.8 is valid under the following assumptions: ideal plug flow conditions are observed, oxygen is present in stoichiometric excess, the fast and slow phases exhibit Arrhenius dependency. The above rate equation was modelled against experimental data for comparison as shown in Figure 6.10. In both cases of calculating the rate constant k for the TOC results and their subsequent Arrhenius parameters, the experimental data had been tested for a first order behaviour (without modification) and second order kinetics. The above equations best suited the experimental data.

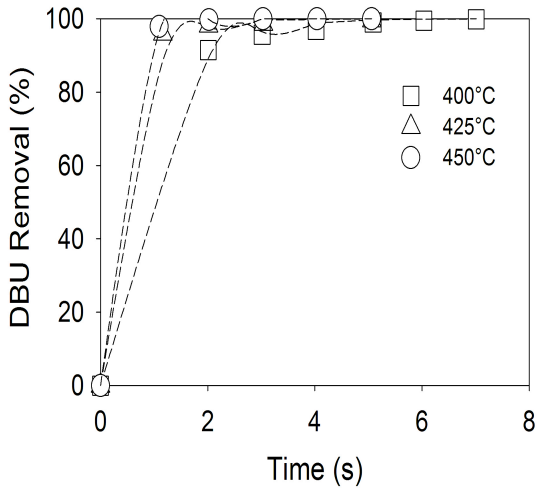

Figure 6.9 DBU removal plotted versus residence time for several temperatures at 25 MPa. Symbols represent experimental data and lines denote kinetic model fitting.

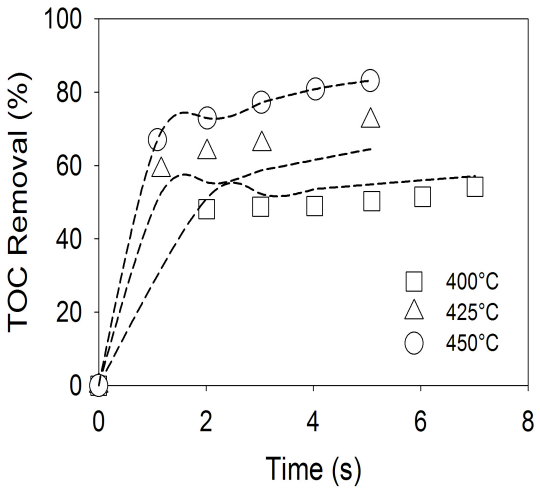

Figure 6.10 TOC removal plotted versus residence time for several temperatures at 25 MPa. Symbols represent experimental data and lines denote kinetic model fitting.

The results above show that there s good agreement between experimental data and the predicted rate data for DBU and TOC.

6.4 Effect of Initial DBU concentration

These experiments were designed to determine the effect of the initial DBU concentration on DBU and TOC removal, and the yield of products. The experiments were carried out at 400ºC, 25 MPa, with a stoichiometric ratio of 1.25. The residence times were varied. The feed concentrations were 6, 12 and 18 mM. The effects of DBU feed concentration on DBU and TOC removal and product yield after 7 seconds residence time is shown in Figure 6.11 and Figure 6.12. At these conditions there is complete breakdown of DBU (> 99%), and TOC removal increased from 54% to 84% as DBU concentration increased. Qi *et al.*(2002), observed a similar trend of increased TOC removal, when the initial feed concentration of aniline was increased ten fold and the stoichiometric ratio was

1.1. This is also in agreement with Veriansyah *et al.* (2007), who found a strong positive dependence between TOC removal and increasing TOC initial concentration.

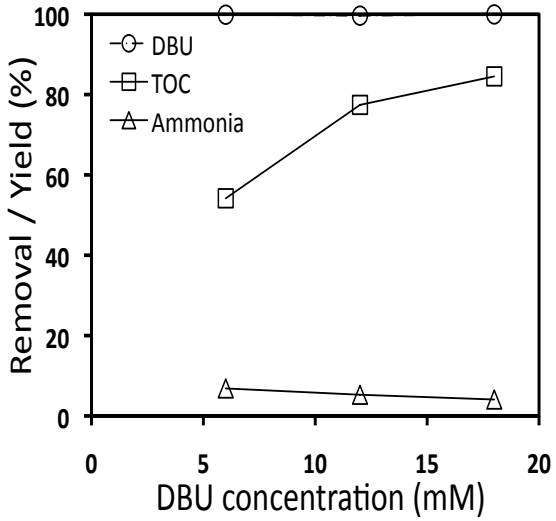

Figure 6.11 Effect of initial DBU concentration on DBU and TOC removal, and the yield of ammonia at 400 ºC, 25 MPa, after 7 s residence time

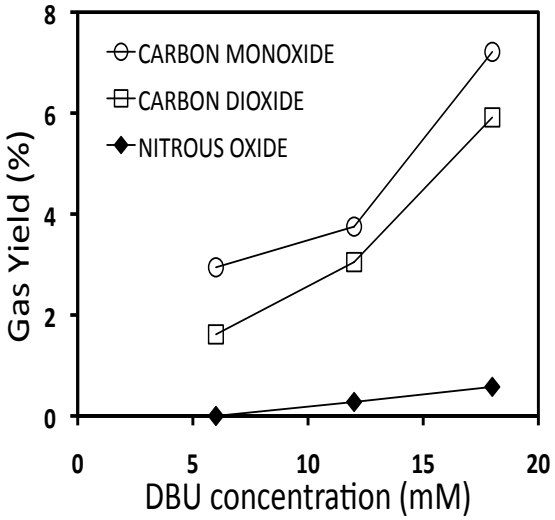

Figure 6.12 Effect of initial DBU concentration on the gas yield at 400 ºC, 25 MPa, after 7 s residence time

Ammonia yield decreased from 7% to 4% as the initial DBU concentration increased. Nitrous oxide was not detected at 6 mM, but was detected at 12 mM and then increased by 0.3% at 18 mM. The increase in TOC removal indicates that high initial DBU concentrations increase the production of free radicals which are necessary for oxidation of any intermediate compounds formed. It is also possible that the increase in free radical concentration slightly inhibits the formation of ammonia, or they could directly react with ammonia, and this interaction results in nitrous oxide as a product. The decrease of ammonia in this instance is favourable because the degradation of ammonia is the rate limiting step in the overall oxidation of organic compounds to nitrogen (Li *et al.*, 1991).

Carbon monoxide and carbon dioxide yield both increased as DBU concentration increased. The yield of carbon monoxide is slightly higher than carbon dioxide (~1%). Figure 6.13 to Figure 6.16b show the effect of initial concentration at varying residence times.

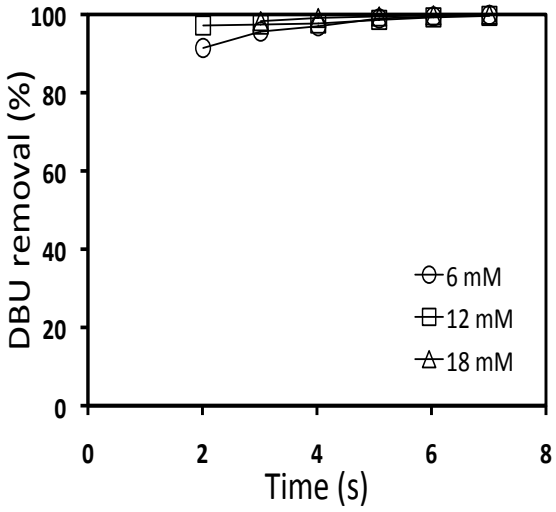

Figure 6.13 Effect of initial DBU concentration on DBU removal at 400 ºC and 25 MPa

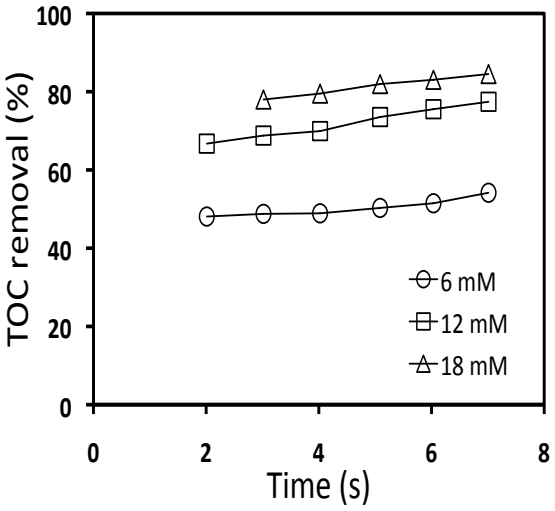

Figure 6.14 Effect of initial DBU concentration on TOC removal at 400 ºC and 25 MPa

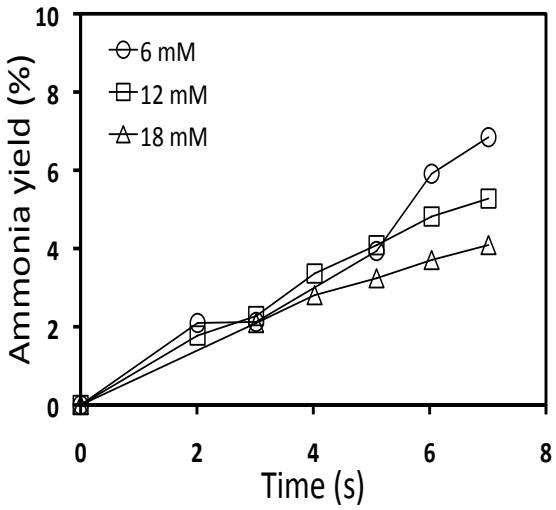

Figure 6.15 Effect of initial DBU concentration on ammonia yield at 400 ºC and 25 MPa

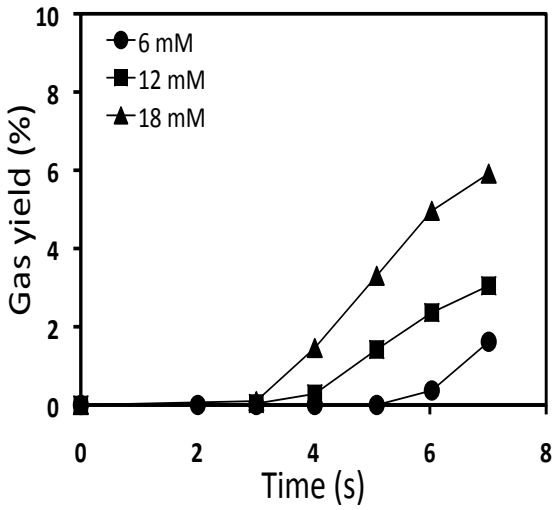

Figure 6.16a Effect of initial DBU concentration on carbon dioxide yield at 400 ºC and 25 MPa

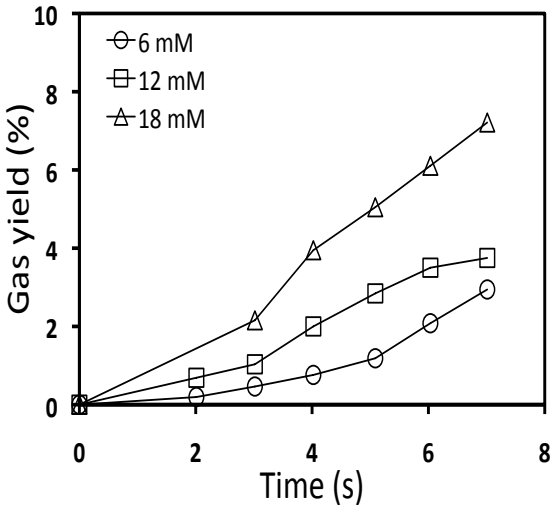

Figure 6.16b Effect of initial DBU concentration on carbon monoxide yield at 400 ºC and 25 MPa

6.5 Oxidation Intermediates

The complete mineralisation of DBU proceeds faster than the TOC removal. This implies that the reaction proceeds through the formation and further oxidation of intermediate organic species. The presence of organic intermediates formed from the hydroxylation or rupturing of the aromatic ring and the scission of a C-N bond, was indicated by the presence of unknown peaks during HPLC analysis.

This was verified by GC-MS analysis (utilising the mass spectrometer as a detector) and matching the peaks obtained with the National Institute of Standards and Technology

(NIST) database. Table 6.3 shows a summary of the intermediate compounds identified in this study.

The results in Table 6.3 and Figure 6.18 show that the decomposition of DBU was initiated by the attack of OH radical (step 1), an oxidising species, which attacks the ring and produces these intermediates. The destruction of these intermediates can be explained through an oxidation (possibly through free radical attack) / hydroxylation reaction (step 2). These intermediates would then undergo further oxidation to yield CO, CO_2, N_2, N_2O and H_2O (step 3). (Aymonier *et al.*, 2000), (Onwudili and Williams, 2007a)

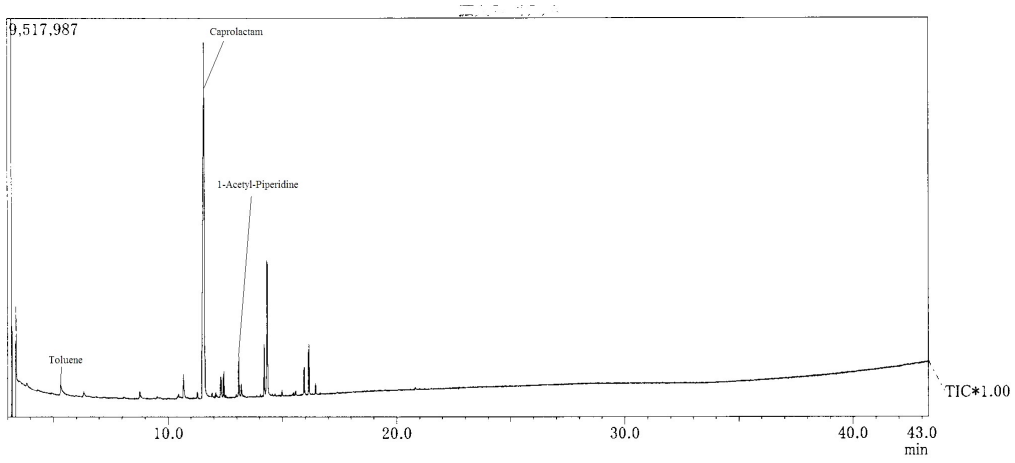

Figure 6.17 GC-MS Chromatograph of SCWO of DBU

Figure 6.17 shows a chromatograph obtained from the oxidation of DBU at 400°C and an initial DBU concentration of 18 mM, after 3 seconds residence time; giving 98% DBU and 78% TOC removal.

Detected Compound	Molecular Weight	Molecular Structure
Caprolactam	113	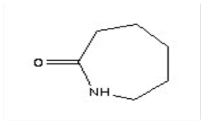
1-Acetyl-Piperidine	127	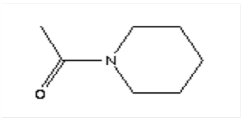
N,N-dimethyl-Formamide	73	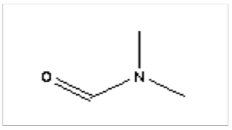
Toluene	92	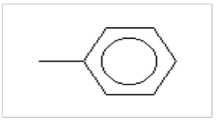
4,5, Dimethyl-Oxazole	97	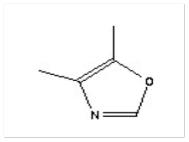
Butyrolactone	86	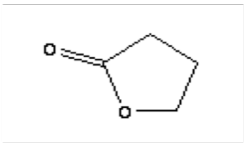
Pentanenitrile	83	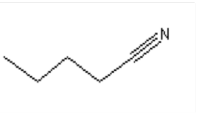

Table 6.3 Summary of Intermediate compounds from the oxidation of DBU

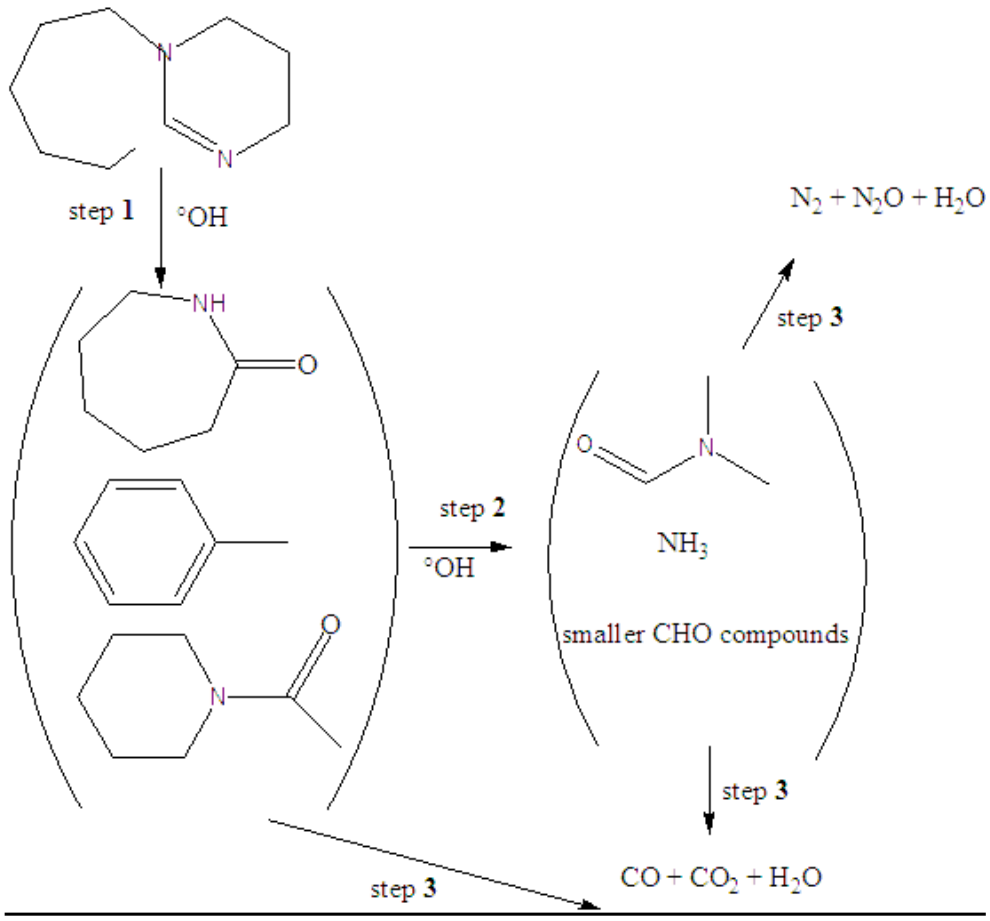

Figure 6.18 A simplified reaction pathway for the supercritical oxidation of DBU

6.6 Summary

The oxidation of DBU solutions were investigated at a temperature range of 400 - 450°C, an initial concentration range of 6 - 18 mM, 25 MPa and an oxidant stoichiometric ratio of 1.25. Temperature increase showed increased DBU and TOC removal efficiency, this was more pronounced for TOC, which showed an increase of 29% at a residence time of 3 seconds. Ammonia yield increased slightly as temperature increased. TOC removal efficiency increased by 31% as the initial DBU concentration increased. DBU removal efficiency was not affected by the increase in initial DBU concentration, while ammonia yield decreased.

The oxidation kinetics were also investigated, and a pseudo first order rate expression was used to satisfactorily predict the oxidation of DBU, with an activation energy of 82 kJ mol-1 and a pre-exponential factor of 2.5×10^{6} s^{-1}. It was found that TOC oxidation progressed as two distinct oxidation steps (fast and then slow) each having a different rate constant. A modified pseudo first order equation was used to evaluate TOC oxidation, the rate expression obtained had good agreement with the experimental data. The activation energy of both phases were 92.3 kJ mol^{-1} and 162.1 kJ mol^{-1} for the fast and slow phase respectively; with pre-exponential factors of 5.1×10^{6} s^{-1} and 9.9×10^{10} s^{-1}

CHAPTER - 7 CONCLUSIONS AND RECOMMENDATIONS

7.1 Conclusions

The research work presented in this thesis focused on the hydrothermal oxidation of nitrogen-containing industrial effluent, using DBU as a model pollutant by different hydrothermal technologies. The oxidation of DBU by WAO, CWAO and SCWO was investigated using laboratory scale systems, the experimental data is presented and discussed throughout this thesis. Kinetic data obtained is also used to develop global kinetic rate expressions for all systems.

For CWAO, a literature review indicated that noble metal catalysts on different supports are more effective for liquid phase oxidation as compared to non-noble metal, which was confirmed by catalyst screening. Ru/Al_2O_3 pellets were selected and used in CWAO experiments. A Ruthenium coated reticulated foam monolith was used as a novel alternative for heterogeneous catalyst instead of Ru/Al_2O_3 pellets. A hazardous industrial effluent was also treated by WAO and CWAO.

7.2 WAO System

A laboratory-scale batch reactor was modified and used for conducting research on the WAO of DBU-containing solutions. This system was used to investigate the destruction efficiency and kinetics at various operating conditions, such as temperature, pressure, oxidant flow-rate, impeller speed and organic concentration.

I. DBU removal in the absence of oxygen was found to be about 30%, but there was no TOC removal, indicating that DBU was not oxidised but instead converted to other compounds. It was concluded that this did not interfere with the study of DBU kinetics.

II. Oxidation results showed that temperature was the primary process parameter affecting DBU and TOC removal. 87% DBU removal was achieved at 240 ºC and 7 MPa, 76% TOC removal was achieved at the same conditions. Ammonia yield increased with temperature resulting in high ammonia concentration, which exceeded the regulated discharge concentration specified by environmental agencies. This indicates that higher temperatures, catalysts or a further treatment step would be required to reduce ammonia concentration. N_2 and CO_2 formation increased with temperature.

III. DBU and TOC removal increased with system pressure, due to increased partial pressure of oxygen in the system. Ammonia yield and gas formation also increased with system pressure.The effect of increased initial DBU concentration on DBU removal was negligible, conversely TOC removal decreased, implying the increased formation of refractory intermediates at higher initial DBU concentrations.

IV. A kinetic analysis was performed to describe the effects of operating parameters on DBU removal. A pseudo first order global rate expression was used to evaluate the rate parameters. The rate expression regressed from the experimental data predicted DBU and TOC removal with good correlation. The rate expression had an Arrhenius activation energy of 78.7 $kJmol^{-1}$ and a pre-exponential factor of 1.62×10^6 min^{-1} for DBU removal at 7 MPa. TOC removal results, showed that it progressed by 3 oxidation steps. The first being an induction phase (time required to build up a sufficient concentration of radicals), a fast phase and then a slow phase. All three phases were found to have Arrhenius dependency and the rate expression was modified to include this. The induction phase decreased with increased temperature.

7.3 CWAO system

A catalyst basket was used in conjunction with the WAO system unit for conducting research on CWAO of DBU-containing solutions. Ru/Al_2O_3 pellets were selected as the experimental catalyst. This system was used to investigate the destruction efficiency and kinetics at various operating conditions, such as temperature, pressure, impeller speed organic concentration, metal loading and catalyst weight.

I. Oxidation results showed that above 500 rpm the rate of oxidation was independent of impeller speed. Ru/Al_2O_3 pellets enhanced DBU and TOC removal compared to WAO at all operating conditions investigated.

II. Temperature was the primary process parameter affecting DBU and TOC removal. Complete DBU removal was achieved at 240 ºC and 7 MPa using 1 g of 3% Ru/Al_2O_3 pellets, 89% TOC removal was achieved at the same conditions. At lower temperatures, DBU removal using 3% Ru/Al_2O_3 pellets was equivalent to that obtained at a temperature 20 ºC higher, under WAO conditions. This enhancement increased for TOC removal to a value of 40 ºC.

III. Ammonia yield decreased with increased temperature, with final ammonia concentrations below the environmental discharge limit of 10 mg/L achieved. A significant ammonia yield decrease of 49.5% was obtained at 240 ºC and 7 MPa using 3% Ru/Al_2O_3 pellets when compared to WAO. This shows 3% Ru/Al_2O_3 pellets is active for ammonia oxidation and would be suited to the oxidation of other N-containing pollutants, because ammonia is a highly refractory N-containing pollutant. N_2 and CO_2 formation increased with temperature and had values higher than those for similar WAO conditions.

IV. Increased system pressure, increased DBU and TOC removal, although a lower ammonia yield is favoured at lower pressures. N_2 and CO_2 formation increased with increased system pressure.

V. Increased initial DBU concentration decreased DBU and TOC removal, while it increased ammonia yield. Changing the metal loading on the catalyst from 3% to 0.5% decreased DBU and TOC removal. Increased catalyst weight had no change on DBU removal, but increased TOC removal slightly. Ammonia yield decreased with increased catalyst weight, while N_2 formation increased.

VI. The activity of 3% Ru/Al_2O_3 pellets decreased when reused for subsequent CWAO runs, because of reduced surface area due to erosion of catalyst support. A novel Ruthenium-coated reticulated foam monolith was compared to 3% Ru/Al_2O_3 pellets for DBU and TOC removal, the pellets were found to be more active for DBU and TOC removal than the reticulated foam. A lower ammonia yield was also found using 3% Ru/Al_2O_3 pellets. The lower activity of the reticulated foam was attributed to the weight of ruthenium metal on the reticulated foam, it was found that as the weight of Ruthenium metal increased, TOC removal increased and ammonia yield decreased. However, the coated reticulated foam's activity for DBU and TOC removal was not affected by consecutive experimental runs. while the activity of 3% Ru/Al_2O_3 pellets decreased significantly after one experimental run.

VII. CWAO using 3% Ru/Al_2O_3 pellets enhanced TOC removal compared to WAO at the same conditions for the treatment of industrial effluent. There was complete removal of ammonia from the industrial effluent using 3% Ru/Al_2O_3 pellets.

VIII. A kinetic analysis was performed to describe the effects of operating parameters on DBU removal. A pseudo first order global rate expression was used to evaluate the rate parameters. The rate expression regressed from the experimental data predicted

DBU and TOC removal with good correlation. The rate expression had an Arrhenius activation energy of 47.5 $kJmol^{-1}$ and a pre-exponential factor of 1.27 x 10^3 min^{-1} for DBU removal at 7 MPa. For TOC, an Arrhenius activation energy of 53.3 $kJmol^{-1}$ and a pre-exponential factor of 4.92 x 10^3 min^{-1} for DBU removal at 7 MPa.

7.4 SCWO system

A laboratory scale SCWO unit, consisting of a continuous tubular reactor was used for conducting research on the SCWO of DBU. This system was used to investigate the destruction efficiency and kinetics at various operating conditions, such as temperature and organic concentration.

I. Oxidation results showed that temperature was the primary process parameter affecting DBU and TOC removal. Near complete DBU removal (> 96%) was observed at above 400 ºC and at 25 MPa, TOC removal increased with temperature. Temperature favoured CO production over that of CO_2, CH_4 production occured in small quantities and at the highest temperature investigated (450 ºC), N_2O production was seen.

II. Ammonia yield increased with temperature, however ammonia concentration sometimes exceeded the discharge concentration. This indicates that higher temperatures would be necessary to achieve greater TOC removal and reduce ammonia yield.

III. TOC removal increased with increasing DBU initial concentration and complete DBU removal was achieved for all DBU concentrations. Ammonia yield decreased with increased DBU initial concentration. CO, CO_2 and N_2O also increased with initial concentration. It is assumed that increased DBU increases the production of free radicals necessary for oxidation.

IV. A kinetic analysis was performed to describe the effects of operating parameters on DBU removal. A pseudo first order global rate expression was used to evaluate the rate parameters. The rate expression regressed from the experimental data predicted DBU and TOC removal with good correlation. The rate expression had an Arrhenius activation energy of 81.8 kJmol^{-1} and a pre-exponential factor of 2.5 x 10^{6} s^{-1} for DBU removal at 25 MPa. TOC removal results, showed TOC removal progressed by 2 distinct oxidation steps. The first being a fast phase and then a slow phase (the slow phase indicates the presence of refractory compounds which are difficult to oxidise). All two phases were found to have Arrhenius dependency and the rate expression was modified to include this.

7.5 Recommendations

The following are recommendations for areas that would benefit from further consideration based on observations or unresolved issues arising from this thesis:

I. **Propose an oxidation reaction pathway for DBU**

Although an extensive study was undertaken for DBU oxidation using the three systems, the formation of oxidation intermediates could not be monitored for WAO and CWAO experiments due to a lack of GC/MS analysis. Consequently, no oxidation reaction pathway could be proposed. Intermediate identification would enable optimisation of the reaction conditions for complete mineralisation of pollutants.

II. **Further Reticulated foam monolith investigation**

Coated Reticulated foam monolith have shown potential as a heterogeneous catalyst. It was found that increased coating weight enhanced TOC removal and decreased ammonia

yield. Further experiments assessing the optimal coating weight should be carried out to achieve comparable or better results compared to Ru/Al_2O_3 pellets, because the reticulated foam monolith has improved stability than the pellets.

III. **Conduct experiments on the converted Batch reactor**

The Batch reactor used for WAO and CWAO experiments was successfully converted into a CSTR. Experiments could not be conducted due to the failure of the high pressure pump for the system. Kinetic data obtained from these experiments would enable the derivation of a design equation and aid in the design and scale-up of a mobile treatment unit for wastewater treatment.

IV. Improved model for DBU oxidation

Taking into account the oxygen mass transfer coefficient, the reaction order for oxygen should be calculated, and used in the global rate equation for DBU oxidation, which would give a more accurate fit for the experimental data The reaction orders should also be ascertained using MATLAB.

V. Further characterisation of catalyst

Further characterisation of the catalyst using techniques such as gas chemisorption, dynamic vapoour sorption would enable its physical properties to be measured more accurately. In addition, X-ray diffraction would identify the species present on the catalyst surface, which would give better insight and understanding of the reaction between the Ru catalyst and DBU.

List of References

Aki S. and Abraham M. A. (1998) An economic evaluation of catalytic supercritical water oxidation: Comparison with alternative waste treatment technologies. *Environmental Progress,* 17**,** 246-255.

Akiya N. and Savage P. E. (2002) Roles of water for chemical reactions in high-temperature water. *Chemical Reviews,* 102**,** 2725-2750.

Andreozzi R., Insola A., Caprio V. and Damore M. G. (1991) Ozonation of pyridine in aqueous-solution - Mechanistic and kinetic aspects. *Water Research,* 25**,** 655-659.

Anikeev V. I., Ermakova A. and Goto M. (2005) Decomposition and oxidation reactions of aliphatic nitro compounds in supercritical water. *Kinetics and Catalysis,* 46**,** 821-825.

Antal M. J., Brittain A., Dealmeida C., Ramayya S. and Roy J. C. (1987) Heterolysis and homolysis in Supercritical water. *Acs Symposium Series,* 329**,** 77-86.

Arslan I. and Balcioglu I. A. (2001) Degradation of Remazol Black B dye and its simulated dye bath wastewater by advanced oxidation processes in heterogeneous and homogeneous media. *Coloration Technology,* 117**,** 38-42.

Ashraf-Ball N. F. (2005) The Treatment of a Toxic Nitrogenous containing Organic compound by Supercritical Water Oxidation and Wet Air Oxidation Processes: Operating Conditions and Reaction Kinetics. *School of Chemical Engineering.* Birmingham, The University of Birmingham.

Aymonier C., Beslin P., Jolivalt C. and Cansell F. (2000) Hydrothermal oxidation of a nitrogen-containing compound: the fenuron. *The Journal of Supercritical Fluids,* 17**,** 45-54.

Baldi G., Goto S., Chow C. K. and Smith J. M. (1974) Catalytic oxidation of formic-acid in water - intraparticle diffusion in liquid-filled pores. *Industrial and Engineering Chemistry Product Research and Development,* 13**,** 447-452.

Barbier J., Delanoe F., Jabouille F., Duprez D., Blanchard G. and Isnard P. (1998) Total oxidation of acetic acid in aqueous solutions over noble metal catalysts. *Journal of Catalysis,* 177**,** 378-385.

Barbier J., Oliviero L., Renard B. and Duprez D. (2002) Catalytic wet air oxidation of ammonia over M/CeO2 catalysts in the treatment of nitrogen-containing pollutants. *Catalysis Today,* 75**,** 29-34.

Barker J. and Kilner M. (1994) The coordination chemistry of the amidine ligand. *Coordination Chemistry Reviews,* 133**,** 219-300.

Benjamin K. M. and Savage P. E. (2004) Hydrothermal reactions of methylamine. *The Journal of Supercritical Fluids,* 31**,** 301-311.

Bermejo M. D., Cantero F. and Cocero M. J. (2008) Supercritical water oxidation of feeds with high ammonia concentrations Pilot plant experimental results and modeling. *Chemical Engineering Journal,* 137**,** 542-549.

Bermejo M. D. and Cocero M. J. (2006) Supercritical water oxidation: A technical review. *AIChe Journal,* 52**,** 3933-3951.

Bermejo M. D., Cocero M. J. and Fernandez-Polanco F. (2004) A process for generating power from the oxidation of coal in supercritical water. *Fuel,* 83**,** 195-204.

Bermejo M. D., Fernandez-Polanco F. and Cocero M. J. (2005) Modeling of a transpiring wall reactor for the supercritical water oxidation using simple flow patterns: Comparison to experimental results. *Industrial and Engineering Chemistry Research,* 44**,** 3835-3845.

Bhargava S. K., Tardio J., Prasad J., Foger K., Akolekar D. B. and Grocott S. C. (2006) Wet oxidation and catalytic wet oxidation. *Industrial and Engineering Chemistry Research,* 45**,** 1221-1258.

Bjerre A. B. and Sorensen E. (1992) Thermal decomposition of dilute aqueous formic-acid solutions. *Industrial and Engineering Chemistry Research,* 31**,** 1574-1577.

Bond G. C. (1987) *Heterogeneous Catalysis: Principles and Applications,* Oxford, Oxford University Press.

Boock L. T., Lamarca C. and Klein M. T. (1993) Hydrolysis and oxidation in Supercritical water. *Endeavour,* 17**,** 180-185.

Cansell F., Beslin P. and Berdeu B. (1998) Hydrothermal Oxidation of Model Molecules and Industrial Wastes. *Environmental Progress,* 17**,** 240-245.

Cao S., Chen G., Hu X. and Yue P. L. (2003) Catalytic wet air oxidation of wastewater containing ammonia and phenol over activated carbon supported Pt catalysts. *Catalysis Today,* 88**,** 37-47.

Chang C. M. J., Li S. S. and Ko C. M. (1995) Catalytic Wet Oxidations of phenol contaminated and *p*-chlorophenol contaminated waters. *Journal of Chemical Technology and Biotechnology,* 64**,** 245-252.

Chen F. Q., Wu S. F., Chen J. Z. and Rong S. X. (2001) COD removal efficiencies of some aromatic compounds in supercritical water oxidation. *Chinese Journal of Chemical Engineering,* 9**,** 137-140.

Chen G., Lei L., Hu X. and Yue P. L. (2003) Kinetic study into the wet air oxidation of printing and dyeing wastewater. *Separation and Purification Technology,* 31**,** 71-76.

Christoskova S. and Stoyanova M. (2001) Degradation of phenolic waste waters over Ni-oxide. *Water Research,* 35**,** 2073-2077.

Cocero M. J., Alonso E., Torio R., Vallelado D. and Fdz-Polanco F. (2000a) Supercritical water oxidation in a pilot plant of nitrogenous compounds: 2-propanol mixtures in the temperature range 500-750 degrees C. *Industrial and Engineering Chemistry Research,* 39**,** 3707-3716.

Cocero M. J., Vallelado D., Torio R., Alonso E. and Fdez-Polanco F. (2000b) Optimisation of the operation variables of a supercritical water oxidation process. *Water Science and Technology,* 42**,** 107-113.

Crain N., Tebbal S., Li L. X. and Gloyna E. F. (1993) Kinetics and Reaction Pathways of Pyridine Oxidation in Supercritical Water. *Industrial and Engineering Chemistry Research,* 32**,** 2259-2268.

Cramer S. D. (1980) The Solubility of Oxygen in Brines from 0ºC to 300ºC. *Industrial and Engineering Chemistry Process Design and Development,* 19**,** 300-305.

Cybulski A. (2007) Catalytic Wet Air Oxidation: Are Monolithic Catalysts and Reactors Feasible? *Industrial and Engineering Chemistry Research,* 46, 4007-4033

Day D. C., Hudgins R. R. and Silveston P. L. (1973) Oxidation of propionic acid solutions. *Canadian Journal of Chemical Engineering,* 51**,** 733-740.

Debellefontaine H., Chakchouk M., Foussard J. N., Tissot D. and Striolo P. (1996) Treatment of organic aqueous wastes: Wet air oxidation and wet peroxide oxidation. *Environmental Pollution,* 92**,** 155-164.

Devlin H. R. and Harris I. J. (1984) Mechanism of the oxidation of aqueous phenol with dissolved oxygen. *Industrial and Engineering Chemistry Fundamentals,* 23**,** 387-392.

Dietrich M. J., Randall T. L. and Canney P. J. (1985) Wet Air Oxidation of Hazardous Organics in Wastewater. *Environmental Progress,* 4.

Ding Z. Y., Frisch M. A., Li L. X. and Gloyna E. F. (1996) Catalytic oxidation in supercritical water. *Industrial and Engineering Chemistry Research,* 35**,** 3257-3279.

Donlagic J. and Levec J. (1998) Does the catalytic wet oxidation yield products more amenable to biodegradation. *Applied Catalysis B-Environmental,* 17**,** L1-L5.

Downey K. W., Snow R. H., Hazlebeck D. A. and Roberts A. J. (1995) Corrosion and chemical agent destruction - Research on supercritical water oxidation of hazardous military wastes. *American Chemical Society Symposium Series,* 608, 313-326

Duprez D., Delanoë F., Barbier J., Isnard P. and Blanchard G. (1996) Catalytic oxidation of organic compounds in aqueous media. *Catalysis Today,* 29**,** 317-322.

Eftaxias A., Font J., Fortuny A., Fabregat A. and Stuber F. (2006) Catalytic wet air oxidation of phenol over active carbon catalyst - Global kinetic modelling using simulated annealing. *Applied Catalysis B-Environmental,* 67**,** 12-23.

Eftaxias A., Font J., Fortuny A., Giralt J., Fabregat A. and Stuber F. (2001) Kinetic modelling of catalytic wet air oxidation of phenol by simulated annealing. *Applied Catalysis B-Environmental,* 33**,** 175-190.

European Economic Community. (2008) Regulation (EC) No 1137/2008 of the European Parliament and of the European Council, 1-54.

Fang H. Y., Chou M. S. and Huang C. W. (1993) Nitrification of ammonia nitrogen in refinery wastewater. *Water Research,* 27**,** 1761-1765.

Forni L., Bahnemann D. and Hart E. J. (1982) Mechanism of the hydroxide ion initiated decomposition of ozone in aqueous solution. *Journal of Physical Chemistry,* 86**,** 255-259.

Fortuny A., Bengoa C., Font J., Castells F. and Fabregat A. (1999) Water pollution abatement by catalytic wet air oxidation in a trickle bed reactor. *Catalysis Today,* 53**,** 107-114.

Foussard J.-N., Debellefontaine H. and Besombes-Vailhe J. (1989) Efficient Elimination of Organic Liquid Wastes: Wet Air Oxidation. *Journal of Environmental Engineering,* 115**,** 367-385.

Freedman D.A. (2005) Statistical Models: Theory and Practice. Cambridge University Press, New York. 1-424

Furuya H., Uwabe R., Sutoh N., Okuwaki A., Amano A. and Okabe T. (1985) Oxidation of coals in liquid phases VII. Oxidation of oxygen containing model compounds of coal by oxygen in concentrated sodium hydroxide. *Bulletin of the Chemical Society of Japan,* 58**,** 3016-3020.

Gallezot P., Laurain N. and Isnard P. (1996) Catalytic wet-air oxidation of carboxylic acids on carbon-supported platinum catalysts. *Applied Catalysis B-Environmental,* 9**,** L11-L17.

Gogate P. R. and Aniruddha B. P. (2003) A review of imperative technologies for wastewater treatment II: hybrid methods. *Advances in Environmental Research,* 8**,** 533-597.

Gomes H. T., Serp P., Kalck P., Figueiredo J. L. and Faria J. L. (2005) Carbon supported platinum catalysts for catalytic wet air oxidation of refractory carboxylic acids. *Topics in Catalysis,* 33**,** 59-68.

Gopalan S. and Savage P. E. (1994) Reaction mechanism for phenol oxidation in supercritical water. *Journal of Physical Chemistry,* 98**,** 12646-12652.

Gopalan S. and Savage P. E. (1995) Phenol oxidation in supercritical water - From global kinetics and product identities to an elementary reaction model in Hutchenson, K.W. and Foster, N.R. (Eds.) *Innovations in Supercritical fluids science and technology*, American Chemical Society, Washington D.C.

Goto S. and Smith J. M. (1975) Trickle bed reactor performance II - Reaction studies. *AIChe Journal,* 21**,** 714-720.

Griffith J. W. and Raymond D. H. (2002) The first commercial supercritical water oxidation sludge processing plant. *Waste Management,* 22**,** 453-459.

Grosjean N., Descorme C. and Besson M. (2010) Catalytic wet air oxidation of N,N-dimethylformamide aqueous solutions: Deactivation of TiO2 and ZrO2-supported noble metal catalysts. *Applied Catalysis B-Environmental,* 97**,** 276-283.

Gulyas H., vonBismarck R. and Hemmerling L. (1995) Treatment of industrial wastewaters with ozone hydrogen peroxide. *Water Science and Technology,* 32**,** 127-134.

Gunale T. L. and Mahajani V. V. (2008a) Studies in wet air oxidation of aqueous morpholine over Ru/TiO2 catalyst: an insight into the fate of the 'N' atom. *Journal of Chemical Technology and Biotechnology,* 83**,** 1154-1162.

Gunale T. L. and Mahajani V. V. (2008b) Studies in wet air oxidation of aqueous morpholine over Ru/TiOcatalyst: an insight into the fate of the N atom. *Journal of Chemical Technology and Biotechnology,* 83**,** 1154-1162.

Gunale T. L. and Mahajani V. V. (2010) An insight into Ru/TiO2 catalyzed wet air oxidation of N-ethylethanolamine in an aqueous solution. *Chemical Engineering Journal,* 159**,** 17-23.

Hamoudi S., Belkacemi K., Sayari A. and Larachi F. (2001) Catalytic oxidation of 4-chloroguaiacol reaction kinetics and catalytic studies. *Chemical Engineering Science,* 56**,** 1275-1283.

Hamoudi S., Larachi F. and Sayari A. (1998) Wet oxidation of phenolic solutions over heterogeneous catalysts: Degradation profile and catalyst behavior. *Journal of Catalysis,* 177**,** 247-258.

Hamoudi S., Sayari A., Belkacemi K., Bonneviot L. and Larachi F. (2000) Catalytic wet oxidation of phenol over PtxAg1-xMnO2/CeO2 catalysts. *Catalysis Today,* 62**,** 379-388.

Hao O. J. and Phull K. K. (1993) Wet oxidation of nitrotoluenesulfonic acid - some intermeadiates, reaction pathways, and byproduct toxicity. *Environmental Science and Technology,* 27**,** 1650-1658.

Hao O. J., Phull K. K., Davis A. P., Chen J. M. and Maloney S. W. (1993) Wet Air Oxidation of Trinitrotoluene manufacturing red water. *Water Environment Research,* 65**,** 213-220.

Harada Y. and Yamasaki K. (1994) Treatment of wastewater and sludge by a catalytic wet oxidation process. *Desalination,* 98**,** 27-39.

Harnby N., Edwards M. F. and Nienow A. W. (1992) *Mixing in the Process Industries* Oxford, Butterworth-Heinemann.

Harradine D. M., Buelow S. J., Dellorco P. C., Dyer R. B., Foy B. R., Robinson J. M., Sanchez J. A., Spontarelli T. and Wander J. D. (1993) Oxidation chemistry of energetic materials in Supercritical water. *Hazardous Waste and Hazardous Materials,* 10**,** 233-246.

Heger K., Uematsu M. and Franck E. U. (1980) The static dielectric constant of water at high pressures and temperatures to 500 MPa and 550 ºC. *Berichte Der Bunsen-Gesellschaft-Physical Chemistry Chemical Physics,* 84**,** 758-762.

Helling R. K. and Tester J. W. (1988) Oxidation of simple compounds and mixtures in Supercritical water - Carbon monoxide, ammonia and ethanol. *Environmental Science and Technology,* 22**,** 1319-1324.

Hoffmann M. M. and Conradi M. S. (1997) Are there hydrogen bonds in supercritical water? *Journal of the American Chemical Society,* 119**,** 3811-3817.

Holgate H. R., Meyer J. C. and Tester J. W. (1995) Glucose hydrolysis and oxidation in Supercritical water. *AIChe Journal,* 41**,** 637-648.

Hussain S. T., Sayari A. and Larachi F. (2001a) Enhancing the stability of Mn-Ce-OWETOX catalysts using potassium. *Applied Catalysis B-Environmental,* 34**,** 1-9.

Hussain S. T., Sayari A. and Larachi F. (2001b) Novel K-doped Mn-Ce-O wet oxidation catalysts with enhanced stability. *Journal of Catalysis,* 201**,** 153-157.

Ichinose S. and Okuwaki A. (1990) Oxidation of coals in Liquid phases X. Mechanism of the cleavage of Benxenecarboxylic acids to Oxalic acid and carbon dioxide by the base catlaysed oxygen oxidation. *Bulletin of the Chemical Society of Japan,* 63**,** 159-165.

Imamura S. (1999) Catalytic and non catalytic wet oxidation. *Industrial and Engineering Chemistry Research,* 38**,** 1743-1753.

Imamura S., Kinunaka H. and Kawabata N. (1982) The Wet oxidation of organic compounds catalysed by CO-BI complex oxide. *Bulletin of the Chemical Society of Japan,* 55**,** 3679-3680.

Ingale M. N., Joshi J. B., Mahajani V. V. and Gada M. K. (1996) Waste treatment of an aqueous waste stream from a cyclohexane oxidation unit: a case study. *Process Safety and Environmental Protection,* 74.

IUPAC. Compendium of Chemical Terminology, 2nd ed. (the "Gold Book"), (1997). Compiled by A. D. McNaught and A. Wilkinson. Blackwell Scientific Publications, Oxford.

Joglekar H. S., Samant S. D. and Joshi J. B. (1991) Kinetics of Wet Air Oxidation of Phenol and Substituted Phenols. *Water Research,* 25**,** 135-145.

Kayan B. and Gizir A. M. (2005) Wet-air oxidation of p-nitrophenol. *Reaction Kinetics and Catalysis Letters,* 84**,** 189-197.

Killilea W. R., Swallow K. C. and Hong G. T. (1992) The fate of nitrogen in Supercritical water oxidation. *Journal of Supercritical Fluids,* 5**,** 72-78.

Kim S. K. and Ihm S. K. (2002) Effects of Ce addition and Pt precursor on the activity of Pt/ Al2O3 catalysts for wet oxidation of phenol. *Industrial and Engineering Chemistry Research,* 41**,** 1967-1972.

Kiwi J., Pulgarin C. and Peringer P. (1994) Effect of fenton and photo-fenton reactions of the degradation and biodegradability of 2-nitrophenols and 4-nitrophenols in water treatment. *Applied Catalysis B-Environmental,* 3**,** 335-350.

Klinghoffer A. A., Cerro R. L. and Abraham M. A. (1998) Catalytic wet oxidation of acetic acid using platinum on alumina monolith catalyst. *Annual Meeting of the American-Institute-of-Chemical-Engineers.* Chicago, Illinois, Elsevier Science Bv.

Kolaczkowski S. T., Beltran F. J., McLurgh D. B. and Rivas F. J. (1997) Wet Air Oxidation of Phenol: Factors that May Influence Global Kinetics. *Process Safety and Environmental Protection,* 75**,** 257-265.

Kolaczkowski S. T., Plucinski P., Beltran F. J., Rivas F. J. and McLurgh D. B. (1999) Wet air oxidation: a review of process technologies and aspects in reactor design. *Chemical Engineering Journal,* 73**,** 143-160.

Koo M., Lee W. K. and Lee C. H. (1997) New reactor system for supercritical water oxidation and its application on phenol destruction. *Chemical Engineering Science,* 52**,** 1201-1214.

Kramer A., Mittelstadt S. and Vogel H. (1999) Hydrolysis of nitriles in supercritical water. *Chemie Ingenieur Technik,* 71**,** 261-267.

Kritzer P. (2004) Corrosion in high-temperature and supercritical water and aqueous solutions: a review. *Journal of Supercritical Fluids,* 29**,** 1-29.

Kritzer P. and Dinjus E. (2001) An assessment of supercritical water oxidation (SCWO) - Existing problems, possible solutions and new reactor concepts. *Chemical Engineering Journal,* 83**,** 207-214.

Kuo C. H., Yuan F. and Hill D. O. (1997) Kinetics of oxidation of ammonia in solutions containing ozone with or without hydrogen peroxide. *Industrial and Engineering Chemistry Research,* 36**,** 4108-4113.

Larachi F. (2005) Catalytic wet oxidation: micro-meso-macro methodology from catalyst synthesis to reactor design. *Topics in Catalysis,* 33**,** 109-134.

Lee D. K. (2003) Mechanism and kinetics of the catalytic oxidation of aqueous ammonia to molecular nitrogen. *Environmental Science and Technology,* 37**,** 5745-5749.

Lee D. K., Cho J. S. and Yoon W. L. (2005) Catalytic wet oxidation of ammonia: Why is N_2 formed preferentially against NO_3? *Chemosphere,* 61**,** 573-578.

Lee D. S. and Gloyna E. F. (1992) Hydrolysis and oxidation of acetamide in Supercritical water.. *Environmental Science and Technology,* 26**,** 1587-1593.

Lee D. S., Park K. S., Nam Y. W., Kim Y. C. and Lee C. H. (1997) Hydrothermal decomposition and oxidation of p-nitroaniline in supercritical water. *Journal of Hazardous Materials,* 56**,** 247-256.

Lee D. S. and Park S. D. (1996) Decomposition of nitrobenzene in supercritical water. *Journal of Hazardous Materials,* 51**,** 67-76.

Levenspiel O. (1972) *Chemical Reaction Engineering - Second Edition*, Willey.

Li H. and Oshima Y. (2005) Elementary Reaction Mechanism of Methylamine Oxidation in Supercritical Water. *Industrial and Engineering Chemistry Research,* 44**,** 8756-8764.

Li L. X., Chen P. S. and Gloyna E. F. (1991) Generalised kinetic model for Wet oxidation of organic compounds. *AIChe Journal,* 37**,** 1687-1697.

Li Puma G. and Yue P. L. (2001) The modeling of a fountain photocatalytic reactor with a parabolic profile. *Chemical Engineering Science,* 56**,** 721-726.

Lin S. H. and Chuang T. S. (1994) Wet Air Oxidation and activated sludge treatment of phenolic wastewater. *Journal of Environmental Science and Health Part a-Environmental Science and Engineering and Toxic and Hazardous Substance Control,* 29**,** 547-564.

Lixiong L., Chen P. and Gloyna E. F. (1991) Kinetic model for wet air oxidation of organic compounds in subcritical and supercritical water. *Supercritical Fluid Enginnering Science,* 24**,** 305-313.

Lopes R. J. G., Silva A. M. T. and Quinta-Ferreira R. M. (2007) Screening of catalysts and effect of temperature for kinetic degradation studies of aromatic compounds during wet oxidation. *Applied Catalysis B-Environmental,* 73**,** 193-202.

Lopez Bernal J., Portela J. R., Nebot Sanz E. and Martinez de la Ossa E. (1999) Wet air oxidation of oily wastes generated aboard ships: kinetic modeling. *Hazardous Materials***,** 61-73.

Luck F. (1996) A review of industrial catalytic wet air oxidation processes. *Catalysis Today,* 27**,** 195-202.

Luck F. (1999) Wet air oxidation: past, present and future. *Catalysis Today,* 53**,** 189-199.

Marshall W. L. and Franck E. U. (1981) Ion product of water substance 0 ºC - 1000 ºC, 1 - 10,000 bars - New international formulation and its background. *Journal of Physical and Chemical Reference Data,* 10**,** 295-304.

Martin A., Luck F., Armbruster U., Patria L., Radnik J. and Schneider M. (2005) Ammonia removal from effluent streams of wet oxidation under high pressure. *Topics in Catalysis,* 33**,** 155-169.

Martin N. and Galey C. (1994) Use of static mixer for oxidation and disinfection by ozone. *Ozone-Science and Engineering,* 16**,** 455-473.

Martino C. J. and Savage P. E. (1997) Supercritical water oxidation kinetics, products, and pathways for CH3- and CHO-substituted phenols. *Industrial and Engineering Chemistry Research,* 36**,** 1391-1400.

Matatov-Meytal Y. I. and Sheintuch M. (1998) Catalytic abatement of water pollutants. *Industrial and Engineering Chemistry Research,* 37**,** 309-326.

McKinseyandCompany (2009) Charting Our Water Future: Economic frameworks to inform decision-making. 2030 Water Resources Group.

Meyer J. C., Marrone P. A. and Tester J. W. (1995) Acetic acid oxidation and hydrolysis in supercritical water. *AIChe Journal,* 41**,** 2108-2121.

Minh D. P., Aubert G., Gallezot P. and Besson M. (2007) Degradation of olive oil mill effluents by catalytic wet air oxidation: 2-Oxidation of p-hydroxyphenylacetic and p-hydroxybenzoic acids over Pt and Ru supported catalysts. *Applied Catalysis B-Environmental,* 73**,** 236-246.

Mishra V. S., Padiyar V., Joshi J. B., Mahajani V. V. and Desai J. D. (1995) Treatment of Acrylonitrile plant wastewater. *Process Safety and Environmental Protection,* 73**,** 243-251.

Modell M., Larson J. and Sobczynski S. F. (1992) Supercritical water oxidation of pulp mill sludges. *Tappi Journal,* 75**,** 195-202.

Ogunsola O. M. (2000) Decomposition of isoquinoline and quinoline by supercritical water. *Journal of Hazardous Materials,* 74**,** 187-195.

Ohta H., Goto S. and Teshima H. (1980) Liquid phase oxidation of phenol in a rotating catlaytic basket reactor. *Industrial and Engineering Chemistry Fundamentals,* 19**,** 180-185.

Oliviero L., Barbier J. and Duprez D. (2003) Wet Air Oxidation of nitrogen-containing organic compounds and ammonia in aqueous media. *Applied Catalysis B,* 40**,** 163-184.

Oliviero L., Barbier J., Duprez D., Guerrero-Ruiz A., Bachiller-Baeza B. and Rodriguez-Ramos I. (2000) Catalytic wet air oxidation of phenol and acrylic acid over Ru/C and Ru-CeO2/C catalysts. *Applied Catalysis B-Environmental,* 25**,** 267-275.

Onwudili J. A. and Williams P. T. (2007a) Reaction mechanisms for the decomposition of phenanthrene and naphthalene under hydrothermal conditions. *Journal of Supercritical fluids,* 39**,** 399-408.

Onwudili J. A. and Williams P. T. (2007b) Reaction mechanisms for the hydrothermal oxidation of petroleum derived aromatic and aliphatic hydrocarbons. *Journal of Supercritical Fluids,* 43**,** 81-90.

Ormad P., Cortes S., Puig A. and Ovelleiro J. L. (1997) Degradation of organochloride compounds by O-3 and O-3/H2O2. *Water Research,* 31**,** 2387-2391.

Paillard H., Brunet R. and Dore M. (1988) Optimal conditions for applying an ozone-hydrogen peroxide oxidising system.. *Water Research,* 22**,** 91-103.

Panayiotou C. (1997) Solubility parameter revisited: an equation-of-state approach for its estimation. *Fluid Phase Equilibria,* 131**,** 21-35.

Perkowski J., Kos L. and Ledakowicz S. (2000) Advanced oxidation of textile wastewaters. *Ozone-Science and Engineering,* 22**,** 535-550.

Pifer A., Hogan T., Snedeker B., Simpson R., Lin M. R., Shen C. Y. and Sen A. (1999) Broad spectrum catalytic system for the deep oxidation of toxic organics in aqueous medium using dioxygen as the oxidant. *Journal of the American Chemical Society,* 121**,** 7485-7492.

Pintar A., Besson M. and Gallezot P. (2001) Catalytic wet air oxidation of Kraft bleaching plant effluents in the presence of titania and zirconia supported ruthenium. *Applied Catalysis B-Environmental,* 30**,** 123-139.

Pintar A. and Levec J. (1994) Catalytic liquid phase oxidation of phenol aqueous solutions - aA kinetic investigation. *Industrial and Engineering Chemistry Research,* 33**,** 3070-3077.

Pinto L. D., Santos L. M. F. d., Al-Duri B. and Santos R. C. D. (2006) Supercritical water oxidation of quinoline in a continuous plug flow reactor - part 1: effect of key operating parameters. 81**,** 912-918.

Portela J. R., Lopez Bernal J., Nebot Sanz E. and Martinez de la Ossa E. (1997) Kinetics of wet air oxidation of phenol. *Chemical Engineering Journal,* 67**,** 115-121.

Portela J. R., Lopez J., Nebot E. and de la Ossa E. M. (2001a) Elimination of cutting oil wastes by promoted hydrothermal oxidation. *Journal of Hazardous Materials,* 88**,** 95-106.

Portela J. R., Nebot E. and de la Ossa E. M. (2001b) Kinetic comparison between subcritical and supercritical water oxidation of phenol. *Chemical Engineering Journal,* 81**,** 287-299.

Prasad J. and Materi G. E. (1990) Comparative study of air- and oxygen-based wet oxidation systems. *7th National Conference of Hazardous Waste and Hazardous Materials Research.* Silver Spring, MD.

Pray H. A., Schweickert C. E. and Minnich B. H. (1952) Solubility of Hydrogen, Oxygen, Nitrogen, and Helium in Water at Elevated Temperatures. *Industrial and Engineering Chemistry,* 44**,** 1146-1151.

Qi X. H., Zhuang Y. Y., Yuan Y. C. and Gu W. X. (2002) Decomposition of aniline in supercritical water. *Journal of Hazardous Materials,* 90**,** 51-62.

Qin J. and Aika K. (1997) Catalytic wet air oxidation of ammonia over alumina supported metals. *Applied Catalysis B,* 16**,** 261-268.

Qin J. and Aika K.-i. (1998) Catalytic wet air oxidation of ammonia over alumina supported metals. *Applied Catalysis B: Environmental,* 16**,** 261-268.

Qin J. Y., Zhang Q. L. and Chuang K. T. (2001) Catalytic wet oxidation of p-chlorophenol over supported noble metal catalysts. *Applied Catalysis B-Environmental,* 29**,** 115-123.

Rebert C. J. and Kay W. B. (1959) The phase behavior and solubility relations of the benzene-water system. *AIChe Journal,* 5**,** 285-289.

Rebrov E. V., de Croon M. H. J. M. and Schouten J. C. (2002) Development of the kinetic model of platinum catalyzed ammonia oxidation in a microreactor. *Chemical Engineering Journal,* 90**,** 61-76.

Rivas F. J., Gimeno O., Portela J. R., de la Ossa E. M. and Beltran F. J. (2001) Supercritical water oxidation of olive oil mill wastewater. *Industrial and Engineering Chemistry Research,* 40**,** 3670-3674.

Rivas F. J., Kolaczkowski S. T., Beltran F. J. and McLurgh D. B. (1998) Development of a model for the wet air oxidation of phenol based on a free radical mechanism. *Chemical Engineering Science,* 53**,** 2575-2586.

Robert R., Barbati S., Ricq N. and Ambrosio M. (2002) Intermediatesin the wet oxidation of cellulose: identification of hydroxyl radical and characterisation of hydrogen peroxide. *Water Research,* 36.

Sadana A. and Katzer J. R. (1974) Involvement of free radicals in aqueous phase catalytic oxidation of phenol over copper oxide. *Journal of Catalysis,* 35**,** 140-152.

Santos A., Yustos P., Durban B. and Garcia-Ochoa F. (2001) Catalytic wet oxidation of phenol: Kinetics of the mineralization rate. *Industrial and Engineering Chemistry Research,* 40**,** 2773-2781.

Sarasa J., Roche M. P., Ormad M. P., Gimeno E., Puig A. and Ovelleiro J. L. (1998) Treatment of a wastewater resulting from dyes manufacturing with ozone and chemical coagulation. *Water Research,* 32**,** 2721-2727.

Satterfield C. N. (1980) *Heterogeneous catalysis in practice,* New York, McGraw-Hill.

Savage P. E., Yu J., Stylski N. and Brock E. E. (1984) Kinetics and mechanism of methane oxidation in supercritical water. *The Journal of Supercritical Fluids,* 12**,** 141-153.

Schutt B. D. and Abraham M. A. (2004) Evaluation of a monolith reactor for the catalytic wet oxidation of cellulose. *Chemical Engineering Journal,* 103**,** 77-88.

Segond N., Matsumura Y. and Yamamoto K. (2002) Determination of Ammonia Oxidation Rate in Sub- and Supercritical Water. *Industrial and Engineering Chemistry Research,* 41**,** 6020-6027.

Shende R. V. and Mahajani V. V. (1994) Kinetics of Wet Air Oxidation of glyoxalic acid and oxalic acid. *Industrial and Engineering Chemistry Research,* 33**,** 3125-3130.

Shende R. V. and Mahajani V. V. (1997) Kinetics of wet oxidation of formic acid and acetic acid. *Industrial and Engineering Chemistry Research,* 36**,** 4809-4814.

Shriner R. L. and Neumanw F. W. (1944) The chemistry of the amidines. *Chemical Reviews,* 35*,* 351-425.

Silva A. M. T., Quinta-Ferreira R. M. and Levec J. (2003) Catalytic and noncatalytic wet oxidation of formaldehyde. A novel kinetic model. *Industrial and Engineering Chemistry Research,* 42**,** 5099-5108.

Skaates J. M., Briggs B. A., Lamparter R. A. and Baillod C. R. (1981) Wet oxidation of glucose. *Canadian Journal of Chemical Engineering,* 59**,** 517-521.

Sonnen D. M., Reiner R. S., Atalla R. H. and Weinstock I. A. (1997) Degradation of pulp-mill effluent by oxygen and Na-5[PV2Mo10O40], a multipurpose delignification and wet air oxidation catalyst. *Industrial and Engineering Chemistry Research,* 36**,** 4134-4142.

Staehelin J. and Hoigne J. (1985) Decomposition of ozone in water in the presence of organic solutes acting as promoters and inhibitors of radical chain reactions. *Environmental Science and Technology,* 19**,** 1206-1213.

Stuber F., Font J., Fortuny A., Bengoa C., Eftaxias A. and Fabregat A. (2005) Carbon materials and catalytic wet air oxidation of organic pollutants in wastewater. *Topics in Catalysis,* 33**,** 3-50.

Su X. L., Zhao Y. L., Zhang R. and Bi J. C. (2004) Investigation on degradation of polyethylene to oils in supercritical water. *Fuel Processing Technology,* 85**,** 1249-1258.

Suárez-Ojeda M. E., Kim J., Carrera J., Metcalfe I. S. and Font J. (2007) Catalytic and non-catalytic wet air oxidation of sodium dodecylbenzene sulfonate: Kinetics and biodegradability enhancement. *Journal of Hazardous Materials,* 144**,** 655-662.

Sugano M., Komatsu A., Yamamoto M., Kumagai M., Shimizu T., Hirano K. and Mashimo K. (2009) Liquefaction process for a hydrothermally treated waste mixture containing plastics. *Journal of Material Cycles and Waste Management,* 11**,** 27-31.

Suwa T., Matsushima A., Suziki Y. and Namina Y. (1961) Synthesis of Nitrous Oxide by Oxidation of Ammonia. *Kohyo Kagaku Zasshi,* 64**,** 1879 - 1888.

Suzuki Y., Tagaya H., Asou T., Kadokawa J. and Chiba K. (1999) Decomposition of prepolymers and molding materials of phenol resin in subcritical and supercritical water under an Ar atmosphere. *Industrial and Engineering Chemistry Research,* 38**,** 1391-1395.

Takayama H., Qin J. Y., Inazu K. and Aika K. (1999) Hydrogen-treated active carbon supported palladium catalysts for wet air oxidation of ammonia. *Chemistry Letters***,** 377-378.

Thomason T. B. and Modell M. (1984) Supercritical water destruction of aqueous wastes. *Hazardous Waste and Hazardous Materials,* 1**,** 453-467.

Thomsen A. B. (1998) Degradation of quinoline by wet oxidation-kinetic aspects and reaction mechanisms. *Water Research,* 32**,** 136-146.

Toepfer B., Gora A. and Li Puma G. (2006) Photocatalytic oxidation of multicomponent solutions of herbicides: Reaction kinetics analysis with explicit photon absorption effects. *Applied Catalysis B-Environmental,* 68**,** 171-180.

Tromans D. (2001) Modelling oxygen solubility in bleaching solutions. *The Canadian Journal of Chemical Engineering,* 79**,** 156-160.

Tukac V. and Hanika J. (1998) Catalytic wet oxidation of substituted phenols in the trickle bed reactor. *Journal of Chemical Technology and Biotechnology,* 71**,** 262-266.

Ukropec R., Kuster B. F. M., Schouten J. C. and van Santen R. A. (1999) Low temperature oxidation of ammonia to nitrogen in liquid phase. *Applied Catalysis B,* 23**,** 45-47.

Vaidya P. D. and Mahajani V. V. (2002) Insight into heterogeneous catalytic wet oxidation of phenol over a Ru/TiO2 catalyst. *Chemical Engineering Journal,* 87**,** 403-416.

Vera Perez I., Rogak S. and Branion R. (2004) Supercritical water oxidation of phenol and 2,4-dinitrophenol. *The Journal of Supercritical Fluids,* 30**,** 71-87.

Veriansyah B., Kim J.-D. and Lee J.-C. (2007) Destruction of chemical agent simulants in a supercritical water oxidation bench-scale reactor. *Journal of Hazardous Materials,* 147**,** 8-14.

Wakabayashi T., Okuwaki A. and Okabe T. (1988) Oxidation of coals in liquid phases VIII. Effect of reactor material and reaction conditions on the formation of oxalate in the oxygen oxidation of acetate in alkaline solutions at elevated temperatures. *Nippon Kagaku Kaishi***,** 299-303.

Webley P. A., Tester J. W. and Holgate H. R. (1991) Oxidation kinetics of ammonia and ammonia-methanaol mixtures in supercritical water in the tmperature range 530 – 700ºC at 246 bar. *Industrial and Engineering Chemistry Research,* 30**,** 1745 - 1754.

Wilhelmi A. R. and Knopp P. V. (1979) Wet Air Oxidation - alternative to incineration. *Chemical Engineering Progress,* 75**,** 46-52.

Willms R. S., Balinsky A. M., Reible D. D., Wetzel D. M. and Harrison D. P. (1987a) Aqueous-phase oxidation: the intrinsic kinetics of single organic compounds. *Industrial and Engineering Chemistry Research,* 26**,** 148-154.

Willms R. S., Reible D. D., Wetzel D. M. and Harrison D. P. (1987b) Aqueous-phase oxidation: rate enhancement studies. *Industrial and Engineering Chemistry Research,* 26**,** 606-612.

Winterbottom J. M. and King M. B. (1999) *Reactor Design for Chemical Engineers,* Cheltenham, Stanley Thornes.

World Health Organisation and United Nations Children's Fund. (2006) Meeting the MDG drinking-water and sanitation target: the urban and rural challenge of the decade, 1-47.

Zhang Q. L. and Chuang K. T. (1998) Kinetics of wet oxidation of black liquor over a Pt-Pd-Ce/alumina catalyst. *Applied Catalysis B-Environmental,* 17**,** 321-332.

APPENDICES

Appendix 1 - Error Analysis

All calculated parameter values were reported at 95% confidence level. The standard deviation of the data sets was calculated using the ANOVA (Analysis OF Variance) statistical data analysis tool in Microsoft Excel. ANOVA was developed by Sir Ronald A. Fisher to compare data sets at 95% confidence levels, and this evolved into Six Sigma set comparisons. Freedman (2005)

Table A 1 shows the standard deviation for TOC removal, obtained during oxidation experiments carried out at 240 ºC and 7 MPa (shown in section 4.4, page 75). It shows that the standard deviation for this data set was a maximum of ± 4.3% at a 95% confidence levels. The standard deviation is the square root of the variance.

Time (min)	Run 1	Run 2	Run 3
0	0	0	0
10	2.01	1.91	3.03
20	54.29	51.57	45.9
30	57.6	57.26	50.9
40	61.89	61.25	55.12
50	64.91	64.38	58.56
60	67.16	67.22	61.55
70	69.91	69.43	63.83
80	71.77	71.35	66.05
90	73.67	72.99	68.55

Anova: Single factor

Time (min)	Run 1	Run 2	Run 3		
SUMMARY					
Groups	**Count**	**Sum**	**Average (%)**	**Variance (%)**	**Standard Deviation (%)**
Row 1	3	0.0	0.0	0.0	0.0
Row 2	3	6.9	2.3	0.4	0.6
Row 3	3	151.8	50.6	18.3	4.3
Row 4	3	165.8	55.3	14.2	3.8
Row 5	3	178.3	59.4	14.0	3.7
Row 6	3	187.9	62.6	12.4	3.5
Row 7	3	195.9	65.3	10.6	3.3
Row 8	3	203.2	67.7	11.4	3.4
Row 9	3	209.2	69.7	10.2	3.2
Row 10	3	215.2	71.7	7.7	2.8

Table A1. Example of experimental error analysis

Appendix 2 - Calculating oxygen partial pressures

The oxygen partial pressure was calculated based on the gas phase product concentration measured by GC-TCD. The mols of gas in the gas syringe were calculated using the ideal gas law based on the volume of the syringe.

$$n = \frac{PV}{RT} \tag{10.1}$$

where

n = mols of gas (mol)

P = Pressure (bar) ($^{x}10^{2}$)

V = Volume (L)

R = Gas law constant (J $K^{-1}mol^{-1}$)

T = Temperature (K)

The mols of gas in the reactor headspace were then calculated, based on the gas composition percentages from the GC-TCD, the molar concentration of oxygen in the reactor headspace was calculated.

The partial pressure of oxygen was calculated from Raoul's law based on x_i, the mole fraction of any individual gas component; P_i - the partial pressure of any individual gas component; P - the total pressure of gas mixture; n_i -the mols of any individual gas component; and n - total mols of gas mixture

$$x_i = \frac{P_i}{P} = \frac{n_i}{n} \qquad (10.2)$$

Appendix 3. Equilibrium constants and liquid phase oxygen concentration at 7 MPa for different temperatures based on equations 4.2 and 4.3 (Section 4.2, page 70)

Temperature (°C)	Equilibrium constant, $k \times 10^{-2}$	Oxygen concentration (mmol)
200	1.4	21
220	1.7	23
240	2.1	25

Table A.2 Calculated equilibrum constant and corresponding oxygen concentration in liquid phase.

Appendix 4. CHEMICAL HAZARD AND RISK ASSESSMENT

Hazardous Substances Policy - Assessment

School/Dept	CHEMICAL ENGINEERING	Assessment Number	
Assessor	OLUWAPONMILE OSIBO	Date of Assessment	25 JAN 2005

Notes Guidance on making an assessment is given in *Chemical Hazard and Risk Assessment (GUIDANCE/22/CHRA/03)*.
Guidance is also available from the attached *Guidance on Completing the Chemical Hazard and Risk Assessment Form*.
Substance data is available in HAZDAT. Use a continuation sheet or word processor to expand any section of this form.
An *MS Word* file for this form is available from

1 LOCATION OF THE WORK ACTIVITY

LAB G34

2 PERSONS WHO MAY BE AT RISK

List names where possible: OLUWAPONMILE OSIBO, IDOKO OCHUMA, SARAH PALMER, NURASHKIN ABDUL AZIZ.

3 ACTIVITY ASSESSED

WET AIR OXIDATION OF DBU

4 MATERIALS INVOLVED Attach copies of data sheet(s)

NAME and CAS NUMBER	AMOUNT	HAZARD	RISK PHRASES	REPORTABLE?
1,8-Diazabicyclo[5.4.0] undec-7-ene 6674-22-2	1g/L (1000 ppm) max	Inhalation Contact with skin Ingestion	Harmful if swallowed Toxic by inhalation Burns on contact with skin Danger of cumulative effects Irritating to the eyes Harmful to aquatic organisms May cause long term effects in the aquatic environment Emits toxic fumes under fire conditions	

If substance is reportable, have you reported it to the Health and Safety Unit? YES/NO (see Note 4)

5 INTENDED USE

Give brief details and attach protocol/ instructions

To be used in small quantities (less than or equal to 1g/L) for Wet Air Oxidation. DBU is charged into a high pressure autoclave and reacted with oxygen, at high temperatures.

6 RISKS to HEALTH and SAFETY from INTENDED USE

From personal exposure or hazardous reactions. Refer to OELs, flash points, etc., as appropriate. Are pregnant women, breast-feeding mothers especially at risk?

Contact with skin can cause dry skin, redness and / or pain. Contact with eyes can cause redness and pain.
If inhaled, may cause irritation and sore throat. If ingested, may cause abdominal pain, diarrhoea, headache, dizziness, vomiting and weakness.

7 CONCLUSIONS ABOUT RISKS

Is level of risk acceptable? Can risk be prevented or reduced by change of substance/procedure? Are control measures necessary?

Acceptable level of risk. Risk can be prevented by using small quantise and suitable PPE

8 CONTROL MEASURES

Additional to *Good Chemical Practice*, e.g., fume cupboard, etc. Any special requirements, e.g., glove type, etc.

Use in small quantities

Wear suitable protective clothing, shoes and safety goggles

Avoid spillages and all precautions must be carefully observed and monitored. Experiments must be supervised

Spillages to be adequately reported and cleaned up according to environmental standards

9 INSTRUCTION/ TRAINING

Specify course(s) and/or special arrangements.

Posters in the vicinity to prevent visitors entering during experiments

Training on special handling of hazardous chemicals and safety

10 MONITORING

Performance of control measures,

Control measures to be monitored and work supervised adequately

Personal exposure	Health Surveillance, specify measures agreed with Health and Safety Unit
N/A	N/A

11 WASTE DISPOSAL PROCEDURE

Collect in clearly labelled waste containers, dispose of via Hazel Jennings according to state and Federal Legislation

12 REVIEW

Enter the date or circumstances for review of assessment (maximum review interval 5 years)

13 EMERGENCY ACTION

TO CONTROL HAZARDS — To stabilize situation eg spread absorbent on liquid spill; eliminate sources of ignition, etc.

Remove supply. Sweep spilled chemical into clearly labelled container. Do not let this chemical into the environment.
Clean up spill according to standards for hazardous chemicals
Report spill to Health and Safety Officer - Bob Badham

TO PROTECT PERSONNEL — Evacuation, protection for personnel involved in clean-up, Special First Aid

Remove contaminated clothes. Rinse and wash skin with soap and water. Avoid exposure, evacuate personnel.
If inhaled, remove to fresh air. If not breathing give artificial respiration. If breathing is difficult, give oxygen.
In case of skin contact, flush with copious amounts of water for at least 15 minutes. Remove contaminated clothing and shoes.
In case of contact with eyes, flush with copious amounts of water for at least 15 minutes. Assure adequate flushing by separating the eyelids with fingers. Call a physician.
If swallowed, wash out mouth with water provided person is conscious. Call a physician. Do not induce vomiting.

TO RENDER SITE OF EMERGENCY SAFE	Clean-up/decontamination

Clean up site wearing suitable PPE, including gloves and goggles. Report all emergencies and seek attention of Safety personnel

14	**EMERGENCY CONTACT**	NAME	OLUWAPONMILE OSIIBO	PHONE	46965

Appendix 5. Hazard and Risk Assessment Summary

Assessment Number

Hazard and Risk Assessment Summary

School/Dept: CHEMICAL ENGINEERING

Location of Activity: G34

Date of Assessment: 25 JAN 2005

Assessor: OLUWAPONMILE OSIBO

Activity Assessed (Attach protocols): WET AIR OXIDATION OF INDUSTRIAL WASTEWATER (DBU)

Assessment of Hazard and Risk									Control Measures Required
HAZARD (List only hazards from which there is a significant risk of serious harm under foreseeable conditions)	**PERSONS AT RISK** (See key, Indicate number)	**PERSONAL HARM?**			**LIKELIHOOD of HARM?**				
		F	Mj	Mn	Y	Pr	Po	R	
Oxygen and Nitrogen gas cylinder leak	Pg		√					√	Use and store below 52°C. Keep cylinders away from all combustible and flammable materials. Do not exceed cylinder outlet pressure of 150 bar. Test cylinders for leaks regularly. Open cylinder outlet valves slowly and close when not in use.
Hot surfaces when the rig is operated	Pg			√				√	Ensure PPE is worn at all times and there is minimal contact with rig surfaces if any at all.
Illness due to prolonged contact with DBU	Pg		√					√	Use small quantities in low concentrations (1g/L or less) at all times. Do not keep large quantities in the laboratory. Keep away all incompatible materials. Wear appropriate PPE at all times. Clean up all spills according to safety regulations. Report all spills immediately

Key

PERSONS AT RISK	
Ug	Undergraduate
Pg	Postgraduate
S	Staff
C	Contractor
V	Visitor
Pa	Patient
Pu	General Public
Yp	Young Person
Nm	New/Expectant Mother

PERSONAL HARM?	
F	Fatality
Mj	Major Injury
Mn	Minor Injury

LIKELIHOOD	
Y	Yes/ Very High
Pr	Probable
Po	Possible
R	Remote

Risk Significance	Y	Pr	Po	R	
F	✓	✓	✓	✓	✓ = Significant risk
Mj	✓	✓	✓	✓	
Mn	✓	✓	X	X	X = Insignificant risk

Date for Review

Major Injury: Loss of or broken limb; Loss of or damaged eye; Loss of consciousness; Acute illness needing medical treatment; Permanent ill health or disability

Appendix 6 - Calculating Reynolds number at Supercritical conditions

Reisdence time (τ) is calculated by dividing reactor volume (V) by the volumetric flowrate (v_{sc}) at the entrance to the reactor at reactor conditions:

$$\tau = \frac{V}{v_{sc}} \quad \text{(A.1)}$$

Table A.3 Table showing calculation of residence times and Reynolds Number at 400 ºC and 25 MPa

Flow (ml/min)	Flow (m3/s)	Flow Super Critical (v_{sc}) (m3/s)	Reactor length (m)	d (m)	Cross sectional Area (m2)	Reactor Volume (m3)	Residence time (s)	μ (Pa s)	Density (kg/m3)	u (m/s)	Reynolds Number
20	3.33E-07	2.00E-06	3.3	1.00E-03	7.85E-07	2.59E-06	1.297	2.92E-05	166.5	2.54E+00	14524
18	3E-07	1.80E-06	3.3	1.00E-03	7.85E-07	2.59E-06	1.441	2.92E-05	166.5	2.29E+00	13071
17	2.83E-07	1.70E-06	3.3	1.00E-03	7.85E-07	2.59E-06	1.526	2.92E-05	166.5	2.16E+00	12345
16	2.67E-07	1.60E-06	3.3	1.00E-03	7.85E-07	2.59E-06	1.622	2.92E-05	166.5	2.04E+00	11619
15	2.5E-07	1.50E-06	3.3	1.00E-03	7.85E-07	2.59E-06	1.730	2.92E-05	166.5	1.91E+00	10893
14	2.33E-07	1.40E-06	3.3	1.00E-03	7.85E-07	2.59E-06	1.853	2.92E-05	166.5	1.78E+00	10167
13	2.17E-07	1.30E-06	3.3	1.00E-03	7.85E-07	2.59E-06	1.996	2.92E-05	166.5	1.65E+00	9440
12	2E-07	1.20E-06	3.3	1.00E-03	7.85E-07	2.59E-06	2.162	2.92E-05	166.5	1.53E+00	8714
11	1.83E-07	1.10E-06	3.3	1.00E-03	7.85E-07	2.59E-06	2.359	2.92E-05	166.5	1.40E+00	7988
10	1.67E-07	9.99E-07	3.3	1.00E-03	7.85E-07	2.59E-06	2.594	2.92E-05	166.5	1.27E+00	7262
10.6	1.77E-07	1.06E-06	3.3	1.00E-03	7.85E-07	2.59E-06	2.448	2.92E-05	166.5	1.35E+00	7698
9	1.5E-07	8.99E-07	3.3	1.00E-03	7.85E-07	2.59E-06	2.883	2.92E-05	166.5	1.14E+00	6536
8.5	1.42E-07	8.49E-07	3.3	1.00E-03	7.85E-07	2.59E-06	3.052	2.92E-05	166.5	1.08E+00	6173
8	1.33E-07	7.99E-07	3.3	1.00E-03	7.85E-07	2.59E-06	3.243	2.92E-05	166.5	1.02E+00	5809
7.6	1.27E-07	7.59E-07	3.3	1.00E-03	7.85E-07	2.59E-06	3.414	2.92E-05	166.5	9.67E-01	5519
7	1.17E-07	6.99E-07	3.3	1.00E-03	7.85E-07	2.59E-06	3.706	2.92E-05	166.5	8.90E-01	5083
6.55	1.09E-07	6.54E-07	3.3	1.00E-03	7.85E-07	2.59E-06	3.961	2.92E-05	166.5	8.33E-01	4756
6.5	1.08E-07	6.49E-07	3.3	1.00E-03	7.85E-07	2.59E-06	3.992	2.92E-05	166.5	8.27E-01	4720
6.45	1.08E-07	6.44E-07	3.3	1.00E-03	7.85E-07	2.59E-06	4.022	2.92E-05	166.5	8.20E-01	4684
6	1E-07	5.99E-07	3.3	1.00E-03	7.85E-07	2.59E-06	4.324	2.92E-05	166.5	7.63E-01	4357
5.85	9.75E-08	5.84E-07	3.3	1.00E-03	7.85E-07	2.59E-06	4.435	2.92E-05	166.5	7.44E-01	4248
5.2	8.67E-08	5.20E-07	3.3	1.00E-03	7.85E-07	2.59E-06	4.989	2.92E-05	166.5	6.61E-01	3776

5.25	8.75E-08	5.25E-07	3.3	1.00E-03	7.85E-07	2.59E-06	4.942	2.92E-05	166.5	6.68E-01	3812
5.1	8.5E-08	5.10E-07	3.3	1.00E-03	7.85E-07	2.59E-06	5.087	2.92E-05	166.5	6.49E-01	3704
5	8.33E-08	5.00E-07	3.3	1.00E-03	7.85E-07	2.59E-06	5.189	2.92E-05	166.5	6.36E-01	3631
4.3	7.17E-08	4.30E-07	3.3	1.00E-03	7.85E-07	2.59E-06	6.034	2.92E-05	166.5	5.47E-01	3123
4	6.67E-08	4.00E-07	3.3	1.00E-03	7.85E-07	2.59E-06	6.486	2.92E-05	166.5	5.09E-01	2905
3.75	6.25E-08	3.75E-07	3.3	1.00E-03	7.85E-07	2.59E-06	6.919	2.92E-05	166.5	4.77E-01	2723
3.7	6.17E-08	3.70E-07	3.3	1.00E-03	7.85E-07	2.59E-06	7.012	2.92E-05	166.5	4.71E-01	2687
3.5	5.83E-08	3.50E-07	3.3	1.00E-03	7.85E-07	2.59E-06	7.413	2.92E-05	166.5	4.45E-01	2542
3	5E-08	3.00E-07	3.3	1.00E-03	7.85E-07	2.59E-06	8.648	2.92E-05	166.5	3.82E-01	2179
2	3.33E-08	2.00E-07	3.3	1.00E-03	7.85E-07	2.59E-06	12.97	2.92E-05	166.5	2.54E-01	1452
1	1.67E-08	9.99E-08	3.3	1.00E-03	7.85E-07	2.59E-06	25.95	2.92E-05	166.5	1.27E-01	726

Appendix 7 - HPLC Calibration Curve

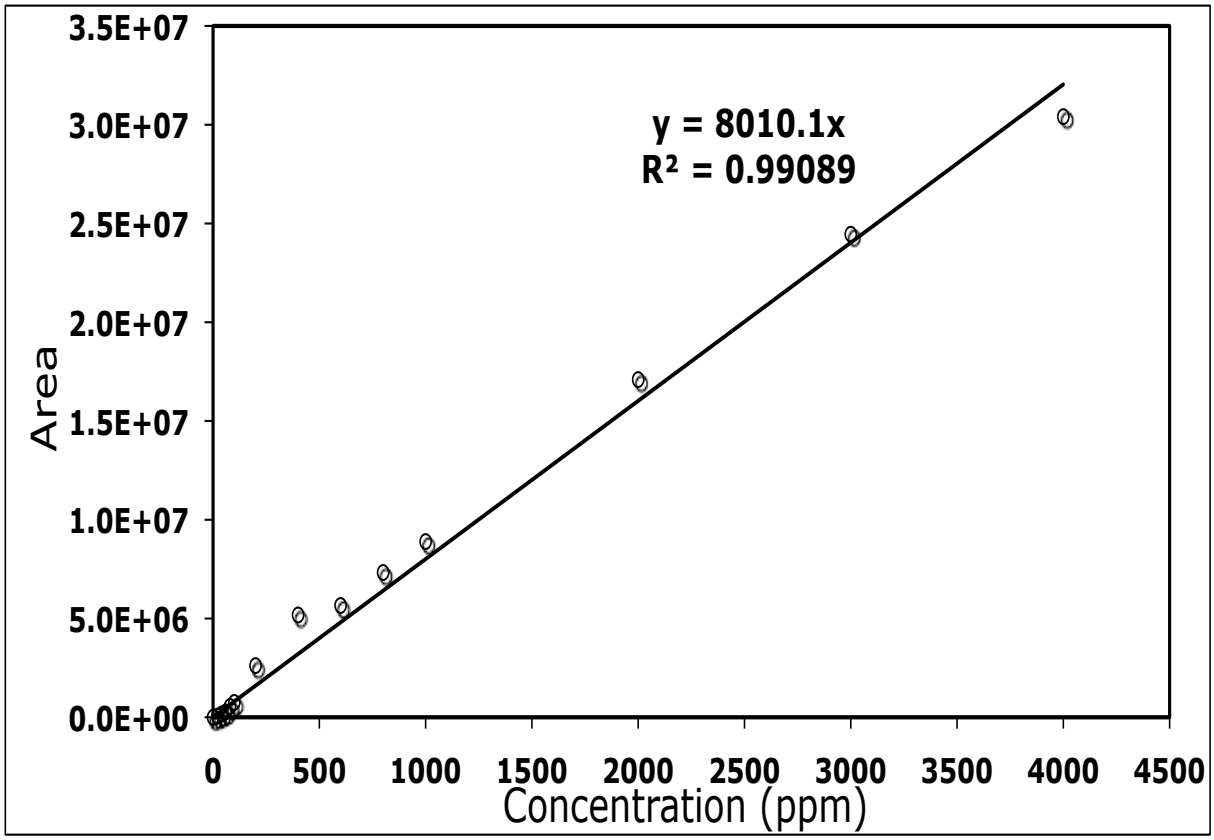

PUBLICATIONS

Oluwaponmile Osibo, Asli Yuksel, Bushra Al-Duri, Mitsuru Sasaki, Motonobu Goto "Hydrothermal Electrolysis of 1,8-diazabicyclo[5.4.0]undec-7-ene (DBU)" Journal of Water Resource and Protection (2010) (Submitted awaiting peer review)

Oluwaponmile Osibo, Yoshito Oshima, Regina Santos, Bushra Al-Duri, "Hydrothermal Oxidation of 1-8 Diazabicyclo [5.4.0] undec-7-ene (DBU) at Subcritical and Supercritical conditions." Proceedings of the 9th International Symposium on Supercritical Fluids, Arcachon (2009).

Idoko J. Ochuma, Oluwaponmile O. Osibo, Robert P. Fishwick, Steve Pollington, Alison Wagland, Joseph Wood and J. Mike Winterbottoma "Three-phase photocatalysis using suspended titania and titania supported on a reticulated foam monolith for water purification" Catalysis Today, 128 (1-2), 100-107 (2007)

Pinto, L., Osibo, O., Santos, R.C.D. and Al-Duri, B, "Removal of Nitrogen - Containing Pollutants from Pharmaceutical Wastewater Streams by Sub-Critical and Supercritical Water Oxidation: A Comparative Study" Proceedings of 7th Italian Conference on Chemical & Process Engineering, Italy. AIDIC Conference Series Vol.7, 281-290 (2005)